UNIVERSIDADE ESTADUAL PAULISTA
"JÚLIO DE MESQUITA FILHO"
Campus de Botucatu

Influência do excesso de cobre e zinco nos aspectos estruturais e funcionais de *Cuphea calophylla* Cham. & Schltdl. (Lythraceae) com ênfase no sistema secretor

Diana Pacheco Seixas

Tese apresentada ao Instituto de Biociências, Câmpus de Botucatu, UNESP, para obtenção do título de Doutor no Programa de Pós-Graduação em Ciências Biológicas (Botânica), AC: Morfologia e Diversidade de Plantas.

BOTUCATU – SP
2022

UNIVERSIDADE ESTADUAL PAULISTA
"Júlio de Mesquita Filho"

INSTITUTO DE BIOCIÊNCIAS DE BOTUCATU

Influência do excesso de cobre e zinco nos aspectos estruturais e funcionais de *Cuphea calophylla* Cham. & Schltdl. (Lythraceae) com ênfase no sistema secretor

Aluna: Diana Pacheco Seixas

Orientadora: Profa. Dra. Tatiane Maria Rodrigues

Coorientadora: Profa. Dra. Carmen Sílvia Fernandes Boaro

Tese apresentada ao Instituto de Biociências, Câmpus de Botucatu, UNESP, para obtenção do título de Doutor no Programa de Pós-Graduação em Ciências Biológicas (Botânica), AC: Morfologia e Diversidade de Plantas.

BOTUCATU – SP
2022

FICHA CATALOGRÁFICA ELABORADA PELA SEÇÃO TÉC. AQUIS. TRATAMENTO DA INFORM.
DIVISÃO TÉCNICA DE BIBLIOTECA E DOCUMENTAÇÃO - CÂMPUS DE BOTUCATU - UNESP
BIBLIOTECÁRIA RESPONSÁVEL: ROSANGELA APARECIDA LOBO-CRB 8/7500

Seixas, Diana Pacheco.
Influência do excesso de cobre e zinco nos aspectos estruturais e funcionais de *Cuphea calophylla* Cham. & Schltdl. (Lythraceae) com ênfase no sistema secretor / Diana Pacheco Seixas. - Botucatu, 2022

Tese (doutorado) - Universidade Estadual Paulista "Júlio de Mesquita Filho", Instituto de Biociências de Botucatu
Orientador: Tatiane Maria Rodrigues
Coorientador: Carmen Sílvia Fernandes Boaro
Capes: 2030203

1. Anatomia vegetal. 2. Estresse oxidativo. 3. Fotossíntese. 4. Metais - Toxicologia.

Palavras-chave: Anatomia vegetal; Estresse oxidativo; Estruturas secretoras; Fotossíntese; Metais tóxicos.

“Dedico este trabalho à minha família que se fez presente e me apoiou em cada etapa; em especial o dedico à Ana Maria Mugnatto Pacheco (minha avó), que infelizmente não pode ver em vida a conclusão deste, mas ela sempre esteve e sempre estará ao meu lado.”

Agradecimentos

A **Deus** pela oportunidade e força para a conclusão deste trabalho.

À **Coordenação de Aperfeiçoamento de Pessoal de Nível Superior - CAPES** - pelo auxílio financeiro para a realização do trabalho (código de Financiamento 001).

Ao **Conselho Nacional de Desenvolvimento Científico e Tecnológico – CNPq** pelo suporte financeiro para este estudo (Edital Universal – Processo 431738/2018-1).

À **Universidade Estadual Paulista "Júlio de Mesquita Filho",** Câmpus de Botucatu, e ao **Programa de Pós-graduação em Ciências Biológicas (Botânica)**, pela estrutura e oportunidade.

À **Profa. Dra. Tatiane Maria Rodrigues** pela oportunidade, orientação, auxílio e ensinamentos em anatomia vegetal; e, também, pela confiança durante este período.

À **Profa. Dra. Carmen Sílvia Fernandes Boaro** pela coorientação e por me auxiliar com o delineamento experimental e com as análises em fisiologia vegetal.

À **Profa. Dra. Marcia Ortiz Mayo Marques** pela disponibilidade, auxílio e toda contribuição para as análises em cromatografia líquida.

Ao **Dr. Felipe Girotto Campos** por auxiliar com o delineamento experimental, montagem do experimento, análises dos resultados em fisiologia vegetal e análises químicas.

Ao **Ruan Serafim da Silva**, aluno de Iniciação Científica, pelo companheirismo e pela colaboração ativa na realização do trabalho experimental e do trabalho em campo.

À **Dra. Taciana Barbosa Cavalcanti** da Empresa Brasileira de Pesquisa Agropecuária – EMBRAPA pela identificação da espécie vegetal do trabalho.

À **Dra. Poliana Ramos Cardoso**, pesquisadora R&D (Innovation Team) na Oxiteno S/A pelo auxílio com a metodologia de histolocalização de peróxido de hidrogênio.

Ao **Centro de Microscopia Eletrônica**, Unesp – Botucatu, pelo processamento de amostras para estudos ultra-estruturais.

Ao **Laboratório Multiusuário de Caracterização de Materiais (LMCMat) – UNESP Sorocaba**, pelas análises em MEV-EDS, em especial agradeço à **Profa. Dra. Elidiane Cipriano Rangel** e a técnica **Gabrielly Ivanof** por todo auxílio e contribuição.

Aos membros da banca de qualificação, **Profa. Dra. Rosani do Carmo de Oliveira Arruda**, **Prof. Dr. Milton Costa Lima Neto** e **Profa. Dra. Elizabeth Orika Ono**, por terem discutido e contribuído para qualidade do trabalho.

Aos membros da banca da defesa, **Profa. Dra. Elizabeth Orika Ono**, **Prof. Dr. Luiz Ricardo dos Santos Tozin**, **Prof. Dr. Filipe Pereira Giardini Bonfim**, **Profa. Dra. Juliana Villela Paulino** e aos suplentes, por aceitarem o convite para contribuir com a qualidade do trabalho.

Aos amigos da pós-graduação em Ciências Biológicas (Botânica), a todos os membros do **LaPAV (Laboratório de Pesquisas em Anatomia Vegetal)** e aos membros do **Laboratório de Crescimento e Fisiologia Vegetal** pela amizade, agradável convívio, ensinamentos e enriquecedoras discussões; além de todo auxílio na montagem e manutenção do experimento.

Não posso deixar de agradecer as pessoas que não estão relacionadas diretamente ao meio acadêmico, mas que foram de suma importância para o trabalho, como o Senhor Ivo, funcionário da fazenda experimental da UNESP de São Manuel que nos auxiliou em todas as vezes que fomos à fazenda para as coletas das plantas.

E aos meus familiares (em especial a minha mãe Ana Beatriz Mugnatto Pacheco; meu pai Luiz Francisco Seixas; minha irmã Laize Pacheco Seixas; meus avós Márcio Pacheco e Ana Maria Mugnatto Pacheco; minha madrinha Maria Cristina Mugnatto Sousa; meu padrinho Paulo Fernando de Sousa) e aos meus amigos que contribuíram para este processo com todo apoio, suporte, companhia e força.

Muito obrigada!

Sumário

Resumo

Áreas destinadas a atividade agropecuária frequentemente apresentam solos contaminados pelo excesso de elementos tóxicos, em especial Zinco (Zn) e Cobre (Cu). Em baixas concentrações esses elementos são micronutrientes essenciais para as plantas, porém, em excesso podem causar alterações na estrutura e funcionamento vegetal. *Cuphea calophylla* Cham. & Schltdl. (Lythraceae) é uma espécie subarbustiva nativa do Brasil popularmente utilizada no tratamento da hipertensão e na produção de saponáceos, sendo naturalmente encontrada em áreas ruderais e de pastagem. Esse trabalho teve como objetivo ampliar o conhecimento sobre o sistema secretor de *C. calophylla* e investigar a influência do excesso de Zn e Cu em aspectos estruturais e funcionais dos órgãos vegetativos da espécie. Indivíduos ocorrentes em área de pastagem com excesso de Zn e Cu e em área preservada foram amostrados; plantas também foram submetidas ao excesso de Zn, Cu e Zn+Cu em condições hidropônicas. Amostras de raiz, caule e folhas foram processadas segundo técnicas usuais em microscopia de luz e microscopia eletrônica de varredura e transmissão; dados morfométricos foram obtidos ao microscópio de luz. Índices de trocas gasosas foram analisados usando analisador de gases por infravermelho (IRGA). O nível de estresse oxidativo foi mensurado por meio da quantificação de peróxido de hidrogênio (H_2O_2) e peroxidação lipídica; moléculas de H_2O_2 foram histolocalizadas com 3,3-diaminobenzidine-DAB. A concentração de Zn e Cu nas estruturas secretoras foi detectada utilizando EDS-MEV. A composição química do extrato produzido pelo eixo vegetativo aéreo foi analisada por cromatografia líquida de alta performance (HPLC). Emergências glandulares volumosas produtoras de substâncias fenólicas, mucilagem e lipídios foram observadas em caules e folhas. Células epidérmicas bicompartimentalizadas secretoras de compostos fenólicos e mucilagem foram observadas no limbo foliar. Hidatódios ocorreram no bordo do limbo foliar e foram aqui descritos pela primeira vez para o gênero. Plantas em área de pastagem e indivíduos submetidos ao excesso de Zn e/ou Cu em hidroponia apresentaram compactação do mesofilo foliar. Plantas mantidas sob excesso de Zn apresentaram maior densidade de células epidérmicas secretoras nas folhas, enquanto que plantas sob excesso de Cu produziram emergências glandulares com menor comprimento. Zn e Cu foram detectados nas emergências glandulares e nas células epidérmicas secretoras sugerindo o envolvimento do sistema secretor na eliminação do excesso desses metais. O excesso de Cu promoveu aumento dos espaços intercelulares nas raízes. Alterações nas membranas internas de mitocôndrias e cloroplastos foram observadas em plantas sob excesso de Zn. Marcação intensa para H_2O_2 foi detectada em folhas e raízes de plantas sob excesso de Zn e/ou Cu. Maior número de compostos químicos foi detectado em plantas sob excesso de Cu, porém a produção de ácido elágico e ácido gálico não

foi alterada com o excesso de Zn e Cu. Apesar do indicativo de estresse oxidativo nas raízes, plantas sob excesso de Zn mantiveram o metabolismo fotossintético, enquanto que plantas sob excesso de Cu tiverem redução na assimilação de carbono. Os resultados obtidos sugerem que *C. calophylla* é tolerante ao excesso de Zn e suscetível ao excesso de Cu. Considerando o aumento exponencial de áreas com solos contaminados por excesso de Cu e Zn devido ao avanço da agropecuária no Brasil, nossos resultados se tornam relevantes uma vez que geram subsídios para predições dos efeitos de ações antrópicas na estrutura e funcionamento dos vegetais, reforçando a importâncias dos esforços para o manejo e conservação de espécies vegetais nativas.

Palavras-chave: anatomia vegetal; estresse oxidativo; estruturas secretoras; fotossíntese; metais tóxicos; ultraestrutura.

Abstract

Areas used for agricultural activity often have soils contaminated by the excess of toxic elements, especially Zinc (Zn) and Copper (Cu). In low concentrations these elements are essential micronutrients for plants, however, in excess they can cause changes in plant structure and function. *Cuphea calophylla* (Lythraceae) is a subshrub species native to Brazil, popularly used in the treatment of hypertension and in the production of saponaceous, being naturally found in ruderal and pasture areas. This work aimed to expand the knowledge about the secretory system of *C. calophylla* and investigate the influence of Zn and Cu excess on structural and functional aspects of vegetative organs. Plants occurring in pasture areas with excess Zn and Cu and in preserved areas were sampled; plants were also subjected to excess Zn, Cu and Zn+Cu under hydroponic conditions. Root, stem and leaf samples were processed according to usual techniques in light microscopy and scanning and transmission electron microscopy; morphometric data were obtained under a light microscope. Gas exchange were measured using infrared gas analyser (IRGA). The level of oxidative stress was measured through the quantification of hydrogen peroxide (H_2O_2) and lipid peroxidation; H_2O_2 molecules were histolocalized with 3,3-diaminobenzidine-DAB. The concentration of Zn and Cu in the secretory structures was detected using EDS-MEV. The chemical composition of the extract produced by the aerial vegetative axis was analysed by high performance liquid chromatography (HPLC). Voluminous glandular emergences producing phenolic substances, mucilage and lipids were observed in stems and leaves. Bi-compartmentalized epidermal cells secreting phenolic compounds and mucilage occurred in the leaf blade. Hydathodes were present at the edge of the leaf blade and were here described for the first time for the genus. Plants in pasture areas and individuals subjected to excess of Zn and/or Cu in hydroponics showed leaf mesophyll compaction. Plants under Zn excess showed higher density of epidermal secretory cells in the leaves, while plants under Cu excess produced glandular emergences with shorter length. Zn and Cu were detected in glandular emergences and in the epidermal secretory cells, suggesting the involvement of the secretory system in the elimination of the excess of these metals. Excessive Cu promoted an increase in intercellular spaces in the roots. Structural changes in the inner membranes of mitochondria and chloroplasts were observed in plants under Zn excess. Intense staining for H_2O_2 was detected in leaves and roots of plants under excess Zn and/or Cu. A greater number of chemical compounds was detected in plants under Cu excess, however the production of ellagic acid and gallic acid was not altered even with Zn and Cu excess. Despite the indicative of oxidative stress in the roots, plants under Zn excess maintained the photosynthetic metabolism, while plants under excess of Cu reduced the carbon

assimilation. The results obtained suggest that *C. calophylla* is tolerant to Zn excess and susceptible to Cu excess. Considering the exponential increase in areas with soils contaminated by excess Cu and Zn due to the advance of agriculture in Brazil, our results become relevant since they generate subsidies for predictions of the effects of anthropic actions on the structure and functioning of plants, emphasising the importance of efforts for the management and conservation of native plant species.

Keywords: oxidative stress; photosynthesis; plant anatomy; secretory structures; toxic metals; ultrastructure.

Introdução geral

A expansão industrial, agroquímica e agropecuária, assim como o excesso de materiais descartados por indústrias e centros urbanos, aumentam excessivamente a contaminação de solos por resíduos potencialmente tóxicos. Neste contexto, encontra-se a contaminação dos solos através de metais tóxicos, os quais muitas vezes são dispersos no ambiente como resquício das atividades antrópicas e podem oferecer riscos aos seres vivos quando em altas concentrações (McBride 1994; Nagajyoti et al. 2010). Duffus, desde 2002, em parceria com a IUPAC (Iternational Union of Pure and Applied Chemistry), defende a utilização da terminologia "metais tóxicos" para se referir a elementos metálicos que, dependo da sua quantidade, podem ser nocivos aos seres vivos, o que faz entrar em desuso a terminologia "metais pesados", visto que nem todos os metais que apresentam alta toxicidade são elementos com alta densidade atômica (maior que 4g/cm3).

Áreas rurais envolvidas com a agropecuária são, geralmente, caracterizadas pela presença de solos contaminados com metais tóxicos, em específico com acúmulo de Zinco (Zn) e Cobre (Cu) (Mantovi et al. 2003; Girotto 2007; Matias et al. 2010; Ambrosini et al. 2016). Este acúmulo se deve à utilização de pesticidas e outros agroquímicos em culturas vegetais (Marsola et al. 2005; Brunetti et al. 2011; Oliveira 2011; Girotto et al. 2013; Brunetto et al. 2014). Além da fertilização dos solos e dos defensivos agrícolas, estudos destacam que regiões utilizadas para pastagem e áreas destinadas à agricultura, que fazem uso da adubação orgânica proveniente de excremento de animais, tendem a apresentar maiores concentrações de Zn e Cu devido à adição de sais para a suplementação alimentar na ração dos animais de manejo (Mantovi et al. 2003; Girotto 2007; Matias et al. 2010; Broetto et al. 2014; Ambrosini et al. 2016; De Conti et al. 2016; Brennan et al. 2019; Scheid et al. 2019).

Zn e Cu são micronutrientes importantes para o desenvolvimento e funcionamento do organismo vegetal (Reeves e Baker 2000; Taiz e Zeiger 2017), atuando como cofatores enzimáticos em diferentes reações essenciais para o metabolismo das plantas (respiração e fotossíntese). Especificamente, o Zn está associado ao metabolismo de grupos fosfato (ATPases), atuando na manutenção da estrutura de ribossomos e no funcionamento da RNA-polimerase. Já o Cu participa diretamente do processo fotossintético através do transporte de elétrons no fotossistema I (Nagajyoti et al. 2010; Hossain et al. 2018; Chandrasekhar e Ray 2020).

Entretanto, o Zn e o Cu em altas concentrações podem provocar disfunções no metabolismo das plantas, alterando o desenvolvimento vegetal (Vangronsveld et al. 1997; Reeves e Baker 2000; Hossain et al. 2018; Hammerschmitt et al. 2020). A toxicidade causada

pelo excesso desses elementos é evidenciada em alterações morfológicas, anatômicas e funcionais nas plantas. Estudos demonstram que o excesso de Zn e Cu em solos contaminados geram espécies reativas ao oxigênio (ERO) no corpo vegetal, como o radical superóxido (O_2^-), hidroxila (OH^-), peróxido de hidrogênio (H_2O_2) e oxigênio singlete ($^1O_2$). As ERO são moléculas instáveis que apresentam oxigênio reduzido, portanto, são altamente reativas, pois buscam seu equilíbrio energético fazendo ligações com diversas moléculas orgânicas. Nessas interações, as ERO desconfiguram moléculas estruturais (ex. lipoproteicas) e ativam rotas enzimáticas levando a distúrbios em vias metabólicas essenciais como na fotossíntese e respiração devido ao estresse oxidativo gerado (Stadtman e Oliver 1991; Parry et al. 1994; Hossain et al. 2018; Hammerschmitt et al. 2020). Em específico, o Zn interfere diretamente no sistema de defesa antioxidante, inativando enzimas antioxidantes e promovendo o estresse oxidativo no corpo vegetal (Gratão et al. 2005). Já o aumento de Cu no organismo vegetal pode promover a produção de ERO de maneira excessiva por meio da reação de Feton, uma vez que o Cu^+ catalisa reações que aumentam a concentração de OH^- (Briat e Lebrun 1999).

De modo geral, o estresse proveniente do excesso de Zn e Cu pode reduzir as taxas de crescimento das plantas e promover alterações nas folhas como clorose, aparecimento de manchas, modificação da morfologia e da área foliar, aumento na emissão de fluorescência das moléculas de clorofila e aceleração da senescência, além de modificar rotas enzimáticas importantes (Taiz e Zeiger 2017; Hossain et al. 2018).

Sabe-se também que o estresse oxidativo em plantas expostas a solos contaminados pelo excesso de Zn e Cu pode levar a alterações anatômicas e subcelulares no corpo vegetal. Estudos descrevem que o excesso de Zn pode provocar a diminuição do volume de células epidérmicas e células do parênquima paliçádico e lacunoso, diminuindo os espaços intercelulares, provocando colapso de feixes vasculares e rompimento de células parenquimáticas do mesofilo, além de reduzir a quantidade de grãos de amido e de amiloplastos (Sridhar et al. 2005, 2007); em raízes, o excesso de Zn pode aumentar os espaços intercelulares do córtex (Kouhi et al. 2016; Somavilla et al. 2018). Já em situação de Cu em excesso, as plantas tendem a apresentar raízes com rupturas na epiderme e alterações na organização concêntrica das camadas de células parenquimáticas do córtex (Guimarães et al. 2016); no limbo foliar pode ocorrer inibição do alongamento de células do parênquima clorofiliano, além do aumento dos espaços intercelulares no mesofilo e aumento do número de cloroplastos nas células fotossintetizantes, os quais passam a apresentar grana mais desenvolvido (Bernal at al. 2006; Bini et al. 2012).

Embora os efeitos morfoanatômicos decorrentes do excesso de Zn e Cu sejam conhecidos na estrutura de algumas espécies vegetais (Sridhar et al. 2005, 2007; Ambrosini et al. 2016; Bini et al. 2012; Somavilla et al. 2018), estudos descrevem que as respostas ao excesso

de metais são muito particulares para cada espécie (Bini et al. 2012; Kouhi et al. 2016; Hossain et al. 2018). Além disso, a maioria dos estudos que avalia a toxicidade proveniente do excesso de metais é limitada a plantas alimentícias ou plantas modelos (Mantovi et al. 2003; Brunetti et al. 2011; Girotto et al. 2013; Kouhi et al. 2016; Schwalbert et al. 2019; Hammerschmitt et al. 2020). Neste sentido, pouco se sabe sobre a influência do excesso de metais tóxicos na morfologia, aspectos subcelulares e funcionamento de plantas nativas.

Em áreas de pastagens, espécies de gramíneas e leguminosas são amplamente utilizadas para o forrageio; entretanto, representantes de mais de 30 famílias botânicas são encontrados naturalmente dispersos nessas áreas, dentre eles representantes da família Lythraceae (Penso et al. 2009). *Cuphea* P. Browne é o maior gênero de Lythraceae, com cerca de 250 espécies distribuídas desde o leste dos EUA até o sul da Argentina (Amarasinghe et al. 1991; Graham e Graham 2014). No Brasil, espécies deste gênero são popularmente conhecidas como sete-sangrias e apresentam uma ampla distribuição, sendo seu principal centro de diversidade em áreas de Cerrado, muitas delas encontradas em regiões ruderais (Cavalcanti 1990).

Espécies de *Cuphea* produzem substâncias com propriedades medicinais (Amarasinghe et al. 1991; Das et al. 2018; Ramírez et al. 2018) com comprovada função antioxidante, além de auxiliar na prevenção de doenças cardiovasculares, hipertensão e na redução do colesterol (Lorenzi e Matos, 2002; Das et al., 2018; Ramírez et al. 2018; Santos et al. 2020). Além disso, essas espécies são ricas em ácidos graxos, sendo fonte de lipídeos para a produção de sabão, detergentes e lubrificantes (Thompson 1984; Phippen 2009). Estudos encontrados na literatura descrevem os sítios de compostos bioativos de espécies de *Cuphea* como sendo tricomas glandulares e células epidérmicas secretoras de mucilagem (Amarasinghe et al. 1991; Lusa e Bona 2011; Klider et a. 2020). Entretanto, faltam estudos detalhados focados na compreensão da morfologia e desenvolvimento do sistema secretor em espécies do gênero.

Cuphea calophylla Cham. e Schltdl. é uma espécie nativa, subarbustiva e ruderal, facilmente encontrada no cerrado paulista em campos, gramados, bordas de matas e em ambientes antropizados como pastagens e beiras de estradas (Lorenzi e Matos 2002; Lusa e Biase 2011). Utilizada na medicina popular para tratamentos de doenças como hipertensão (Lorenzi e Matos 2002; Ramírez et al. 2018), as propriedades medicinais de *C. calophylla* têm sido relacionadas com a produção de substâncias fenólicas detectadas em extratos do seu eixo vegetativo aéreo, as quais atuam diretamente como antioxidantes, dentre elas estudos destacam o ácido elágico e o ácido gálico (Ramírez et al. 2018; Klider at al. 2020; Santos et al. 2020). Além disso, há relatos sobre o potencial comercial dessa espécie para a produção de saponáceos (Thompson 1984).

Desse modo, conhecer os aspectos estruturais e funcionais de *C. calophylla* e a influência do excesso de Cu e Zn no desenvolvimento e funcionamento de seu eixo vegetativo é de grande relevância quando se considera: a) sua ampla distribuição no Brasil, em especial em áreas antropizadas; b) a importância do sistema secretor vegetal na produção de substâncias bioativas e sua utilização pela medicina popular e indústria farmacêutica; c) o avanço da agropecuária e o aumento das áreas ocupadas por solos contaminados pelo uso de pesticidas e fertilizantes químicos ou orgânicos no Brasil, em especial no interior paulista.

Esse trabalho teve como objetivo ampliar o conhecimento sobre o sistema secretor do eixo vegetativo aéreo de *C. calophylla* e investigar a influência do excesso de Zn e Cu em aspectos estruturais e funcionais dos órgãos vegetativos. Os resultados obtidos foram organizados em dois capítulos redigidos no formato de artigos científicos. O primeiro capítulo teve como objetivo ampliar o conhecimento sobre o sistema secretor do eixo vegetativo aéreo de *C. calophylla*. O segundo capítulo, de cunho experimental, teve como objetivo analisar a influência do excesso de Zn e Cu nos aspectos estruturais, fisiológicos e bioquímicos dos órgãos vegetativos de *C. calophylla* utilizando indivíduos ocorrentes naturalmente em áreas preservadas e áreas de pastagem e indivíduos cultivados em meio hidropônico em casa de vegetação. Nossos resultados geram subsídios para estudos com abordagem ecológica, taxonômica e farmacológica, dentre outras, além de trazerem importantes informações para predições dos efeitos de ações antrópicas na estrutura e funcionamento das plantas e para o manejo de espécies vegetais.

Referências bibliográficas

AMARASINGHE, V.; GRAHAM, S.A.; GRAHAM, A. Trichome morphology in the genus *Cuphea* (Lythraceae). **Botanical Gazette**, 152, p.77-90, 1991.

AMBROSINI, V.G.; SORIANI, H.H.; ROSA, D.J.; TIECHER, T.L.; GIROTTO, E.; SIMÃO, D.G.; MELO, G.W.B.; ZALAMENA, J.; BRUNETTO, G. **Impacto do excesso de cobre e zinco no solo sobre videiras e plantas de cobertura.** In: Calagem, adubação e contaminação em solos cultivados com videiras. Embrapa Uva e Vinho, p.91-110, 2016.

BERNAL, M.; RAMIRO, M.V.; CASES, R.; PICOREL, R.; YRUELA, I. Excess copper effect on growth, chloroplast ultrastructure, oxygen-evolution activity and chlorophyll fluorescence in *Glycine max* cell suspension. **Physiologia plantarum**, 127, p.312-325, 2006.

BINI, C; WAHSHA, M.; FONTANA, S.; MALECI, L. Effects of heavy metals on morphological characteristics of *Taraxacum officinale* web growing on mine soils in NE Italy. **Journal of Geochemical Exploration**, 123, p.101-108, 2012.

BRENNAN, R.F.; PENROSE, B.; BELL, R.W. Micronutrients limiting pasture production in Australia. **Crop and Pasture Science**, 70, p.1053-1064, 2019.

BRIAT, J.F.; LEBRUN, M. Plant responses to metal toxicity. Comptes Rendus de l'Académie des Sciences, series III, **Sciences de la vie**, 322, p.43-54, 1999.

BROETTO, T.; TORNQUIST, C.G.; BAYER C.; CAMPOS, B.C.; MERTEN, C.G.; WOTTRICH, B. Soils and surface waters as affected by long-term swine slurry application in oxisols of Southern Brazil. **Pedosphere**, 24, p.585-594, 2014.

BRUNETTI, G.; FARRAG, K.; ROVIRA, P.S.; NIGRO, F.; SENESI, N. Greenhouse and field studies on Cr, Cu, Pb and Zn phytoextraction by *Brassica napus* from contaminated soils in the Apulia region, Southern Italy. **Geoderma**, 160, p.517-523, 2011.

BRUNETTO, G.; MIOTTO, A.; CERETTA, C.A.; SCHMITT, D.E.; HEINZEN, J.; DE MORAES, M.P.; CANTON, L.; TIECHER, T.L.; COMIN, J.J.; GIROTTO, E. Mobility of copper and zinc fractions in fungicide-amended vineyard sandy soils. **Archives of Agronomy Soil Science**. 60, p.609-624, 2014.

CAVALCANTI, T.B. Flora da Serra do Cipó, Minas Gerais: Lythraceae. **Boletim de Botânica da Universidade de São Paulo**, 12, p.67-93, 1990.

CHANDRASEKHAR, C.; RAY, J.G. Plant Response to Excess of Copper in Soils: A Review. In: **Metal toxicity in plants**. New York: Nova Science Publishers, 2020.

DAS, A.; CHAUDARY, S.K.; BHAT, H.R.; SHAKYA, A. *Cuphea carthagenensis*: a review of its ethnobotany, pharmacology and phytochemistry. **Bulletin of Arunachal Forest Research**, 33, p.01-14, 2018.

DE CONTI, L.; CERRETA, C.A.; FERREIRA P.A.A.; LOURENZI, C.R.; GIROTTO, E.; LOURENSINI, F.; TIECHER, T.L.; MARCHEZEN, C.; ANCHIETA, M.G.; BRUNETTO, G. Soil solution concentrations and chemical species of copper and zinc in a soil with a history of pig slurry application and plant cultivation. **Agriculture, Ecosystems and Environment**, 216, p.374-386, 2016.

DUFFUS, J.H. “Heavy metals” - A meaningless term? Pure and applied chemistry, 5, p.793-807, 2002.

GIROTTO, E. **Cobre e zinco no solo sob uso intensive de dejeto líquido de suínos**. Universidade Federal de Santa Maria, Centro de Ciências Rurais, p.01-121, 2007.

GIROTTO, E.; CERETTA, C.A.; ROSSATO, L.V.; FARIAS, J.G.; TIECHER, T.L.; DE CONTI, L.; SCHMATZ, R.; BRUNETTO, G.; SCHETINGER, M.R.C.; NICOLOSO, F.T. Triggered antioxidant defense mechanism in maize grown in soil with accumulation of Cu and Zn due to intensive application of pig slurry. **Ecotoxicology and Environmental Safety**. 93, p.145-155, 2013.

GRAHAM, S.A.; GRAHAM, A. Ovary, fruit, and seed morphology of the Lythraceae. **International Journal of Plant Sciences**, 175, p.202-240, 2014.

GRATÃO, P.L.; POLLE, A.; LEA, P.J.; AZEVEDO, R.A. Making the life of heavy metal-stressed plants a little easier. **Functional plant biology**, 32, p.481-494, 2005.

GUIMARÃES, P.R.; AMBROSINI, V.G.; MIOTTO, A.; CERETTA, C.A.; SIMÃO, D.G.; BRUNETTO, G. Black oat (*Avena strigosa* Schreb.) growth and root anatomical changes in sandy soil with different copper and phosphorus concentrations. **Water Air Soil Pollution**. 227, n.192, 2016.

HAMMERSCHMITT, R.K.; TIECHER, T.L.; FACCO, D.B.; SILVA, L.O.; SCHWALBERT, R.; DRESCHER, G. L.; TRENTIN, E.; SOMAVILLA, L.M.; KULMANN, M.S.S.; SILVA, I.C.B.; TAROUCO, C.P.; NICOLOSO, F.T.; TIECHER, T.; MAYER, N.A; KRUG, A.V.; BRUNETTO, G. Copper and zinc distribution and toxicity in ‘Jade’/‘Genovesa’ young peach tree. **Scientia Horticulturae**, 259, n.108763, 2020.

HOSSAIN, M.A.; KAMIYA, T.; BURRITT, D.; TRAN, L.S.P.; FUJIWARA, T. (EDS.). **Plant macronutrient use efficiency: molecular and genomic perspectives in crop plants.** Academic Press, Elsevier Inc, 2018.

KLIDER, L. M. MACHADO, C.D.; ALMEIDA, V.P.; TIRLONI, C.A.S.; MARQUES, A.A.M.; PALOZI, R.A.C.; LORENÇONE, B.R.; ROMÃO, P.V.M.; GUARNIER, L.P.; CASSERIMO, N.S.; SILVA, D.B.; CAVALCANTI, T.B.; RAMAN, V.; KHAN, I.A.; JUNIOR, A.G.; BUDEL, J.M. Cuphea calophylla var. mesostemon (Koehne) SA Graham: A Whole-Ethnopharmacological Investigation. **Journal of Medicinal Food**, 24, p.394-410, 2020.

KOUHI, S.M.M.; LAHOUTI, M.; GANJEALI, A.; ENTEZARI, M.H. Anatomical and ultrastructural responses of *Brassica napus* after long-term exposure to excess zinc. **Turkish Journal of Biology**, 40, p.652-660, 2016.

LORENZI, H.; MATOS, F.J.A. **Plantas medicinais no Brasil: nativas e exóticas cultivadas**. Nova Odessa: Instituto Plantarum, p.512, 2002.

LUSA, M.G.; BIASI, L.A. Estaquia de *Cuphea calophylla* subsp. *mesostemon* (Koehne) Lourteig (Lythraceae). **Revista Brasileira de Plantas Medicinais,** 13, p.52-57, 2011.

MANTOVI, P.; BONAZZI, G.; MAESTRI, E.; MARMIROLI, N. Accumulation of copper and zinc from liquid manure in agricultural soils and crop plants. **Plant and Soil**, 250, p.249-257, 2003.

MARSOLA, T.; MIYAZAWA, M.; PAVAN, M.A. Acumulação de cobre e zinco em tecidos do feijoeiro em relação com o extraído do solo. **Revista Brasileira de Engenharia Agrícola e Ambiental**, 9, p.92-98, 2005.

MATIAS, J.L.; CERETTA, C.A.; NESI, C.N.; GIROTTO, E.; TRENTIN, E.E.; LOURENZI, C.R.; VIEIRA, R.C. Cupper, zinc and manganese in soils of two watersheds in Santa Catarina with intensive use of pig slurry. **Revista Brasileira de Ciências do Solo**, 34, p.1445-1454, 2010.

MCBRIDE, M.B. **Environmental chemistry of soil.** New York: Oxford University Press, p.406, 1994.

METCALFE, C.R.; CHALK, L. **Anatomy of the dicotyledons: leaves, stem and wood in relation to taxonomy with notes one economics uses**. Oxford: Clarendon Press, 1950.

NAGAJYOTI, P.C.; LEE, K.D.; SREEKANTH, T.V.M. Heavy metals, occurrence and toxicity for plants: a review. **Environmental Chemistry Letters**, 8, p.199-261, 2010.

OLIVEIRA, E.A.B. **Avaliação de método alternativo para extração e fracionamento de substâncias húmicas em fertilizantes orgânicos**. Instituto Agronômico de Campinas, 53, p.01-05, 2011.

PARRY, A.D.; TILLER, A.S.; EDWARDS, R. The effects of heavy metals and root immersion on isoflavonoid metabolism in Alfalfa (*Medicago sativa* L.). **Plant Physiology**, 106, p.195-202, 1994.

PENSO, S.; BAUER, M.O.; CHICHORRO, J.F.; GONDIM, C.A.; VASCONCELOS, L.V. Caracterização estacional de uma pastagem natural do cerrado Mato-Grossense submetida ao pastejo. **Ciência Animal Brasileira**, 10, p.124-134, 2009.

PHIPPEN, W.B. **Oil Crops**. New York: Springer Verlag**,** 4, p.544, 2009.

RAMÍREZ-ATEHORTÚA, A.M.; MORALES-AGUDELO, L.; OSORIO, E.; LARA-GUZMÁN, O.J. The traditional medicinal plants *Cuphea calophylla, Tibouchina kingii*, and *Pseudelephantopus spiralis* attenuate inflammatory and oxidative mediators. **Evidence-Based Complementary and Alternative Medicine**, p.01-11, 2018.

REEVES, R.D.; BAKER, A.J.M. **Metal-accumulating plants**. In: Raskin I, Ensley BD (eds) Phytoremediation of toxic metals: using plants to clean up the environment. New York: Wiley, p.193-229, 2000.

SANTOS, M. C., TOSON, N. S., PIMENTEL, M. C., BORDIGNON, S. A., MENDEZ, A. S., & HENRIQUES, A. T. Polyphenols composition from leaves of *Cuphea* spp. and inhibitor potential, in vitro, of angiotensin I-converting enzyme (ACE). **Journal of ethnopharmacology**, 255, p.112781, 2020.

SCHEID, D.L.; SILVA, R.F.D.; SILVA, V.R.D.; ROS, C.O.D.; PINTO, M.A.B.; GABRIEL, M.; CHERUBIN, M.R. Changes in soil chemical and physical properties in pasture fertilised with liquid swine manure. **Scientia Agricola**, 77, e 20190017, p. 01-10, 2019.

SCHWALBERT, R.; SILVA, L.O.; SCHWALBERT, R.A.; TAROUCO, C.P.; FERNANDES, G.S.; MARQUES, A.C.; COSTA, C.C.; HAMMERSCHMITT, R.K.; BRUNETTO, G.; NICOLOSO, F.T. Physiological responses of soybean (*Glycine max* (L.) Merrill) cultivars to copper excess. **Anais da Academia Brasileira de Ciências**, 91, e20190121, p.01-15, 2019.

SOMAVILLA, L.M.; SIMÃO, D.G.; TIECHER, T.L.; HAMMERSCHIMITT, R.K.; OLIVEIRA, J.M.S.; MAYER, N.A.; PAVANELLO, E.P.; TRENTIN, E.; BELLES, S.W.; BRUNETTO, G. Structural changes in roots of peach rootstock cultivars grown in soil with high zinc content. **Science Horticulturae**, 237, p.1-10, 2018.

SRIDHAR, B.B.M.; DIEHL, S.V.; HAN, F.X.; MONTS, D.L.; SU, Y. Anatomical changes due to uptake and accumulation of Zn and Cu in Indian mustard (*Brassica juncea*). **Environmental and Experimental Botany**, 54, p.131-141, 2005.

SRIDHAR, B.B.M.; HAN, F.X.; DIEHL, S.V.; MONTS, D.L.; SU, Y. Effects of Zn e Cu accumulation on structural and physiological characteristics of barley plants. **Brazilian Plant Physiology**, 19, p.15-22, 2007.

STADTMAN, E.R.; OLIVER, C.N. Metal-catalyzed oxidation of proteins. Physiological consequences. **Journal of Biological Chemistry**, 266, p.2005–2008, 1991.

TAIZ, L.; ZEIGER, E.; MØLLER, I.M.; MURPHY, A. **Fisiologia e desenvolvimento vegetal**. Artmed Editora, 2017.

THOMPSON, A.E. *Cuphea* - a potential new crop. **Hort Science**, p.352-354, 1984.

VANGRONSVELD, J.; COLPAERT, J.V.; VAN TICHELEN, K.K. Reclamation of a bare industrial area contaminated by non-ferrous metals: physicochemical and biological evaluation of the durability of soil treatment and revegetation. **Environmental pollution**, 94, p.131-140, 1997.

Capítulo 1:

Expanding knowledge and clarifying aspects on the secretory system in aerial vegetative organs of *Cuphea calophylla* Cham. & Schltdl., Lythraceae

Abstract

Cuphea calophylla Cham. & Schltdl. is a Lythraceae subshrub that occurs in different environmental conditions. Their aerial portions have medicinal properties and are used for soap production. We assessed the structure, ultrastructure, and histochemistry of the secretory cells and tissues in *C. calophylla* leaves and stems to further understand its secretory system. Hydathodes with epithem, tracheary elements, and water pores occurred at the leaf border and are reported here for the first time in a *Cuphea* species. Glandular emergences occurred in the leaves and stems and were constituted by a wide basis and a narrower apical portion that exudated sticky material. Phenolic compounds, mucilage, and lipids were produced in cells of the glandular emergences which exhibited Golgi bodies, vesicles, smooth endoplasmic reticulum, oil drops, and plastids. The epidermis of the leaf blade was characterized by bi-compartmentalized secretory cells divided by a cellulosic septum in their equatorial region. These cells contained phenolic compounds in the upper compartment and mucilage in the lower compartment. These results expand the knowledge on the secretory system in Lythraceae, and shed light on the sites producing bioactive compounds in *C. calophylla*, highlighting the potential of native plants to produce substances with ecological, medicinal, and economic importance.

Keywords: histology; secretory emergences; secretory epidermal cells; hydathodes; ultrastructure.

Introduction

Lythraceae, a family of angiosperms belonging to Myrtales, is widely distributed in the subtropics and tropics of both the hemispheres. A few species occur in tempered regions (Cavalcanti and Graham 2002; Graham and Granham 2014) and can inhabit aquatic to extremely arid environments as well (Graham 2007). Representatives of Lythraceae comprise several species known for their different morphotypes of glandular and non-glandular appendages on leaves and stems and by the presence of epidermal mucilaginous cells on leaves and seeds (Metcalfe and Chalk 1950; Panigrahi and Panigrahi 1983; Lusa and Bona 2011).

Cuphea P. Browne is the largest genus of Lythraceae and comprises about 250 species distributed from the eastern United States to southern Argentina. Its primary diversity nucleus is the Brazilian mountains and the secondary nucleus is in Central America (Amarasinghe et al. 1991; Cavalcanti 1990; Cavalcanti and Graham 2002; Graham and Graham 2014). Species of this genus range from herbaceous to small shrubs, annuals, and perennials, and several of them have great potential in the chemical, food, and pharmacological industries (Amarasinghe et al. 1991; Das et al. 2018).

In Brazil, some species of *Cuphea* are widely used in folk medicine for the treatment of cardiovascular disease and lowering cholesterol, and the whole plant is used as tea, syrup, or hydroalcoholic extracts that are orally ingested (Lorenzi and Matos 2002). Several studies have demonstrated that the bioactive properties of water and hydroalcoholic extracts of the *Cuphea* species are mainly because of the presence of tannins, flavonoids, sterols, carbohydrates, unsaturated fatty acids, and alkanes (Ribeiro et al. 1988; Schuldt et al. 2004; Elgindi et al. 2011; Das et al. 2018; Ramírez et al. 2018). *Cuphea* species have also been explored as oil sources for soap and detergent manufacturing (Miller et al. 1964; Thompson 1984; Graham and Knapp 1989; Phippen 2009). In addition, their lipophilic content, together with other carbohydrates and antioxidants, make them suitable for use in the food industry as a component of functional food (Graham and Knapp 1989; Kumar et al. 2018).

Cuphea calophylla Cham. & Schltdl. is native to Argentina, Bolivia, Paraguay, and Brazil and is widely distributed in different habitats such as natural fields, dirty fields, humid fields, forest edges, open fields, road edges, and pastures (Cavalcanti and Graham 2002; Lusa and Biasi 2011). In Brazil, this species is popularly known as “sete-sangrias” or “red-ganxumam” and is also used in folk medicine (Cavalcanti and Graham 2002; Lorenzi and Matos 2002). Water and hydroalcoholic extracts from its aerial vegetative shoots have been tested and found to be a powerful diuretic, antioxidant, and anti-inflammatory, which justifies its use in folk medicine and indicates that this plant is a source of substances for the bioprospection of drugs that treat hypertension (Ribeiro et al. 1988; Elgindi et al. 2011; Ramírez et al. 2018; Klider et al. 2020). In addition, the lipids produced in the leaves and stems are a source of raw material for soap production (Thompson 1984; Phippen 2009).

Knowledge of the morphological and anatomical features of the *Cuphea* species, mainly about the structures secreting bioactive compounds, is important for plant management to achieve better industrial performance (Hirsinger and Knowles 1984; Amarasinghe et al. 1991). In addition, this knowledge is taxonomically important for environmental conservation actions by aid on identifying the native flora and recognizing evolutionary traits in the group (Cavalcanti 1990; Graham et al. 1993; Cavalcanti and Graham 2002). Thus, in this paper, we

describe the structure, ultrastructure, and histochemistry of the secretory cells and tissues in the leaves and stems of *C. calophylla*, expanding our understanding of the secretory system in this species.

Material and methods

Plant material

C. calophylla is a small subshrub (maximum 50 cm) with vegetative and reproductive shoots densely covered by a dense indumentum. The stem is erect to decumbent. Its leaves are simple, opposite, petiolate (small petioles, 1 mm in length), and vary in shape from oval, cordiform, to rounded. It blooms throughout the year, with fruiting predominant from August to November (Cavalcanti and Graham 2002).

Vegetative basal branches were collected from adult *C. calophylla* plants (n = 5) from a remnant of the Atlantic Forest in the Botanical Garden of the Institute of Biosciences (22°53'09.7″ S, 48°29'59.8″ W), São Paulo State University, Botucatu city, São Paulo State, Brazil. We obtained samples from the shoot apex, middle portion of the leaf blade from fully expanded leaves located at the third node in the stem, median portion of the petiole at this same node, young stem portions located 1.0 cm below the shoot apex, and a stem under secondary growth located 0.5 cm above the ground.

Vouchers with reproductive material were deposited in the Irina Delanova Gemtchújnicov Herbarium (BOTU), Institute of Biosciences of Botucatu, under registration number 35187. The plant material was identified by Dr. Taciana Barbosa Cavalcanti from the Empresa Brasileira de Pesquisa Agropecuária (EMBRAPA), a specialist of the *Cuphea* genus.

Light microscopy

Stem and leaf samples were fixed in formaldehyde, acetic acid, and alcohol - FAA 50 (Johansen, 1940), dehydrated in an ethanol series, embedded in methacrylate resin (Leica Historesin) and cross-sectioned with a semi-automatic rotating microtome. Sample of the shoot apex were longitudinal-sectioned. The sections (5 μm thick) were stained with toluidine blue pH 4.7 (O'Brien et al. 1964), and permanent slides were mounted with Entellan® (Merck).

Histochemical tests were conducted on fresh materials. Cross sections of leaf blades and young stems were obtained by hand using a razor blade and treated with 1% acid phloroglucinol solution for lignin (Johansen 1940), Sudan IV for total lipids (Johansen 1940), Nadi's reagent for essential oils and resin (David and Carde 1964), 10% solution of ferric chloride for phenolic compounds (Johansen 1940), mercuric bromophenol blue for proteins (Mazia et al. 1953), Wagner's reagent for alkaloids (Furr and Mahlberg 1981), periodic acid/Schiff reagent (PAS)

for non-cellulosic polysaccharides (Taboga and Vilamaior 2013), and 0.02% solution of ruthenium red for polysaccharides and pectin (Jensen 1962). The PAS and ruthenium red tests were also applied to leaf sections embedded in methacrylate resin. The control tests followed the protocols described by the respective authors.

All slides from conventional microscopy and histochemical tests were analysed using a BX 41 microscope (Olympus, Japan), and all relevant results were documented using a coupled C-7070 digital camera (Olympus, Japan).

Stereomicroscope analysis

To evaluate the distribution of leaf and stem glandular appendages, fresh samples were analysed using an M205C stereomicroscope (Leica, Germany) coupled with a DFC425 digital camera (Leica, Germany). Some samples were previously treated with PAS (Taboga and Vilamaior 2013), ruthenium red (Jensen 1962), Sudan IV (Johansen 1940), ferric chloride (Johansen 1940), and Nadi's reagent (David and Carde 1964) to detect the chemical properties of the exudate drops from such appendages.

Scanning electron microscopy (SEM)

Samples from the middle region of the leaves were fixed in 2.5% glutaraldehyde in 0.1 M phosphate buffer (pH 7.3) for 24 h, post-fixed in 1% osmium tetroxide, dehydrated in an ethylic series, dried in a critical point dryer, and coated with gold. The samples were analyzed using a compact JEOL JSM-6010 scanning electron microscope.

Transmission electron microscopy (TEM)

Conventional transmission electron microscopy was conducted on the leaves to investigate the subcellular features of the secretory cells. Leaf blade samples were fixed in 2.5% glutaraldehyde in 0.1 M phosphate buffer (pH 7.3) for 24 h, post-fixed with 1% osmium tetroxide aqueous solution in the same buffer for 1 h, dehydrated in an acetone series, and embedded in Araldite resin. Ultra-thin sections (70 nm) were stained with uranyl acetate (Watson 1958) and lead citrate (Reynolds 1963). The samples were examined using a Tecnai Spirit transmission electron microscope (FEI, USA) at 80 kV. The relevant results were documented using a digital image capture system coupled to an electron microscope.

Results

Hydathodes

Hydathodes were observed at the leaf border (Fig. 1a; 1b). In some cases, they were associated with glandular emergence (Fig. 1a). Hydathodes were covered by the epidermis with ordinary cells (Fig. 1a; 1b). On the adaxial leaf surface, modified stomata with a subjacent chamber constituted the water pores (Fig. 1a; 1b). Subjacent to the epidermis, there was a remnant of chlorophyll tissues of the mesophyll followed by an enlarged portion of the epithem tissue (Fig. 1a; 1b). The epithem tissues were composed of compactly arranged parenchyma cells with thin walls and were devoid of chloroplasts (Fig. 1a; 1b). Terminal tracheary elements of the veins were immersed in the epithem (Fig. 1a; 1b). Ultrastructurally, epithem cells had thin walls, plasmalemma with irregular contours, abundant cytoplasm, voluminous nuclei with irregular shapes and evident nucleoli, and vacuoles (Fig. 1c; 1d). The cytoplasm presented numerous mitochondria, plastids with starch grains and plastoglobuli, smooth and rough endoplasmic reticulum, polysomes, multivesicular bodies, free vesicles, and oil drops. Vacuoles with membranous inclusions were commonly observed in epithem cells (Fig. 1c; 1d). Electron-dense bodies, membranous inclusions, and myelin figures were observed inside the vacuoles of some cells.

Glandular emergences

Glandular emergences occurred on the entire surface of the young stem (Fig. 2a-c) and petioles. In the leaf blade, they were distributed throughout the abaxial and adaxial surfaces, interspersed with non-glandular trichomes, and were more abundant on the veins (Fig. 2d-e); a glandular emergence was also present on the leaf border (Fig 2f).

Glandular emergences are multicellular and multiseriate, with a wide basis and a narrower tapering apical portion (Fig. 2a; 2c-d). Some of these were naturally reddish (Fig 2a, 2c). Drops of sticky, transparent, and abundant exudates were observed on their apex (Fig 2a).

Along the shoot apex, glandular emergences at different developmental stages were observed (Fig. 3a). First, a single protodermal was divided anticlinally (Fig. 3b). One of the daughter cells had a denser cytoplasm and was protruding (Fig. 3c). Periclinal divisions on this cell originated from a four-celled structure (Fig. 3d). Then, these protodermal cells divided successively in several planes, giving rise to a multicellular protuberance (Fig. 3e-f). Subsequently, a number of periclinal and anticlinal divisions occurred in the developing protuberance, and at this stage, cells from the ground meristem subjacent to the developing protuberance started to divide and elongate tangentially toward the expanded basis (Fig. 3g). These elongated cells were integrated on the basis of protuberance (Fig. 3h). Additional cell divisions and growth occurred, giving rise to an elongated appendage (Fig. 3i).

The fully differentiated glandular appendage exhibited an enlarged basal portion and a narrow tapering upper portion (Fig. 2a; 2c-d; 3i). The whole appendage was covered by a layer of tangentially elongated epidermal cells with thick pectin-cellulosic walls and a developed vacuoma. The basal enlarged portion was filled with round to oval ground cells with relatively thick non-lignified wall cells, and a group of polyhedral and smaller cells with thinner pectin-cellulosic walls occurred centrally in the basal portion. The narrow and tapering superior portion was filled exclusively by elongated ground cells with thick walls (Fig. 3i). The cells present in the most distal region of the tapering portion exhibited lignified walls (Fig. 3i, insert). The apex of the secretory emergence culminated in two cells that left a small opening between them, an apical pore (Fig. 3i, insert).

Histochemical tests revealed the presence of phenolic compounds, mucilage, and total lipids in the exudate drops on the apex of the glandular emergences (Fig. 3j-l) and in the cells along their bodies (Fig. 3m-o).

Ultrastructurally, epidermal tangentially-elongated cells had thick cellulosic walls with lamellar features (Fig. 4a). The pit fields connect the epidermal cells between themselves (Fig. 4a). The cytoplasm was reduced and confined to the cell periphery due to the presence of a voluminous central vacuole (Fig. 4a; 4b). Plastids with structured thylakoids, mitochondria with evident cristae, smooth endoplasmic reticulum, Golgi bodies, and numerous vesicles were found in the cytoplasm (Fig. 4b). Oil drops were observed inside the plastids (Fig. 4c). The voluminous vacuole contained oil drops, flocculent electron-dense material, and dark bodies. The oil drops were surrounded by a flocculent electron-dense material (Fig. 4a; 4b; 4d; 4e).

The cells that filled the enlarged basal portion of the secretory emergences had walls with lamellar features and loosely arranged cellulose microfibrils (Fig. 4d; 4e; 4f). Lipid impregnation were immersed in the cell wall matrix and in the corners of the cells (Fig. 4d; e; f). Numerous pit-fields with plasmodesmata connect the cells with each other (Fig. 4d; e). The cytoplasm was reduced and contained mitochondria, smooth and rough endoplasmic reticulum, polysomes, plastids with starch grains, and plastoglobuli (Fig. 4g; 4h). A few of the plastids contained oil drops and were devoid of grana (Fig. 4g; 4h). Vesicles were also observed in the cytoplasm, and images suggested fusion of vesicles to the plasmalemma (Fig. 4e; 4h). The vacuole was large and contained oil drops and flocculent electron-dense inclusions (Fig. 4d-h).

Secretory epidermal cells

Voluminous secretory epidermal cells were observed on the adaxial surface of the leaf blade (Fig. 5a). These cells originated from the anticlinal divisions on the protodermis (Fig. 5b). After acquiring an isodiametric shape, the nucleus migrated to the basal pole of the cell (Fig.

5b). A thin septum was visible in the equatorial region of the differentiating secretory cells, creating two compartments (Fig. 5c; 5d; 5e). The vacuoles were developed and the cytoplasm was reduced (Fig. 5e). At this stage, the developing septum in the equatorial region of the cell was constituted by a dense portion of cytoplasm, giving the bi-compartmentalized aspect to the differentiating cell (Fig. 5e). Two large vacuoles, one in each cell pole, characterized the cells at this developmental stage (Fig. 5e). These vacuoles contained fibrillar and membranous inclusions (Fig. 5e). Both the portions of cytoplasm, in the equatorial and in the bottom of the developing cells, were electron-dense, and were rich in rough and smooth endoplasmic reticulum, ribosomes, Golgi bodies, vesicles, and mitochondria (Fig. 5f-h). Plastids with poorly developed inner membrane systems were also observed in these cells (Fig. 5f). The nucleus with an evident nucleolus was confined to the basal pole of the developing cell (Fig. 5f). In this region, large vesicles were observed merging with the tonoplast (Fig. 5f). Golgi bodies and small vesicles were particularly abundant in the equatorial portion of the cytoplasm (Fig. 5g; 5h), and the vesicles fused to form a presumptive cell plate. In the latter developmental stage, wall material with fibrillar aspect was deposited at the equatorial region of the developing cell on both sides of the forming cell plate (Fig. 5i). This nascent cross-wall became continuous with the anticlinal cell walls, giving rise to the cell wall septum.

The fully developed epidermal secretory cells were voluminous and had thick outer periclinal walls with a cuticle containing villous ornaments (Fig. 6a; 6b). A wall septum divided the cells into two true compartments (Fig. 6b). The upper compartment was smaller and contained phenolic compounds (Fig. 6c). This cell portion maintained a narrow portion of electron-dense cytoplasm located above the septum and contained mitochondria, Golgi bodies, and vesicles (Fig. 6d). The lower compartment was larger and had a large vacuole filled with a homogenous substance, which was histochemically identified as mucilage (Fig. 6b; 6e; 6f). The cytoplasm adjacent to the vacuole contained voluminous vesicles filled with material that had an aspect similar to that filling the vacuole (Fig. 6g).

Apparently non-secreting cells occurred on the side of cells with mucilage in the leaf epidermis of *C. calophylla* (Fig. 5a).

Discussion

In this paper, we bring novelties on the structural features of the secretory system in Lythraceae, particularly in *C. calophylla*, clarifying important aspects of the histology, ultrastructure, and development of secretory cells and tissues.

To the best of our knowledge, this is the first report of the occurrence of hydathodes in *Cuphea* species. The presence of hydathodes in the Lythraceae family has been described only

in the *Lafoensia* species (Graham et al. 1993). Functionally, hydathodes are considered to be sites of guttation, which is the discharge of water to the leaf surface (Fahn 1979). Salts, sugars, and other substances can be released along with water from the hydathodes (Evert 2006). Studies suggest that hydathodes also act in water absorption (Rundel 1982; Martin and von Willert 2000) and control the water balance in plants (Pedersen 1993; Cerutti et al. 2019), in addition to acting in the reacquisition of solutes from the transpiration stream (Wilson et al. 1991). However, this structure can also be a pathway for microorganisms, being considered as a site of several plant infections (Carlton et al. 1998; Cerutti et al. 2019).

Hydathodes have been reported in plants of various life forms and in various ecological habitats, from submerged aquatic plants to plants growing in relatively dry conditions (Martin and von Willert 2000). *C. calophylla* is distributed in a wide range of environments, such as natural fields, humid field, forest edges, and pastures (Cavalcanti and Graham 2002; Lusa and Biasi 2011). Considering the several roles of hydathodes in the release of water excess in environments with high humidity (Pedersen 1993; Pedersen et al. 1997), the absorption of dew water deposited on the leaf surface under dry conditions (Rundel 1982; Martin and von Willert 2000), and reabsorption of solutes from transpiration (Wilson et al. 1991), the presence of hydathodes on *C. calophylla* is important for the colonization of environments with different characteristics.

In *C. calophylla*, hydathodes occurred at the leaf border, and their inner structure followed the general characteristics of hydathodes: tracheary elements are inserted into a specific parenchyma tissue in the mesophyll called epithem and water pores were observed in the epidermis (Fahn 1979; Cerutti et al. 2019). In *C. calophylla* hydathodes, the water pores are constituted by non-functional stomata. In the epithem, the presence of cells with sinuous walls and abundant cytoplasm with large nuclei, polysomes, well-developed endoplasmic reticulum, and numerous mitochondria and vesicles ensures a high metabolic activity of these cells in order to maintain the flow of water and aqueous solutions (Pedersen et al. 1997; Cerutti et al. 2019). In addition, the presence of plastids with starch grains in the epithem cells may help the metabolic activity of these cells by acting as an energy source (Fahn 1979). In *C. calophylla* hydathodes, we were not able to detect the continuation of the bundle sheath toward the epidermis, as reported for other species (Evert 2006). Such sheaths are responsible for connecting the plant vasculature to the environment through the hydathode pores, mediating and boosting the guttation (Cerutti et al. 2019). The lack of this sheath has already been observed in Rosaceae (Lersten and Curtis 1982) and in several monocots such as wheat and rice plants (Maeda and Maeda 1988; Evert 2006).

Among the Lythraceae representatives, *Cuphea* species contain all the aerial organs bearing the indumentum with the greatest morphological diversity (Lusa and Bona 2011). The morphology of these appendages is taxonomically important (Amarasinghe et al. 1991; Beentje 2010) and is useful for differentiating between *Cuphea* species with similar morphological features (Amarasinghe et al. 1991). In the leaves and stems of *C. calophylla*, we detected a morphotype of secretory appendages with similar morphologies to those described previously for aerial organs of Lythraceae, including *Cuphea* species. These studies have described such secretory appendages as secretory trichomes (Solereder 1908; Metcalf and Chalk 1950; Amarasinghe et al. 1991; Cavalcanti and Graham 2002; Lusa and Biasi 2011; Lusa and Bona 2011; Klider et al. 2020). However, our ontogenetic observations showed that the glandular appendages in the leaves and stems of *C. calophylla* are glandular emergences, as they have a mixed origin, arising from both protodermal and sub-protodermal tissues in the leaf primordium and shoot apex (Evert 2006).

The secretory ability of the emergence of *C. calophylla* leaves and stems is evidenced by the presence of sticky and transparent exudates on their apex. These physical properties of the exudate are a hurdle to tiny herbivores such as aphides or mealybugs (Karban and Baldwin 2007). As *Cuphea* species are commonly found interspersed in the cultivation of economically important plants, their glands are agronomically important (Amarasinghe et al. 1991). The viscous exudate released from the glandular appendages can clog the machinery and hinder seed harvest (Hirsingera and Knowles 1984). Phenolic compounds, mucilage, and total lipids were histochemically detected in the glandular emergence of *C. calophylla*. Phenolic compounds are efficient against UVB radiation, and are also important preventing herbivory (Harbone 1993; Liakoura et al. 1997; Bredenkamp and Van Wyk 1999; Silva et al. 2016). Mucilage is important for water maintenance and detoxification of plant organisms as it captures toxic elements (Bredenkamp and Van Wyk 1999; Windsor et al. 2000; Kumar et al. 2018; Galloway et al. 2020). The action of mucilage in the maintenance of the water potential in the leaves (Ascensão and Pais, 1998; Silva et al. 2016; Seixas et al. 2021) is important for this species if it is considered that these plants can occur in a wide range of environments, including dry areas. Lipophilic contents may be the chemical components that provide the sticky propriety of the exudate, in addition to playing an important role in protecting against herbivores and pathogens (Fahn 1979; Tozin et al. 2017). Despite previous studies describing terpenes in the exudate of *Cuphea* glandular appendages (Amarasinghe et al. 1991; Lusa and Bona 2011), such substances were not histochemically detected in our study.

The cellular ultrastructure of the basal enlarged portion of the secretory emergence in *C. calophylla* corroborates the histochemical results and probe the production of secretions with

mixed composition. Golgi bodies and numerous vesicles indicate the intense synthesis of hydrophilic substances such as non-cellulosic polysaccharides (Werker 2000; Silva et al. 2016; Tozin et al. 2016). The presence of starch grains in plastids indicates that these organelles can be the source of carbohydrates for the production of the hydrophilic fraction of the secretion (Paiva and Machado 2008). Images suggesting the fusion of vesicles to the plasmalemma indicate the granulocrine processes of secretions from the producing cells (Evert 2006). The abundant plasmodesmata connecting the cells suggests that hydrophilic substances can be transported via the symplast (Silva et al. 2016). On the other hand, smooth endoplasmic reticulum, plastids containing osmiophilic inclusions, and oil drops in the cytoplasm demonstrate the production of lipophilic substances (Evert et al. 2006; Tozin and Rodrigues 2016). Oil droplets can cross cell boundaries and accumulate in intercellular spaces (Paiva 2016; Tozin and Rodrigues 2016).

These oil bodies are probably released by ecrine processes and accumulate inside the cell wall matrix and in the corner among the cells in the secretory emergences. Our results indicate that the basal enlarged portion of secretory emergence is responsible for secretory production, as already mentioned by Amarasinghe et al. (1991) for appendages with similar morphology. We were also able to detect that the upper portion of the glandular emergences constituted of elongated cells are involved in transporting secretions toward the emergence apex. In this route, the hydrophilic substances appear to move by symplast while the lipophilic substances move preferentially in an apoplastic manner. A similar mechanism was observed in secretory emergences in other plant groups (Silva et al. 2020). In *C. calophylla*, the apex of secretory emergence is characterized by the presence of an opening where two apical cells meet. Since the secretion reaches the emergence apex, it is released outside of the apical pore.

The epidermis of the adaxial leaf surface of *C. calophylla* was characterized by the presence of bi-compartmentalised secretory cells containing phenolic compounds in the upper compartment and mucilage in the lower compartment. Epidermal cells containing mucilage have been described for other Lythraceae species (Solereder 1908; Metcalf and Chalk 1950; Panigrahi and Panigrahi 1983; Meira 2000; Little et al. 2004; Lusa and Bona 2011; Kshirsagar 2019), including *Cuphea calophylla* (Klider et al. 2020), and have been considered as an important diagnostic feature of the family (Keating 1984; Little et al. 2004).

The compartmentalisation of the secretory epidermal cells is described in Lythraceae as well as in species belonging to other families (Bredenkamp and Van Wyk 1999; Seixas et al. 2021) as a result of the existence of a wall-like septum (Gregory and Bass 1989). Our transmission electron microscopy analyses revealed that this septum is actually constituted by a true cellulosic cell wall, and the alignment and fusion of small vesicles in the equatorial region

of the differentiating secretory epidermal cells forming a cell plate is particularly interesting. The process of septum establishment in these cells is similar to phragmoplast-mediated cytokinesis (Chapman et al. 2001). However, the developmental processes of the secretory epidermal cells in *C. calophylla* do not involve nuclear division, discarding the occurrence of biseriate epidermis. This is important as this type of epidermis has often been incorrectly described as uni-, bi-, or multi-seriate in different plant species (Bredenkamp and Van Wyk 1999).

The subcellular sites of mucilage deposition detected here differ from those considered by Klider et al. (2020), who described the epidermal cells in the leaves of *C. calophylla* as containing mucilage on the periclinal external wall. Epidermal cells with mucilage have been reported in several plant groups (Solereder 1908; Metcalfe and Chalk 1950; Gregory and Bass 1989; Matthews and Endress 2006) as cells with a mucilaginous inner cell wall and distinct cytoplasm or entirely mucilaginous cells with an indistinct cytoplasm (Metcalfe and Chalk 1950; Napp-Zinn 1973). In the majority of cases, mucilage is deposited between the cell wall and the plasmalemma, and in exceptional cases, mucilage is considered to accumulate in vacuoles (Gregory and Bass 1991 and references therein). However, the structural interpretation of these cells in the literature contains several inaccuracies and erroneous structural interpretations (Bredenkamp and Van Wyk 1999), probably due to the absence of a more detailed analysis. In *C. calophylla*, we demonstrated that mucilage accumulates inside a large vacuole located in the lower portion of the leaf epidermal cells. The large vacuole grows because of the fusion of abundant and voluminous vesicles that sprout from the Golgi apparatus. As the vacuole grows and the volume of mucilage increases by this granulocrine process of secretion deposition, the volume of the cytoplasm decreases and becomes visible as a dark line (Mauseth, 1980). The production of mucilage by the Golgi bodies (Young et al. 2008) and the granulocrine process of carbohydrate secretion is commonly reported for secretory cells in different plant groups (Paiva 2009; Machado et al. 2014), including bryophytes (Ligrone 1986).

In contrast to other plants (Fahn 1988), we were not able to detect microscopic evidence of the exudation of mucilage outward the protoplast in *C. calophylla*, as the mucilage remains inside the vacuole. Nevertheless, non-secreting epidermal cells occurred on the side of cells with mucilage in the leaf epidermis of *C. calophylla*, which can be correlated with phenological aspects and seasonal changes on the mucilage accumulation along the year (Schmid 1948; Esdom and Schanze 1954, *apud* Gregory and Bass 1989) and with the plant age (Kuntze 1891, *apud* Gregory and Bass, 1989) as the carbohydrate storage in mucilage can be resorbed at different times of the year (Gregory and Bass 1989). As previously mentioned, the epidermal cells rich in mucilage in *C. calophylla* probably serve as a regulator of hydration within the leaf,

accumulating water and avoiding the loss of humidity to the environment (Ascensão and Pais 1998; Werker 2000; Silva et al. 2016).

Phenolic compounds were deposited in the vacuoles of the upper compartment of the leaf epidermal cells of *C. calophylla*. The association with phenolic compounds is reported here for the first time in *Cuphea* species. This association, as seen in our results, is frequently described for mucilaginous secretory cells (Gregory and Bass 1989; Bredenkamp and Van Wyk 1999; Kumar et al. 2018; Seixas et al. 2021), probably because of the tannin potential to absorb mucilage (Radlkofer 1875, apud Gregory and Bass, 1989). Phenolic compounds play an important role as natural antioxidants, capturing excess reactive oxygen species and deleterious ions (Bredenkamp and Van Wyk 1999; Kumar et al. 2018), and can also protect plants against UVB radiation (Windsor et al. 2000).

In general, our histochemical tests detected total lipids, mucilage, and phenolic compounds in the secretory system of *C. calophylla*. In addition to the ecological roles played by the secretory system, the substances produced by *C. calophylla* have medicinal and economical properties (Graham and Knapp 1989; Kumar et al. 2018) with high potential for use in the bioprospection of drugs (Ramírez et al. 2018) and in the food (Graham and Knapp 1989) and soap industries (Phippen 2009). Therefore, leaves and young stems are relevant as sources of bioactive substances.

These results expand and improve our knowledge of the secretory system in Lythraceae, particularly in *C. calophylla*, and can present taxonomic importance of the plant group. Our data shed light on the sites producing bioactive compounds in the vegetative aerial organs of this species and highlight the potential of native plants to produce substances with ecological, medicinal, and economic importance.

References

Amarasinghe V, Graham SA, Graham A (1991) Trichome morphology in the genus *Cuphea* (Lythraceae). Bot gaz 152: 77-90

Ascensão L, Pais MS (1998) The leaf capitate trichomes of *Leonotis leonurus*: histochemistry, ultrastructure and secretion. Ann Bot 81: 263–271

Beentje HJ (2010) The Kew plant glossary: an illustrated dictionary of plant terms. Royal Botanic Gardens, Kew

Bredenkamp CL, Van Wyk AE (1999) Structure of mucilaginous epidermal cell walls in *Passerina* (Thymelaeaceae). Bot J Linn Soc 129: 223-238

Carlton WM, Braun EJ, Gleason ML (1998) Ingress of *Clavibacter michiganensis* subsp. michiganensis into tomato leaves through hydathodes. Phytopathology 88: 525-529

Cavalcanti TB (1990) Flora da Serra do Cipó, Minas Gerais: Lythraceae. Boletim de Botânica da Universidade de São Paulo 12: 67-93

Cavalcanti TB, Graham S (2002) Lythraceae. In: Flora fanerogâmica do Estado de São Paulo. Instituto de Botânica, São Paulo

Cerutti A, Jauneau A, Laufs P, Leonhardt N, Schattat MH, Berthomé R, Routaboul JM, Noël LD (2019) Mangroves in the leaves: anatomy, physiology, and immunity of epithemal hydathodes. Annu Rev Phytopathol 57: 91-116

Chapman RL, Borkhsenious O, Brown RC, Henk MC, Waters D A (2001) Phragmoplast-mediated cytokinesis in Trentepohlia: results of TEM and immunofluorescence cytochemistry. Int J Syst Evol Microbiol 51: 759-765

Das A, Chaudary SK, Bhat HR, Shakya A (2018) *Cuphea carthagenensis*: a review of its ethnobotany, pharmacology and phytochemistry. Bull Arunachal Forest Res 33: 01-14

David R, Carde JP (1964) Coloration differentielledês inclusions lipidique et terpeniques des pseudophylles du pine maritime au moyen du react if Nadi. C R Biol 257: 1338-1340

Elgindi MR, Ayoub N, Milad R, Hassan, R (2011) A comprehensive review of *Cuphea* (Lythraceae). Res J Pharm Biol Chem Sci 2: 847-855

Evert RF (2006) Esau's plant anatomy. Meristems, cells and tissues of the plant body. Their structure, function and development, 3rdedn. Wiley, New Jersey

Fahn A (1979) Secretory tissues in plants. Academic, London

Fahn A (1988) Secretory tissues in vascular plants. New Phytol 108: 229-257

Furr M, Mahlberg PG (1981) Histochemical analyses of laticifers and glandular trichomes in *Cannabis sativa*. J Nat Prod 44: 153–159

Galloway AF, Knox P, Krause K (2020) Sticky mucilages and exudates of plants: putative microenvironmental design elements with biotechnological value. New Phytol 225: 1461-1469

Graham SA (2007) Lythraceae. In: The families and genera of vascular plants: Flowering Plants· Eudicots. Springer, Berlin

Graham SA, Knapp SJ (1989) *Cuphea:* A new plant source of medium-chain fatty acids. Crit Rev Food Sci Nutr 28: 139-173

Graham SA, Crisci JV, Hoch PC (1993) Cladistic analysis of the Lythraceae sensu lato based on morphological characters. Bot J Linn Soc 113: 1-33

Graham SA, Graham A (2014) Ovary, fruit, and seed morphology of the Lythraceae. Int J Plant Sci 175: 202-240

Gregory M, Baas P (1989) A survey of mucilage cells in vegetative organs of the Dicotyledons. Israel J Bot 38: 125-174

Harbone, JB (1993) Introduction to ecological biochemistry. Academic press University of reading, United Kingdom

Hirsinger F, Knowles PF (1984) Morphological and agronomic description of selected *Cuphea* germplasm. Econ Bot 38: 439-451

Jensen WA (1962) Botanical histochemistry: principles and practice. Freeman, San Francisco

Johansen DA (1940) Plant microtechnique. McGraw–Hill, New York

Karban R, Baldwin IT (2007) Induced responses to herbivory. University of Chicago Press, Chicago

Keating R (1984) Leaf histology and its contribution to relationships in the Myrtales. Ann Missouri Bot Gard 71: 801-823

Klider LM, Machado CD, Almeida VP, Tirloni CAS, Marques AAM, Palozi RAC, Lorençone BR, Romão PVM, Guarnier LP, Casserimo NS, Silva DB, Cavalcanti TB, Raman V, Khan IA, Junior AG, Budel JM (2020) *Cuphea calophylla* var. *mesostemon* (Koehne) SA Graham: A Whole-Ethnopharmacological Investigation. J Med Food 24: 394-410

Kshirsagar AA (2019) Morphological and anatomical studies of *Cuphea ignea* L. (Family Lythraceae). Bioinfolet 16: 123-124

Kumar SS, Girish Patil BG, Giridhar P (2018) Mucilaginous polysaccharides from vegetative parts of *Bixa orellana* L.: Their characterization and antioxidant potential. J Food Biochem 43: e12747

Lersten NR, Curtis JD (1982) Hydathodes in *Physocarpus* (Rosaceae: Spiraeoideae). Can J Bot 60: 850-855

Liakoura V, Stefanou M, Manetas Y, Cholevas C, Karabourniotis G (1997) Trichome density and its UV-B protective potential are affected by shading and leaf position on the canopy. Environ Exp Bot 38: 223-229

Ligrone R (1986) Structure, development and cytochemistry of mucilage-secreting hairs in the moss *Timmiella barbuloides* (Brid.) Moenk. Ann Bot 58: 859-868

Little AA, Stockey RA, Keating RC (2004) *Duabanga*-like leaves from the Middle Eocene Princeton chert and comparative leaf histology of Lythraceae sensu lato. Am J Bot 91: 1126–1139

Lorenzi H, Matos FJA (2002) Plantas medicinais no Brasil: nativas e exóticas cultivadas. Instituto Plantarum, Nova Odessa

Lusa MG, Biasi LA (2011) Estaquia de *Cuphea calophylla* subsp. *mesostemon* (Koehne) Lourteig (Lythraceae). Rev Bras Pl Med 13: 52-57

Lusa MG, Bona C (2011) Caracterização morfoanatômica e histoquímica de *Cuphea carthagenensis* (Jacq.) J.F. Macbr. (Lythraceae). Acta bot bras 25: 517-527

Machado SR, Teixeira SDP, Rodrigues TM (2014) Bacterial leaf glands in *Styrax camporum* (Styracaceae): first report for the family. Botany 92: 403-411

Maeda E, Maeda K (1988) Ultrastructural studies of leaf hydathodes: II. Rice (*Oryza sativa*) leaf tips. Jpn J Crop Sci 57: 733-742

Martin CE, Von Willert DJ (2000) Leaf epidermal hydathodes and the ecophysiological consequences of foliar water uptake in species of *Crassula* from the Namib Desert in southern Africa Plant Biol 2: 229-242

Matthews ML, Endress PK (2006) Floral structure and systematics in four orders of rosids, including a broad survey of floral mucilage cells. Plant Syst Evol 260: 199-221

Mauseth JD (1980) A stereological morphometric study of the ultrastructure of mucilage cells in *Opuntia polyacantha* (Cactaceae). Bot Gaz 141: 374–378

Mazia D, Brewer PA, Alfert M (1953) The cytochemical staining and measurement of protein with mercuric bromphenol blue. Biol Bull 104: 57–67

Meira RMSA (2000) Anatomia foliar e estudos morfologicos em especies de *Lafoensia* Vand. (Lythraceae) nativas do Brasil. Universidade Estadual de Campinas, São Paulo

Metcalfe CR, Chalk L (1950) Anatomy of the dicotyledons, systematic anatomy of the leaf and stem. Clarendon Press, Oxford

Miller RW, Earle FR, Wolff IA, Jones Q (1964). Search for new industrial oils, IX. *Cuphea*, a versatile source of fatty acids. J Am Oil Chem Soc 41: 279-280

Napp-Zinn K (1973) Anatomie des Blattes. II. Angiospermen A, 1. Handbuch der Pflanzenanatomie, Spezieller Teil VIII 2A. Borntraeger, Berlin

O'Brien TP, Feder N, McCully ME (1964) Polychromatic staining of plant cell walls by toluidine blue O. Protoplasma 59: 368–373

Paiva EAS (2009) Occurrence, structure and functional aspects of the colleters of *Copaifera langsdorffii* Desf. (Fabaceae, Caesalpinioideae). C R Biol 332: 1078-1084

Paiva EAS (2016) How do secretory products cross the plant cell wall to be released? A new hypothesis involving cyclic mechanical actions of the protoplast. Ann Bot 117: 533–540

Paiva EAS, Machado SR (2008) The floral nectary of Hymenaea stigonocarpa (Fabaceae, Caesalpinioideae): Structural aspects during floral development. Ann Bot 101: 125-133

Panigrahi SG, Panigrahi G (1983) Studies on evolutionary trends and adaptive radiation in four genera of Lythraceae. Evol Bot Biost: 211-219

Pedersen O (1993) Long-distance water transport in aquatic plants. Plant Physiol 103: 1369-1375

Pedersen O, Jørgensen LB, Sand-Jensen K (1997) Through-flow of water in leaves of a submerged plant is influenced by the apical opening. Planta 202: 43-50

Phippen WB (2009) Oil Crops. Springer Verlag, New York

Ramírez-Atehortúa AM, Morales-Agudelo L, Osorio E, Lara-Guzmán OJ (2018) The traditional medicinal plants *Cuphea calophylla*, *Tibouchina kingii*, and *Pseudelephantopus*

spiralis attenuate inflammatory and oxidative mediators. Evid Based Complement Alternat Med: 1-11

Reynolds ES (1963) The use of lead citrate at high pH as an electron-opaque stain in electron microscopy. J Cell Biol 17: 208–212

Ribeiro RDA, Barros F, Melo MMRF, Muniz C, Chieia S, Wanderley MG, Gomes C, Trolin G (1988) Acute diuretic effects in conscious rats produced by some medicinal plants used in the state of São Paulo, Brasil. J Ethnopharmacol 24: 19-29

Rundel PW (1982) Water uptake by organs other than roots. In: Physiological Plant Ecology II. Springer, Berlin

Schuldt EZ, Farias MR, Ribeiro-do-Valle RM, Ckless K (2004) Comparative study of radical scavenger activities of crude extract and fractions from *Cuphea carthagenensis* leaves. Phytomedicine 11: 523-529

Seixas DP, Palermo FH, Rodrigues TM (2021). Leaf and stem anatomical traits of *Muntingia calabura* L. (Muntingiaceae) emphasizing the production sites of bioactive compounds. Flora 278: 151802

Silva SCDM, Tozin LRDS, Rodrigues TM (2016) Morphological and histochemical characterization of the secretory sites of bioactive compounds in leaves of *Lantana camara* L. (Verbenaceae). Botany 94: 321-336

Silva SCDM, Machado SR, Nepi M, Rodrigues TM (2020) Structure and function of secretory glochids and nectar composition in two Opuntioideae (Cactaceae) species. Botany 98: 425-437

Solereder H (1908) Systematic Anatomy of the Dicotyledons: a hand-book for laboratories of pure and applied botany. Carendon press, Oxford.

Taboga SR, Vilamaior PSL (2001) Citoquimica. In: A célula. Manole LTDA, Barueri, pp 42-50

Thompson AE (1984) *Cuphea* - a potential new crop. Hortic Sci 19: 352-354

Tozin LRS, Rodrigues TM (2016) Morphology and histochemistry of glandular trichomes in *Hyptis villosa* Pohl ex Benth. (Lamiaceae) and differential labeling of cytoskeletal elements. Acta bot bras 31: 330-343

Tozin LRS, Silva SCM, Rodrigues TM (2016) Non-glandular trichomes in Lamiaceae and Verbenaceae species: morphological and histochemical features indicate more than physical protection. N Z J Bot 54: 446-457

Tozin LRS, Marques MOM, Rodrigues TM (2017) Herbivory by leaf-cutter ants changes the glandular trichomes density and the volatile components in an aromatic plant model. AoB Plants 9: plx057

Watson ML (1958) Staining of tissue sections for electron microscopy with heavy metals. J. Biophys. Biochem. Cytol 4: 475-478

Werker E (2000) Trichome diversity and development. Adv Bot Res 31: 1–35

Windsor JB, Symonds VV, Mendenhall J, Lloyd AM (2000) *Arabidopsis* seed coat development: morphological differentiation of the outer integument. Plant J 22: 483-493

Wilson TP, Canny MJ, Mccully ME (1991) Leaf teeth, transpiration and the retrieval of apoplastic solutes in balsam poplar. Physiol Plant 83: 225-232

Young RE, McFarlane HE, Hahn MG, Western TL, Haughn GW, Samuels AL (2008) Analysis of the Golgi apparatus in *Arabidopsis* seed coat cells during polarized secretion of pectin-rich mucilage. Plant Cell 20: 1623-1638

Figures

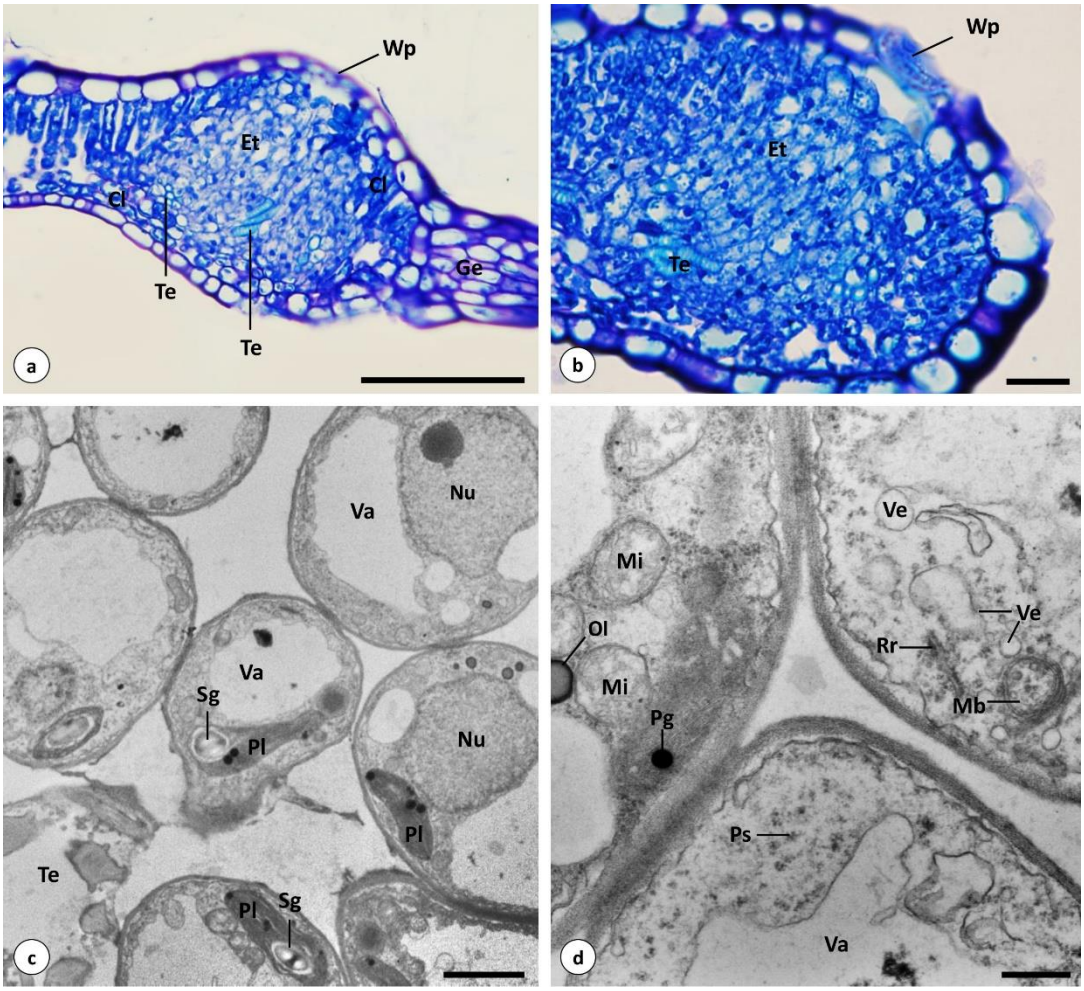

Figure 1. Photomicrographs (**a**, **b**) and transmission electronmicrographs (**c**, **d**) of hydathodes in cross-sectioned leaves of *Cuphea calophylla.* **a**. Hydathode associated with glandular emergence in the leaf border. **b**. Detail showing epithem, tracheary elements and water pore. **c**. Epithem cells with thin walls, voluminous nucleus with nucleolus, vacuoles and plastids with starch grains. **d**. Epithem cells with thin walls, sinuous plasmalemma and cytoplasm rich in organelles. **Cl** - chlorophyll parenchyma; **Et** - epithem; **Ge** - glandular emergence; **Mb** - multivesicular body; **Mi** - mitochondria; **Nu** - nucleus; **Ol** - oil drop; **Pg** - plastoglobuli; **Pl** - plastid; **Ps** - polysome; **Rr** - rough endoplasmic reticulum; **Sg** - starch grain; **Te** - tracheary element; **Va** - vacuole; **Ve** - vesicle; **Wp** - water pore. Scale bars: 150 µm (a); 50 µm (b); 5 µm (c); 1 µm (d).

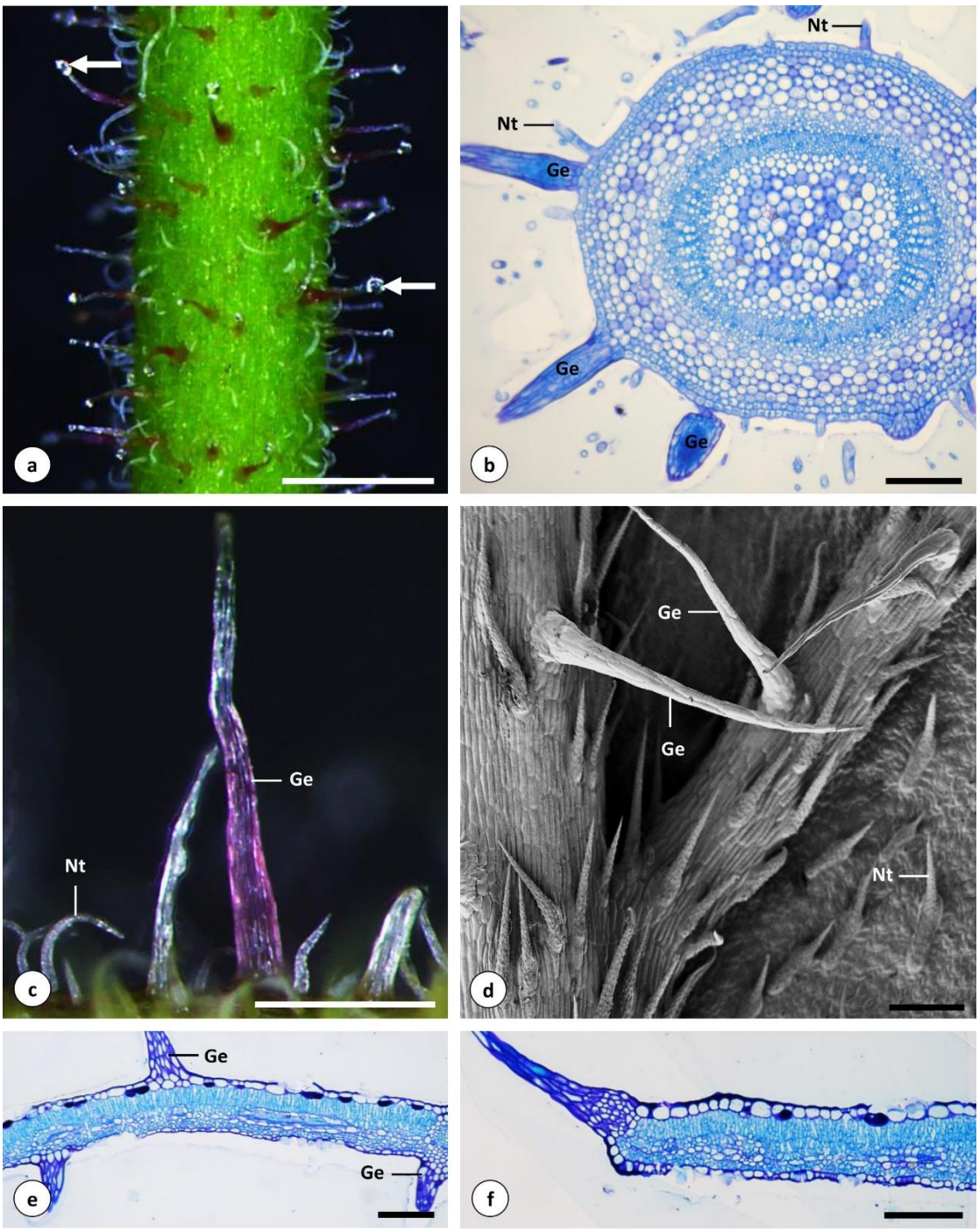

Figure 2. Glandular emergences on stem (**a-c**) and leaves (**d-f**) of *Cuphea calophylla*. **a**. Photography under stereomicroscopy showing glandular emergences with exudate drops (white arrows) on their apex. **b**. Photomicrography of cross sectioned stem showing voluminous glandular emergences. **c**. Detail of figure **a** showing glandular emergence with reddish aspect. **d**. Scanning electron micrography of abaxial surface of the leaf blade showing glandular emergences distributed mainly on the veins. **e**. Photomicrography of leaf blade in cross section showing glandular emergences on both leaf surfaces. **f**. Photomicrography of leaf blade in cross section with glandular emergence on the leaf border. **Ge** - glandular emergence; **Nt** - non-glandular trichome. Scale bars: 1 mm (a); 250 µm (c); 150 µm (b, e, f); 100 µm (d).

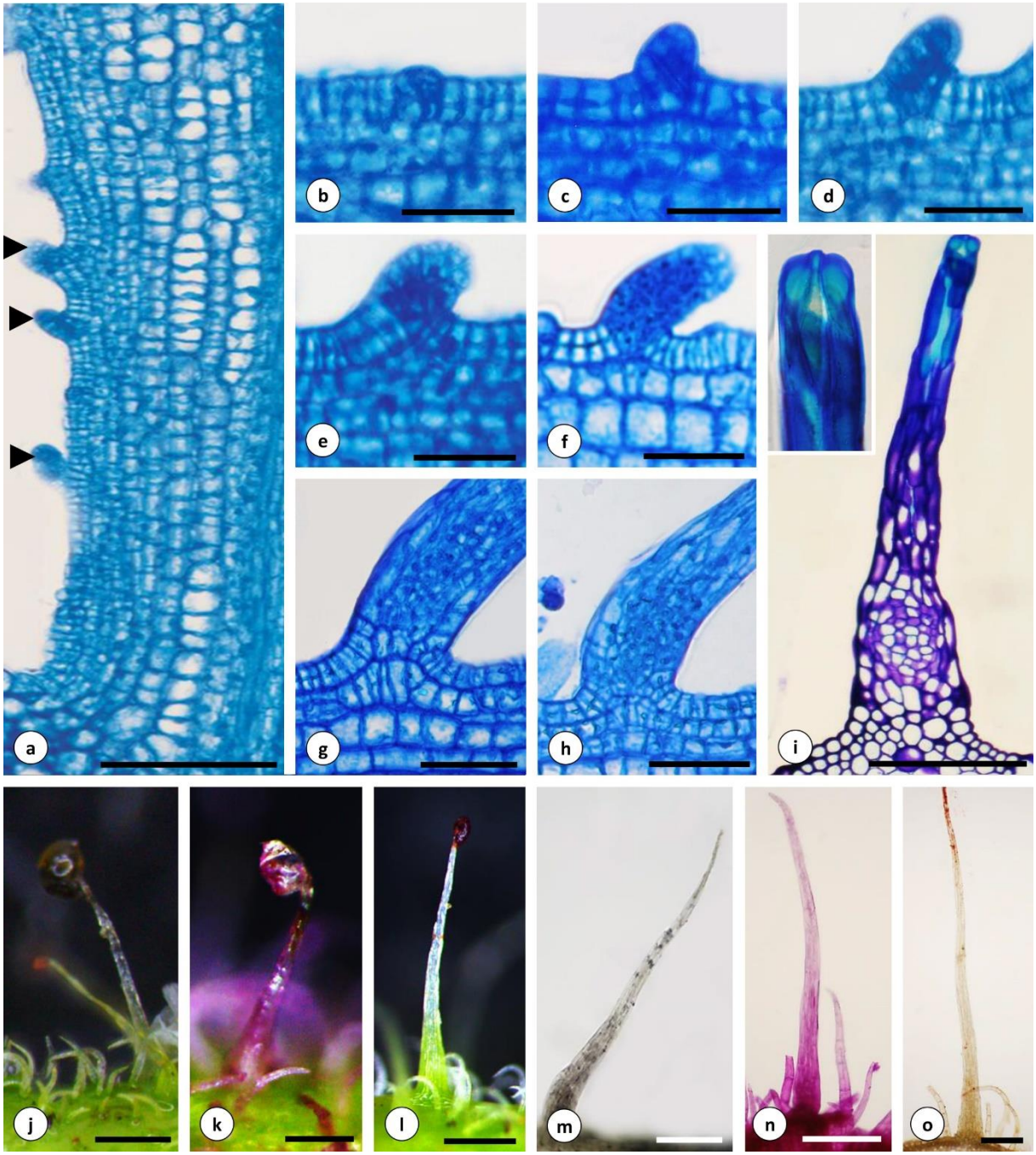

Figure 3. Photomicrographies (**a-i**; **m-o**) under light microscopy and photographs under stereomicroscope (**j-l**) of *Cuphea calophylla* stem. **a**. Shoot apex in longitudinal section showing glandular emergences in different developmental stages (arrowheads). **b-h**. Sequential developmental stages of the glandular emergences in longitudinal sections of the shoot apex. **b**. Anticlinal division of a single protodermal cell. **c**. Protrusion of a daughter cell from the protodermis. **d**. Four-celled primordium. **e, f.** Multicellular protuberance. **g**. Division and tangential elongation of ground cells toward the expanded basis of the developing emergence. **h**. Ground cells integrated on the expanded basis of the developing emergence. **i**. Cross section of the young stem showing a fully differentiated glandular emergence with enlarged basal portion and a narrow tapering upper portion. In the inset, observe the opening on the emergence apex. **j-o.** Glandular emergences of stem treated with different reagent. **j, m**. Detection of phenolic compounds by ferric chloride. **k**. Detection of polysaccharides and pectin by ruthenium

red. **l**, **o**. Detection of total lipids by Sudan IV. **n**. Detection of polysaccharides by PAS. Scale bars: 250 µm (j, l); 150 µm (a, m-o); 125 µm (k); 50 µm (f-i); 25 µm (b-e).

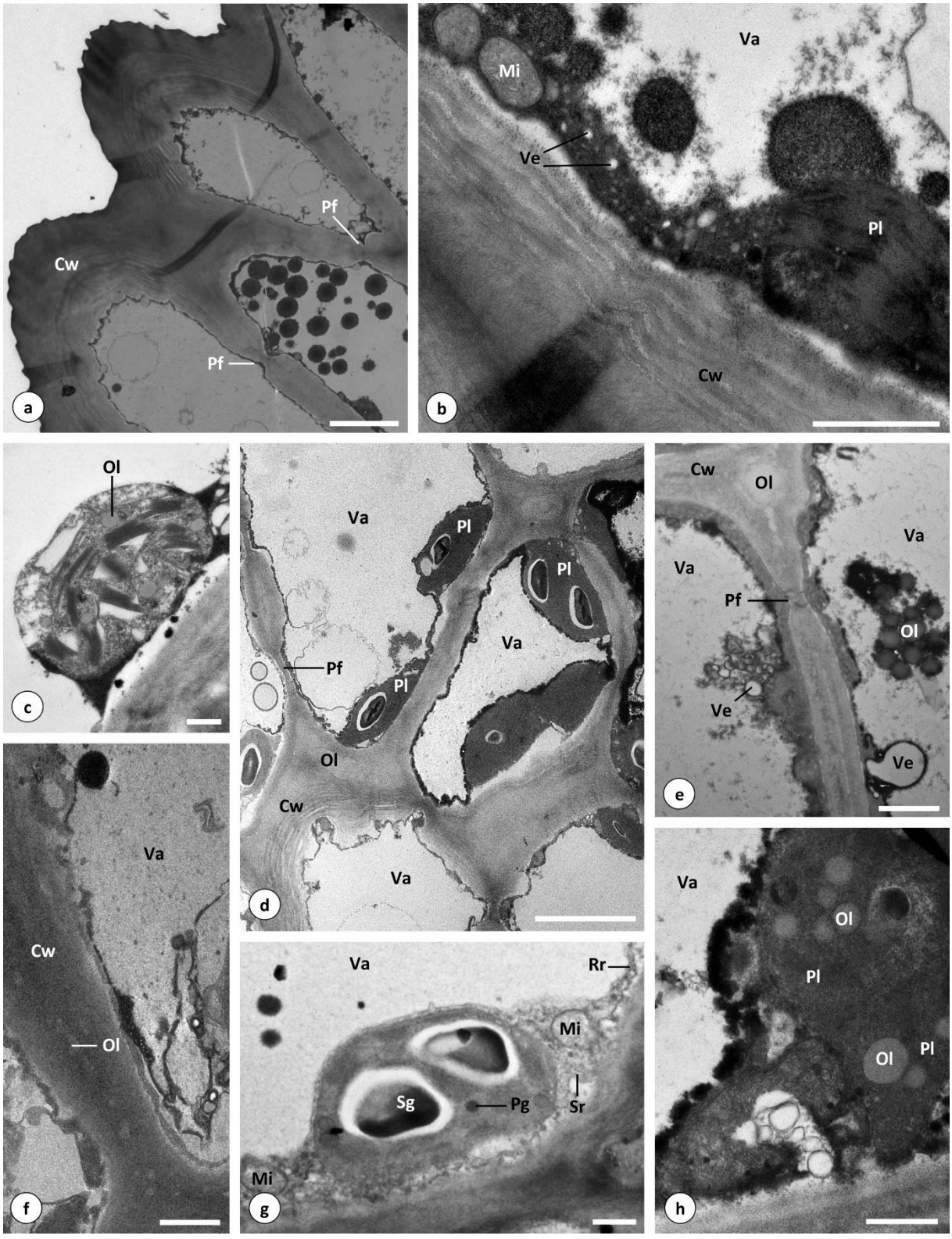

Figure 4. Transmission electronmicrographs of the glandular emergences in *Cuphea calophylla* leaves. **a-c** Epidermal tangentially-elongated cells. **a.** Cells with thick walls with lamellar features and pit fields, reduced cytoplasm and large vacuoles. **b**. Detail showing thick walls, reduced cytoplasm and vacuole with dense bodies and fibrillar material. **c**. Plastid with thylakoids and oil drops. **d-h.** Enlarged basal portion of the glandular emergence. **d**. Cells with thick walls incrusted with oil material, developed vacuoles and electron-dense cytoplasm with plastids containing starch grains. **e-f**. Cells with walls with pit-fields, large vacuoles containing membranous

material, fibrillar inclusions and oil content and reduced cytoplasm. Observe accumulations of oil material immersed in the cell wall and filling the corner among cells. **g**. Reduced cytoplasm with mitochondria, rough and smooth endoplasmic reticulum, polysome, and plastid with plastoglobuli and starch grain. **h**. Plastids with oil inclusions and vacuole with electron-dense bodies. **Cw** - cell wall; **Mi** - mitochondria; **Ol** - oil drop; **Pg** - plastoglobuli; **Pf** - pit field; **Pl** - plastid; **Rr** - rough endoplasmic reticulum; **Sg** - starch grain; **Sr** - smooth endoplasmic reticulum; **Va -** vacuole; **Ve** - vesicle. Scale bars: 10 µm (a, e); 2 µm (b, d, g); 1 µm (c, f, h).

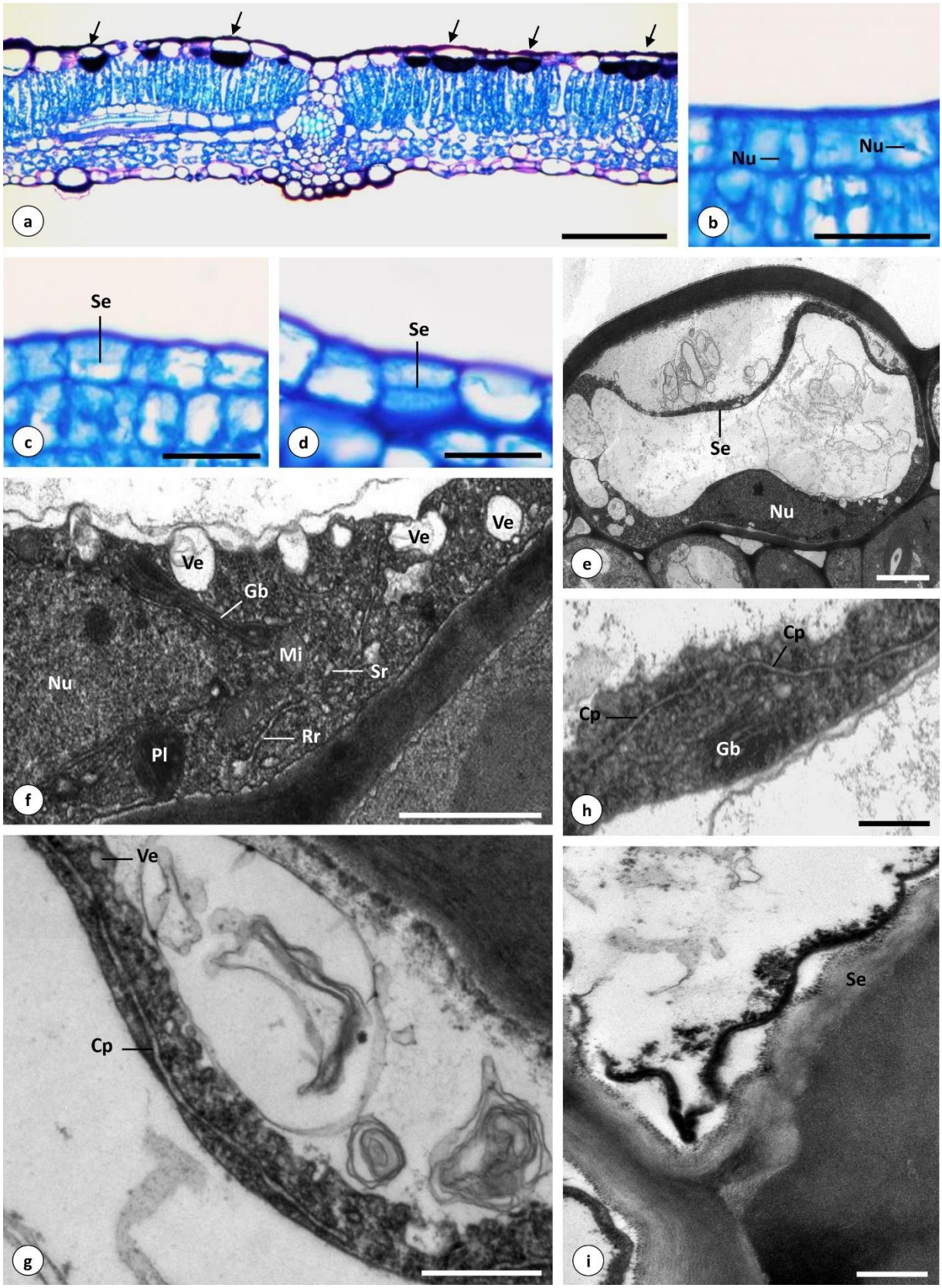

Figure 5. Photomicrographies (**a-d**) and transmission electron micrographs (**e-i**) of *Cuphea calophylla* leaves. **a**. Cross section of a fully expanded leaf with secretory epidermal cells (arrows) on the adaxial leaf surface. **b-d**. Developmental stages of the secretory epidermal cells in leaf primordium. **b**. Isodiametric cells originated from the anticlinal divisions on the protodermis; nucleus is observed in the basal pole of the cell. **c**. Septum deposition in the equatorial cell region. **d**. Stablished septum creating two compartments. **e**. Bi-compartmentalized cell

showing stablishing septum in the equatorial cell region; observe the nucleus in the basal pole of the cell. **f**. Basal portion of the cell showing nucleus and dense cytoplasm with proliferative Golgi bodies and abundant vesicles. **g-h**. Equatorial region of the cell with Golgi bodies and vesicles, and presumptive cell plate. **i**. Fully differentiated secretory epidermal cell showing equatorial septum separating two cellular compartments. **Cp** - cell plate; **Gb** - Golgi body; **Mi** - mitochondria; **Nu** - nucleus; **Pl** - plastid; **Rr** - rough endoplasmic reticulum; **Se** - septum; **Sr** - smooth endoplasmic reticulum; **Ve** - vesicle. Scale bars: 100 µm (a); 50 µm (b); 25 µm (c, d); 5 µm (e); 2 µm (f); 1 µm (g, h, i).

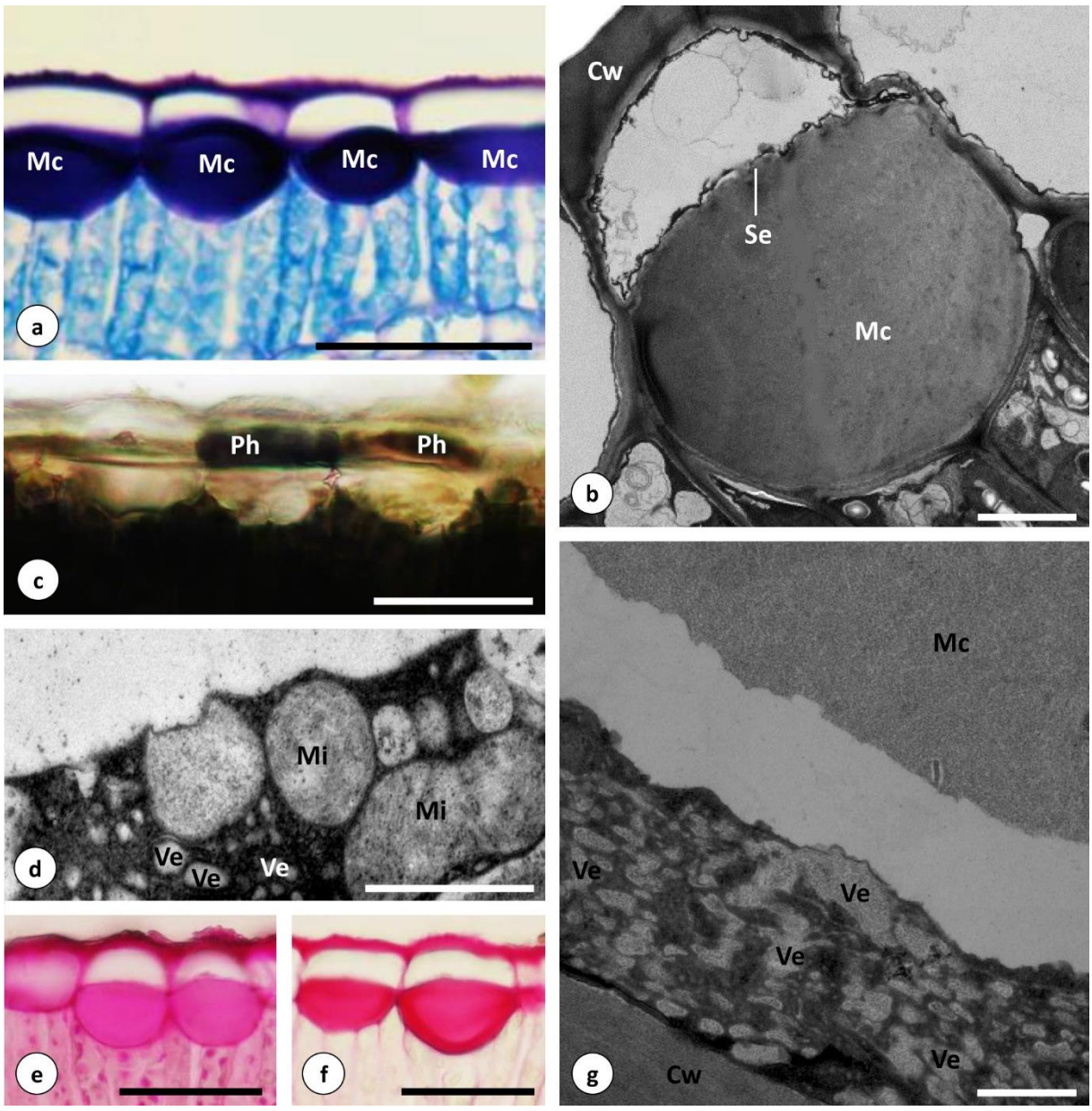

Figure 6. Photomicrographs (**a**, **c**, **e**, **f**) and transmission electron micrographs (**b**, **d**, **g**) of the fully differentiated secretory epidermal cells in *Cuphea calophylla* leaves. **a**. Bi-compartmentalized cells with lower compartment filled with mucilage. **b**. Cell with cellulosic septum in the equatorial portion. Observe the lower compartment filled with mucilage. **c**. Phenolic compounds in the upper compartment of the epidermal cells marked by ferric chloride. **d**. Portion of electron-dense cytoplasm above the septum with vesicles and mitochondria. **e-f**. Detection of polysaccharides on the lower compartment of the epidermal cells by PAS (e) and ruthenium red (f). **g**. Portion of cytoplasm in the bottom side of the cells with abundant and voluminous vesicles filled with mucilage. **Cw** - cell wall; **Mc** - mucilage; **Mi** – mitochondria; **Ph** - phenolic compounds; **Se** - septum; **Ve** - vesicle. Scale bars: 50 µm (a, c, e, f); 10 µm (b); 2 µm (d); 1 µm (g).

Capítulo 2:

The structural and functional responses of *Cuphea calophylla* Cham. & Schltdl. (Lythraceae) to excess of zinc and copper

Abstract

Cuphea calophylla (Lythraceae) is a subshrub with medicinal and economical potential. It is easily found in pasture areas, which soils are commonly contaminated with high concentrations of zinc (Zn) and copper (Cu). We investigated the structural and functional responses of *C. calophylla* to Zn and/or Cu excess in plants naturally occurrent in preserved area of Atlantic Forest and pasture and plants under controlled conditions. Individuals were subjected to different concentrations of Zn and/or Cu under hydroponic conditions in greenhouse: reference solution with 0.11g/L of Zn and 0.04g/L of Cu (T1 - control); reference solution adding 0.22g/L of Zn (T2); reference solution adding 0.10g/L of Cu (T3); and reference solution adding 0,22g/L of Zn and 0,10g/L of Cu (T4). Samples of leaves and roots were processed for structural analysis under light and scanning and transmission electron microscopy; Zn and Cu were detected by energy-dispersive X-ray spectroscopy (EDS). Gas exchange variables were measured using infrared gas analyser (IRGA). Oxidative stress was determined by H_2O_2 quantification and lipid peroxidation and H_2O_2 were histolocalized with 3,3-diaminobenzidine-DAB. The chemical composition of the extract of the aerial axis was analysed by high-performance liquid chromatography (HPLC). Plants from pasture area and plants from T2 and T3 presented a more compact leaf mesophyll. In the root, Cu excess promoted larger intercellular spaces in the cortex and vessel members with thicker walls. Chlorosis and leaf wrinkling regions were observed in all treatments, except in the control. Stain of H_2O_2 was intense in leaves and roots of plants from T2, T3 and T4. Alterations in the organelle membranes were detected in plants from T2; changes in chloroplasts and accumulation of electron-dense bodies in the intercellular spaces occurred in the root cortex of plants from T3. The number of chemical compounds was higher in the extract of plants from T3; however, the production of ellagic and gallic acids was not affected. Zn and Cu were detected in the secretory structures, suggesting their involvement in the detoxification of these metals. Despite the oxidative stress in the roots, plants under Zn excess maintained their photosynthetic metabolism, while plants under Cu excess had a decreased in the carbon assimilation. These results suggest that *C. calophylla* may have a tolerance to Zn and a susceptibility to Cu excess.

Keywords: anatomy; biochemistry; leaf; metal toxicity; oxidative stress; photosynthesis; root; ultrastructure.

Introduction

Areas destined for agriculture are becoming a global concern due to the soil contamination by potentially toxic elements. The extensive and excessive use of pesticides and other agrochemicals, synthetic or organic, increases the availability of nitrogen (N), phosphorus (P) and potassium (K) in soils, but it also promotes an increase in the concentration of other elements which, in excess, can be harmful to living beings, such as zinc (Zn) and copper (Cu) (Marsola et al. 2005; Brunetto et al. 2014).

Many studies have demonstrated that soils frequently used for pasture tend to have higher concentrations of Zn and Cu as a consequence of supplementary salts addiction in the food of cattle, as a feeding supplementation (Mantovi et al. 2003; Brennan et al. 2019). In the same way, intensification of the agronomic production system, with recurrent use of organic fertilization derived from animals from large livestock production modifies the availability of Zn and Cu on soils, leading to a soil contamination (Silva et al. 2005; Brennan et al. 2019; Hossain et al. 2018).

In low concentrations, Zn and Cu are essential for plants being considered micronutrients. Both these elements act as enzyme cofactors in essential biochemical reactions in the body of plants. Zn is generally associated with the metabolism of phosphate group molecules (ATPases) and carbohydrates, acting also in the maintenance of ribosome structure and in the functioning of RNA-polymerase. Not least, Cu has an effective participation in the metabolic processes of plants, as in cellular respiration, carbohydrate metabolism and in the photosynthetic process, mainly participating in the electron's transport in photosystem I (Nagajyoti et al. 2010; Hossain et al. 2018). However, in high concentrations these elements become toxic and can lead to an unbalance in plant metabolism.

The toxicity due to Zn and Cu excess promotes oxidative stress in plant cells, increasing the concentration of reactive oxygen species (ROS), and triggering a series of antioxidant responses that alter essential metabolic pathways for plants and biosynthesis production, such as photosynthesis and mitochondrial respiration (Yruela 2005; Giampaoli et al. 2012; Girotto et al. 2013; Bulgarelli et al. 2016; Hammerschmitt et al. 2020). Studies describe that excess of Zn promotes reduction in the leaf area, leaf blade chlorosis and curls, compaction of mesophyll, disruption of chlorenchyma cells, reduction in the number of chloroplasts per cell and degradation of photosynthetic pigments (Sridhar et al. 2005, 2007; Kouhi et al. 2016; Hammerschmitt et al. 2020). Regarding the excess of Cu, it can promote chlorosis in leaves, inhibit cells division and elongation, promote a reduction in the size of vascular bundles and an irregular formation and degradation of chloroplasts and mitochondria, suppressing chlorophyll

biosynthesis (Guimarães et al. 2016; Martins et al. 2016; Li et al. 2017; Hammerschmitt et al. 2020).

Despite the changes frequently reported in the literature, the reactions and features expressed by plants exposed to metal excess do not follow a stablished pattern, making it difficult to predict the expressions of toxicity in different plant species, especially regarding morphological and anatomical changes (Bini et al. 2012; Kouhi et al. 2016; Li et al. 2017; Hossain et al. 2018). Besides, the vast majority of studies related to toxicity by Zn and Cu excess are limited to genetically selected species of feed and/or test model species (Mantovi et al. 2003; Brunetti et al. 2011; Yang et al. 2011; Girotto et al. 2013; Kouhi et al. 2016; Tiecher et al. 2018; Schwalbert et al. 2019; Hammerschmitt et al. 2020). Thus, the influence of these metals excess on the development of native/wild species is little discussed. Therefore, studies about native species naturally found in areas contaminated by metals become necessary for a better understanding of the influence of these metals on the development of such plants, promoting useful information for their management and conservation.

Cuphea calophylla Cham. e Schltdl. is a subshrub species native from Brazil, easily found in pasture and/or grassland areas and popularly known as “sete-sangrias” (Lusa and Biasi 2011; Facco 2015). The extracts of their aerial vegetative axis are widely used for the treatment of diseases related to hypertension (Lorenzi and Matos 2002; Ramírez et al. 2018). Their antioxidant activity is mainly derived from the presence of ellagic acid and gallic acid in the extracts from their aerial organs (Klider et al. 2020; Santos et al. 2020). In addition, this species is used for soup manufacturing due to their lipid contents (Thompson 1984).

The aim of this study was to investigate the structural and functional responses to Zn and/or Cu excess of *C. calophylla* plants naturally growing in the field and plants under controlled conditions.

Material and Methods

Plant material and field experiment

Cuphea calophylla is a subshrub that can reach up 50 cm height. Non-glandular trichomes and glandular emergences occur throughout all their aerial vegetative axis. Their leaves are opposite, with tiny petioles (1-2 mm) and the leaf blade varies in shape from oval, heart-shaped to rounded (Cavalcanti and Graham 2002).

In order to compare the morphoanatomical features of plants living in a preserved area and in pasture field, we sampled ten adult plants (n=10) of *C. calophylla* occurring in a preserved remnant of Atlantic forest in the Botanical Garden (S 22°53'09,7”, W 48°29'59.8”) of Institute of Biosciences of Botucatu, IBB, UNESP, in Botucatu municipality, São Paulo

State, Brazil; other ten adult plants (n=10) were sampled from a population stablished in an area of cattle pasture at the UNESP Experimental Farm (S 22°46'21.0'', W 48°33'52.9'') located in São Manuel municipality, São Paulo State, Brazil. The climate in both areas is Cfa according to Köppen classification with hot temperate humid climate, with average temperature above 22 ºC in the hottest month (Cunha and Martins 2009).

To evaluate the physicochemical characteristics of the soils, especially the concentration of micronutrients (Zn and Cu), soil samples (n=2 for each sample region) were collected at a depth of 20-30 cm, dried in 40°C, passed through a 2 mm sieve and stored in paper bags. The samples were sent to the Department of Soils and Environmental Resources, FCA, UNESP, Botucatu, where the standard/basic analysis (pH (CaCl2), MO, H + Al, P-resin, Ca, Mg, K, S, B, CTC, V%), and micronutrient analysis (SOQ-A + SOQ-B) were performed.

Plants with reproductive material were collected from both the study areas and vouchers were deposited in the Irina Delanova Gemtchújnicov Herbarium (BOTU), of the Institute of Biosciences of Botucatu, IBB, UNESP (under registration numbers 35186 and 35187). The identification of the taxon was confirmed by Dr. Taciana Barbosa Cavalcanti, specialist in the genus.

Greenhouse experiment

Stem fragments in vegetative stage were collected from 120 adult plants of *C. calophylla* occurring in a remnant of Atlantic Forest in the Botanical Garden of the Institute of Biosciences of Botucatu, IBB, UNESP. Cuttings obtained from the stem fragments were placed in trays containing medium-grained vermiculite mixed with vegetable soil and kept in a greenhouse with constant irrigation until the rooting and formation of the first leaves (adapted from Lusa and Biasi 2011). Subsequently, plant samplings were transferred to hydroponic condition in treatments with different concentrations of Zn and Cu, as described below.

Firstly, a pilot experiment was carried out to determine the solution of the control treatment and the solutions with maximum concentrations of Zn and Cu supported by plants of *C. calophylla* that would allow the emerge of new branches. For that, 35 plants were transferred to 750 ml pots filled with nº 2 Hoagland and Arnon (1950) nutrient solution. These plants were separated into seven groups with 5 repetitions in each one. Each plant group received different concentrations of Zn and Cu: a) Tp1 (reference ionic solution nº 2 of Hoagland and Arnon (1950) at 50%, which presents 0.11g/ L for Zn and 0.04g/L of Cu); b) Tp2 (reference ionic solution with Zn at 0.165g/L); c) Tp3 (reference ionic solution with Zn at 0.22g/L); d) Tp4 (reference ionic solution with Zn at 0.275g/L); e) Tp5 (reference ionic solution with Cu at

0.06g/L); f) Tp6 (reference ionic solution with Cu at 0.08g/L); g) Tp7 (reference ionic solution with Cu at 0.10g/L).

The plants in the pilot experiment had their morphological aspects (height growth, appearance of new branches, chlorosis and leaf deformations, etc.) daily evaluated. The mortality of these plants was also considered. Thus, the solutions selected for the experiment were:

- T1 = control (reference ionic solution nº 2 of Hoagland and Arnon (1950) at 50%, which presents 0.11g/ L for Zn and 0.04g/L of Cu);
- T2 = excess of Zn (reference ionic solution with Zn at 0.22g/L);
- T3 = excess de Cu (reference ionic solution with Cu at 0.10g/L);
- T4 = solution with the excess of Zn (0.22g/L) and Cu (0.10g/L).

Ten repeats, with three plants each (n=30), were maintained for each treatment for four weeks, until the formation and complete expansion from new leaves. After this period, samples were collected for subsequent analysis.

Throughout the experimental period, the solutions were kept with an ionic conductivity of 1.19 mS and pH 5.7, these solutions were changed weekly in order to maintain the constancy of these variables. The experiments were carried out in a greenhouse under controlled conditions (24-25°C; and mean relative humidity 82%) in randomized blocks.

Morphological features

Morphological analyses of the aerial vegetative axis of 10 plants from each treatment of the greenhouse experiment were performed. The following features were analysed: a) aspect and diameter of the apical buds; b) length of the stem; c) diameter of the young stem (1.5 cm below the apical bud); d) appearance (colour, presence or absence of stains and winding) of the leaf blade; e) area, length and width of the leaf blade from the second pair of fully expanded leaves formed after the treatments; and f) length of the root system.

Diameter and length measurements were performed using a digital calliper and a millimetre ruler, respectively. The area of the leaf blade was determined using an Area Meter equipment (LICOR-3100). The morphological features of the plants were photodocumented with a Canon EOS Rebel T6 camera.

Light microscopy

Root portions (approximately 1.5 cm above the root apex) and samples from the median region of the leaf blade of the second pair of fully expanded leaves formed after the treatments

were collected from 10 plants of each treatment in greenhouse. Likewise, samples were collected from the median region of the leaf blade from the second pair of fully expanded leaves of plants (n=10) occurring in the Atlantic Forest remnant and pasture area.

The collected samples were fixed in mixture of formaldehyde, acetic acid and 50% alcohol (Johansen 1940), dehydrated in an ethylic series, embedded in methacrylate resin (Leica Historesin®) and cross-sectioned with a semi-automatic rotating microtome (Leica RM2155). The cross sections (5 µm thick) were stained with toluidine blue pH 4.7 (O'Brien et al. 1964), and permanent slides were mounted with Entellan® (Merck).

For the leaf blade, the following features were analysed: a) length of glandular emergencies; b) density of glandular emergencies; c) thickness of the outer periclinal wall of epidermal cells in the adaxial surface of the leaf blade, d) area and density of the secretory epidermal cells on the adaxial surface of the leaf blade, e) thickness of the leaf blade; f) thickness of the palisade and the spongy parenchyma, g) width of palisade parenchyma cells, h) area occupied by the intercellular spaces in the spongy parenchyma, h) area of the vascular bundles immersed in the mesophyll, j) distance between the smallest veins in the mesophyll, and k) area occupied by vascular tissues in the midrib. For root samples, we analysed: a) epidermis thickness, b) cortex thickness, c) area occupied by intercellular spaces in the cortex, d) area of the vascular cylinder, and e) cell wall thickness of the metaxylem vessel elements.

The slides were analysed using an Olympus BX 41 light microscope and the relevant aspects were documented with a coupled Olympus C-7070 digital camera. Morphometric measurements were performed using the Image J software. In order to density calculation of the glandular emergences, the whole abaxial leaf surfaces were photographed in a Leica M205C stereomicroscope and glandular emergences were counted in the Image J software.

Gas exchange

Gas exchange indices were evaluated in the last week of the greenhouse experiment, before the destructive analysis (microscopical and biochemical analysis). Measurements were performed using the second pair of fully expanded leaves formed after the application of treatments (n=7) using an Infra-Red Gas Analyzer with a coupled portable modulated light fluorometer (Infra-Red Gas Analyzer - IRGA, model GFS 3000 FL with LED-Array/PAM-Fluorometer 3055-FL, Walz). The following variables were analysed: net CO_2 assimilation rate (A_{net}, µmol CO_2 m^{-2} s^{-1}), stomatal conductance (g_s, mmol m^{-2} s^{-1}), transpiration rate (E, mmol H_2O vapor m^{-2} s^{-1}), internal CO_2 concentration in the leaf (C_i, µmol CO_2 mol^{-1}), instantaneous carboxylation efficiency of enzyme ribulose 1,5-biphosphate carboxylase - RuBisCO (A_{net}/C_i, µmol m^{-2} s^{-1} Pa^{-1}) and instantaneous water use efficiency (iWUE, µmol CO_2 (mmol $H_2O)^{-1}$)

(Zhang et al. 2001), with light saturating of 1200 μmol $m^{-2}s^{-1}$ photosynthetic photon flux density (DFFF) in the period between 9 and 11 am.

Quantification of the hydrogen peroxide (H_2O_2)

Samples of root and aerial vegetative axis were collected from five plants from each treatment (n=5) in the greenhouse. The samples were ground with liquid nitrogen and stored under -20°C. For the quantification of hydrogen peroxide (H_2O_2), 100 mg of each sample was subjected to 1 ml of 0.1% trichloroacetic acid (TCA) and vortexed homogenized. Subsequently, the samples were centrifuged at 12000 RPM for 15 minutes at 4°C in a refrigerated centrifuge. The supernatant was immediately subjected to the following reaction in the dark for one hour: 0.5 ml of extract + 0.5 ml of 0.1 M Phosphate Buffer (pH 7.0) + 2.0 ml of 1 M KI. After this period, the reaction was read in a spectrophotometer at 390 nm and the concentration of H_2O_2 was calculated using the curve of 0-100 μM of H_2O_2 (Alexieva et al. 2001).

Level of lipid peroxidation

For each treatment in greenhouse, 100 mg of fresh root and fresh aerial vegetative axis from five plants (n=5) were collected. The collected samples were macerated in a mortar with the addition of 2 ml of the reaction solution consisting of thiobarbituric acid (0.25%, m/v) and trichloroacetic acid (10%, m/v). The resulting material was placed in sealed test tubes and placed in a water bath at 95°C for 1 hour. The solution was centrifuged at 12000 RPM for 40 minutes at 25°C and the supernatant was collected and read in a spectrophotometer at wavelengths of 532 nm and 600 nm. The concentration of malondialdehyde (MDA) was calculated using an extinction coefficient equal to 155 $mM^{-1}cm^{-1}$ (Heath and Packer 1968).

***In situ* detection of hydrogen peroxide (H_2O_2)**

Fresh root samples (1.5 cm above the root apex) and the median portion of the leaf blade of fully expanded leaves from three plants (n=3) of each experimental treatment in greenhouse were cross-sectioned by hand using a razor blade. The obtained sections were treated in a freshly prepared 0.5% solution of 3,3-diaminobenzidine DAB (Sigma-Aldrich, St. Louis, MO, USA) for 60 minutes in the dark. Then, the sections were washed in 70% alcohol, followed by deionized water, and mounted in water between slides and coverslips (Rossetti and Bonatti 2000). The control test was performed using 1M ascorbic acid solution.

The results were immediately analysed and photodocumented with an Olympus BX 41 light microscope with a coupled Olympus C-7070 digital camera.

Transmission electron microscopy (TEM)

In order to investigate the subcellular aspects of roots and leaves of *C. calophylla* under Zn and/or Cu excess, samples of roots and median region of fully expanded leaf blades formed after the treatments in greenhouse were fixed in 2.5% glutaraldehyde in 0.1M phosphate buffer (pH 7.3) for 24 h, post-fixed with 1% osmium tetroxide aqueous solution in the same buffer for 1 h, dehydrated in an acetone series and embedded in Araldite resin. Ultra-thin sections (70 nm) were stained with uranyl acetate (Watson 1958) and lead citrate (Reynolds 1963). The samples were examined using a FEI Tecnai Spirit transmission electron microscope at 80 kV. The relevant results were documented with a digital system of image capture coupled to the electron microscope.

Scanning electron microscopy and energy-dispersive X-ray spectroscopy (EDS)

In order to detect the presence of Zn and Cu in the secretory structures of the leaves, leaf samples formed after treatments with isolate excess of Zn and Cu (T2 and T3, respectively) in greenhouse were fixed in 2.5% glutaraldehyde in 0.1M phosphate buffer (pH 7.3) for 24 h, post-fixed in 1% osmium tetroxide, dehydrated in an ethylic series, dried in a critical point dryer and coated with gold. The samples were analysed using a compact JEOL JSM-6010 scanning electron microscope with an energy dispersive X-ray spectroscopy (EDS) detector attached.

Chemical compounds and identification of phenolic composition by High-Performance Liquid Chromatography (HPLC)

Plants from each treatment (n=3) performed in greenhouse had 200 mg of their aerial vegetative axis (dried at 38°C) crushed and the extract was solubilized in methanol and deionized water (7:3, v/v) at concentration 5 mg/mL. Each extract was filtered with cotton and the volume was made up with solvent extractor (methanol). Samples were filtered with a Millex LCR filter (non-sterile 0.45 μm 13 mm PTFE membrane) and placed in amber glass bottles at 4°C. The extracts were injected in a High-Performance Liquid Chromatography (uv HPLC focused Thermo Fisher-Scientific) with gradient pump and UVVIS detector and a C18 reverse phase column (150 × 4.6 mm and 5 μm particle diameter). The mobile phase consisted of a 0.5% gradient acetic acid in ultrapure acid water with 0,1% of formic acid pH=2,53 (A), methanol (B) and acetonitrile (C), HPLC grade, with a flow rate of 1 mL/min for 30 min and detection wavelength 365 nm, following the literature (Dembogurski et al. 2018; Klider et al. 2020). Data were processed by Chromeleon 7 CDS software version 7.2.1.5833 (Thermo Fisher Scientific) and chromatographic profile were analysed for each extract. In order to confirm the presence of ellagic acid and gallic acid and quantify those compounds in the extracts, authentic

standards were injected into the equipment. The ellagic acid standard used was Sigma, degree of purity ≥ 95% and the calculated curve was y = 2,2687x +0,2134, R^2 =1; the acid gallic standard used was Vetec, degree of purity ≥ 99% and the calculate curve was y = 0,4012x - 0,2826, R^2 = 1. Concentrations of these compounds described above were calculated and expressed here in mg of the identify substance per g of plant material dry mass (aerial vegetative axis).

Statistical analyses

The data analyses referring to the measurement of morphological, anatomical and physiological parameters of the studied plants had the normality tested with Shapiro-Wilk's test. Concerning the data comparison between plants from the Atlantic Forest remnant and pasture area, when parametric the data were compared using ANOVA and when nonparametric those were compared by van der Waerden test. Regarding the data comparing plants from the different treatments of the greenhouse experiment, when parametric the data were compared using ANOVA and when nonparametric those were compared by ANOVA/Kruskal-Wallis test. In all analyses the trust gap was 95% ($p < 0.05$). Referring to data of the density of the secretory structures, a data transformation using a square root was performed in order to generate a constant variable. After that, the data were submitted to the same test conditions previously described.

Results

Soil analyses

The concentration of Zn and Cu in the soil samples varied between the field areas. In general, soil samples from the pasture area showed higher concentrations of Zn and Cu when compared to samples from the Atlantic Forest remnant (Table 1). It was also possible to identify highest pH in soil of the pasture areas, in addition to variations of other nutrients concentrations, such as higher concentrations of B, Ca and Mg (Table 1).

External morphology of plants under experimental conditions in the greenhouse

In all treatments, leaf primordia occurred in the apical buds. For plants from the control treatment (T1) the leaf primordia showed a greenish colour (Fig. 1a), without any type of chlorosis; 3% of the individuals analysed showed a slight reddish colour in the basal portion of the leaf blade of the young leaves in the expansion process. Plants from T2, T3 and T4 produced leaf primordia and young expanding leaves with scattered chlorosis regions, wrinkled appearance and reddish basal portion (Fig. 1b-d).

Regarding the appearance of the fully expanded leaves, plants from T1 (Fig. 1e) presented greenish-coloured leaf blade with turgid aspect and absence of chlorosis. In T2 (Fig. 1f), plants presented greenish-coloured leaf blades with scattered regions of chlorosis or chlorosis areas concentrated in their basal portion; all plants from this treatment presented leaf blade with a withered aspect, wrinkled and twisted edge facing downwards. In T3 (Fig. 1g), plants showed leaf blade with dark green colour; some plants produced leaf blades with scattered regions of chlorosis and/or reddish edges; portions of the base and, mainly, portions close to the midrib showed a wrinkled appearance. In the plants fromT4 (Fig. 1h) the leaf blade showed scattered regions of chlorosis giving a senescent aspect to the leaves; some individuals also presented a wrinkled leaf blade and twisted edge.

In the measured morphological characteristics, differences were observed only in the leaf blade area. Plants from T3 presented leaves with smaller leaf blade area compared to plants from the control (T1) and T2 (Table 2).

Anatomical aspects of the plants from field conditions and plants from greenhouse experiment

The leaves of *C. calophylla,* from both the field (Fig. 2a, b) and greenhouse (Fig. 2c-f) plants, were amphistomatic, with uniseriate epidermis containing non-glandular hairs and Large glandular emergences occurred on the whole leaf blade surface. Voluminous bi-compartmentalized secretory cells containing phenolic compounds and mucilage were abundant in the adaxial surface of the leaf blade. Mesophyll was dorsiventral and collateral vascular bundles were immersed on it.

The leaves of plants living in the pasture area had higher density of the glandular emergence and secretory epidermal cells in comparison to leaves of plants from the remnant of Atlantic Forest (Table 3). On the other hand, plants living in the Atlantic Forest remnant exhibited leaf blade with wider palisade parenchyma cells, larger intercellular spaces in the spongy parenchyma, larger 4th order vascular bundles and greater distance between the 4th order vascular bundles (Table 3).

Regarding the plants treated with different concentrations of Zn and Cu in the greenhouse, individuals from the control treatment produced longer glandular emergences than plants from T3 and T4 (Table 4). The thickness of the outer periclinal wall of the epidermal mucilaginous cells was greater in the plants from the control treatment (T1) when compared to the plants from T3 and T4 (Table 4). The density of those secretory epidermal cells was higher in the plants from the T2 in comparison to plants from T4 (Table 4). The area occupied by the intercellular spaces in the spongy parenchyma was greater in plants from T1 than in plants from

the T3 and T4, while the area of the 4th order vascular bundles was greater in the plants from T3 and T4 treatment when compared to the plants from T1 (Table 4). In addition, the distance between the 4th order vascular bundles was smaller in the plants from T3 treatment when compared to the plants from T1 and T2 (Table 4).

The roots of *C. calophylla* plants treated with different concentrations of Zn and Cu in greenhouse exhibited uniseriated epidermis, cortex with six to eight layers of parenchyma cells and well delimited endodermis, and central vascular cylinder with pericycle and primary xylem and phloem (Fig. 3a-d). The area of the intercellular spaces in the cortex was greater in the plants from T3 and T4 than in the plants from the control treatment (Table 5). Plants from T3 exhibited vessel members with thicker walls when compared to plants from T1 and T2 (Table 5).

Gas exchange measurements

Plants from T2 had a higher transpiration rate (*E*) when compared to plants from the other treatments (Fig. 4a). Individuals from T2 had higher stomatal conductance (g_s) than plants from T3 and T4 (Fig. 4b). Plants from T1 and T2 presented higher values of carbon assimilation (*A*) and RuBisCO efficiency (A_{net}/Ci) than plants from T3 and T4 (Fig. 4c and d, respectively). For instantaneous water use efficiency (iWUE), plants from T3 and T4 presented lower values than plants from T1 (Fig. 4e). The values of internal CO_2 concentration in the leaf (*Ci*) did not change among the treatments (Fig. 4f).

Hydrogen peroxide (H_2O_2) production and lipid peroxidation in the aerial shoots and root

Plants from T1 and T4 treatments had higher concentrations of hydrogen peroxide in the aerial shoots than plants from T2 (Fig. 5a). Differences in the lipid peroxidation in the aerial portions were not observed among plants from the different treatments (Fig. 5b).

Regarding the root, a higher concentration of hydrogen peroxide was found in plants from T4 than plants from T3 (Fig 5c). The lipid peroxidation was more intense in the roots of plants from T2 than in plants from T1 (Fig. 5d).

***In situ* detection of hydrogen peroxide (H_2O_2) in the leaf blade and root**

The leaf blade of the plants from T1 showed mild DAB staining on the mesophyll (Fig. 6a); on the midrib of these plants a light staining for H_2O_2 were observed in cells from the vascular system (Fig. 6b). Plants from T2 showed intense reaction for H_2O_2 in both palisade and spongy parenchyma (Fig. 6c); in the midrib the H_2O_2 were marked in the cells of the vascular system, especially in the xylem, and in few parenchymal cells of the cortex (Fig. 6d).

For plants from T3, H_2O_2 stains were intensely marked in the palisade parenchyma cells (Fig. 6e); in the midrib the H_2O_2 were histolocalized in the xylem cells and in some parenchyma cells of the cortex (Fig. 6f). For plants from T4, intense staining for H_2O_2 occurred in the spongy parenchyma cells and mainly in the palisade parenchyma (Fig. 6g); in the midrib the H_2O_2 were located in the xylem cells and in several parenchyma cells of the cortex (Fig. 6h).

For the roots, plants from T1 showed light staining for H_2O_2 in the exoderm and endoderm (Fig. 7a). For plants from T2, T3 and T4, H_2O_2 were intensely marked in the endoderm, pericycle and phloem cells (Fig. 7b-d). In plants from T3, in addition to these regions, cells from the median portion of the cortex also showed positive reaction for DAB (Fig. 7c).

Subcellular aspects of the leaf blades and roots

The leaf blade of plants from T1 had chlorenchyma cells in the mesophyll with thin walls, dense cytoplasm, vacuoles with different sizes and nucleus with evident nucleolus (Fig. 8a, b). Mitochondria with developed cristae, Golgi bodies, endoplasmic reticulum, and abundant chloroplasts were observed in both the palisade and spongy parenchyma cells (Fig. 8a-d). The chloroplasts exhibited irregular contour, developed thylakoids and contained starch grains and plastoglobuli (Fig. 8a-d). Electron-dense inclusions, membranous material and fibrillar content occurred in the vacuoles (Fig. 8b-d). The palisade parenchyma cells had vesicles and oil droplets in the cytoplasm (Fig. 8b, c). Peroxisomes were observed in the spongy parenchyma cells (Fig. 8d).

In the leaves of plants from T2, the plastids were very large with lenticular to reniform shape, and contained poorly developed internal membranes, starch grains and small plastoglobules (Fig. 8e-g); however, some of them were devoid of starch grains (Fig. 8g). The mitochondria were abundant, voluminous and contained dilated cristae (Fig. 8f, g). The vacuoles contained membranous inclusions (Fig. 8e); myelin figures were observed (Fig. 8e). In plants from T3, chlorenchyma cells had a dense cytoplasm with granular aspect characterized by the abundance of polysomes (Fig. 8 h, i). Golgi bodies and vesicles were also abundant (Fig. 8 h, i). Mitochondria cristae were less evident than in the control treatment (Fig. 8, insert). Myelin figures were commonly observed (Fig. 8h). The plastids had well-developed thylakoids (Fig. 8h-i). Membranous and fibrillar material occurred in the vacuoles (Fig. 8i). In the palisade cells, the chloroplasts were voluminous and rectangular to square in shape and occupied the entire width of the cells (Fig. 8h). Electron-dense bodies occurred in the spaces among the spongy cells (Fig. 8i).

Chlorenchyma cells of leaves of plants from T4 presented a dense granular cytoplasm, with Golgi bodies and abundant vesicles (Fig. 8j-k). The mitochondria cristae were poorly developed (Fig. 8k); membranous inclusions and myelin figures occurred in the vacuoles (Fig. 8j). Chloroplasts from palisade parenchyma cells were large and rectangular to square in shape (Fig. 8j). Juxtaposition points between two or more chloroplasts and between chloroplasts and mitochondria were frequently observed in both types chlorenchyma cells (Fig. 8k, l).

The roots of plants from T1 had sinuous epidermal cells with cytoplasm containing ribosomes, smooth endoplasmic reticulum, mitochondria with developed cristae, Golgi bodies and a lot of vesicles (Fig. 9a). Vacuoles were small and electro-lucent (Fig. 9a). The cortical parenchyma cells had thin walls with plasmodesmata and a large vacuole that compressed the cytoplasm in cell periphery (Fig. 9b). Plastids with thylakoids, mitochondria with developed cristae, rough and smooth endoplasmic reticulum, Golgi bodies and a lot of vesicles were observed in the cortical parenchyma cells (Fig. 9b-d). In the phloem, the sieve tube members exhibited thin walls, mitochondria with developed cristae, and endoplasmic reticulum; membranous inclusions were observed in the phloem cells (Fig. 9e). In the xylem, the vessel members had thick walls with electron-dense bodies adhered to their internal face (Fig. 9f); the xylem parenchyma cells exhibited dense and abundant rich in organelles (Fig. 9f).

In plants from T2, the epidermal cells had plasma membrane with sinuous contour and flocculent and electron-dense cytoplasm with few organelles (Fig. 9g). In the cortical parenchyma cells, the vacuoles were developed and the cytoplasm was electron-dense and reduced; the mitochondria had unclear cristae (Fig. 9h), and plastids with poorly developed internal membrane (Fig. 9i); electron-dense bodies occurred mainly attached in the internal face of the tonoplast (Fig. 9h, i). Endodermal cells had large nucleus, vacuole and abundant electron-dense cytoplasm with well-developed rough and smooth endoplasmic reticulum (Fig. 9j). The phloem cells had apparently thicker walls in comparison to the control treatment (Fig. 9k). The vessel members presented more abundant electron-dense bodies adhered in the internal face of the cell in comparison to T1 (Fig. 9l). For plants from T3, root epidermal cells had a wide vacuole with membrane inclusions and accumulation of electron-dense bodies in the periplasmic space (Fig. 9m). Cortical parenchyma cells had grainy and reduced cytoplasm and a wide vacuole with membrane inclusions (Fig. 9n); electron-dense material accumulated in the spaces in the corner of parenchyma cells (Fig. 9n, insert). Endodermal cells exhibited rough endoplasmic reticulum, mitochondria with poorly developed cristae, peroxisomes and vesicles (Fig. 9o). The sieve tube members exhibited features similar to T1. Vessel members had abundant electron-dense material adhered to the inner cell surface similar to T2. Electron-dense bodies were observed in the periplasmic and in the intercellular spaces in the vascular

parenchyma cells (Fig. 9p). Plants from T4 had epidermis with developed vacuoles with membranous inclusions and electron-dense granular cytoplasm containing abundant mitochondria with grainy matrix (Fig. 9q). The cortical parenchyma cells exhibited cytoplasm with mitochondria with grainy matrix, plastids with thylakoids and small starch grains, peroxisomes, vesicles, and vacuoles with fibrillar material (Fig. 9r). The 3endodermal cells had features similar to the other parenchyma cells. Electron-dense bodies accumulated in the intercellular spaces among the cortical cells (Fig. 9s). Parenchyma cells from the vascular system had grainy cytoplasm, mitochondria with grainy matrix, plastids with thylakoids and vesicles (Fig. 9t); the vacuoles contained fibrillar material (Fig. 9t) and membranous inclusions (Fig. 9u).

Detection of Zn and Cu in the secretory structures

The EDS spectrum of the secretory structures of *C. calophylla* plants under Zn and Cu excess detected these elements in the apical portion of the glandular emergence and inside the secretory epidermal cells (Fig. 10a-d). In plants from T2, the apical portion of the glandular emergences showed higher atomic proportion of Cu than Zn, while the glandular emergence of plants from T3 presented more Zn than Cu (Fig. 10a-b). In regard the secretory epidermal cells, plants from both treatments showed higher atomic proportion of Zn than Cu (Fig. 10c-d).

Chemical composition of the aerial vegetative axis

The analyses in high-performance liquid chromatography (HPLC) of the extracts obtained from *C. calophylla* detected differences in the number of compounds produced by plants under the four treatments. Plants from T4 and T3 produced greatest number of peaks in the chromatogram. Plants from the control treatment (T1) had the lowest number of peaks. Plants from T2 were not different from those of T1, T3 and T4 (Table 6).

Regarding the production of their medicinal compounds, there was no differences between the quantity of ellagic acid and gallic acid produced by plants from the four treatments (Table 6).

Discussion

Our results showed that excessive Zn and/or Cu can induce structural and functional changes in *C. calophylla* plants under experimental controlled conditions and that plants living in a pasture area exhibit anatomical differences in comparison to plant living in a preserved area of Atlantic Forest.

The differential data on the morphometrical anatomical features of leaves between *C. calophylla* of pasture and preserved areas can be related to the distinctive features of the soil between the areas. Samples of soil from pasture area showed higher concentrations of nutrients, as Mg, Ca, B, and especially Zn and Cu, than the soils sampling from the conserved area in the Atlantic Forest remnant. These results corroborate the studies about the quality of soils in areas destined to agriculture, which describe that pasture areas tend to have higher concentration of micronutrients in the soil, mainly zinc (Zn) and (Cu), due to the addition of supplementary salts in the food of livestock animals (Verkleji 1993; Mantovi et al. 2003; Girotto 2007; Matias et al. 2010; Ambrosini et al. 2016; Brennan et al. 2019; Scheid et al. 2019).

In addition, the soil samples from the pasture area had lower acidity level in comparison to that found in the Atlantic Forest remnant. It is known that the increase in soil pH may promote changes in the cation exchange points of its particles, which decreasing the mobility and availability of ions for plants absorption and, particularly, change the availability of Zn and Cu (Mantovi et al. 2003; Girotto et al. 2007; De Conti et al. 2016; Brennan et al. 2019). However, the pH values found for both studied regions are still within the Zn and Cu absorption range (Bell and Dell 2008; De Conti et al. 2016), therefore it is not a limiting factor for their absorption by the studied plants.

Plants of *C. caloplylla* from pasture area had leaves with more compact tissues, smaller width of palisade parenchyma cells, smaller area of intercellular spaces, smaller area of 4th order vascular bundles and smaller distance between it than plants from the preserved area. These differential morphometrical anatomical data between plants from the different areas are in agreement with data obtained by different authors in studies involving Zn and Cu excess. Reduction in mesophyll cell size, narrowing of intercellular spaces, and structural changes of vascular bundles have been reported in plants under Zn excess (Sridhar et al. 2005 2007; Kouhi et al. 2016). Likewise, plants subjected to Cu excess may present reduction in the vascular tissues, especially the xylem, as a way to reduce the translocation of this mineral through the plant's body (Martins et al. 2016). Regarding the influence of Cu on leaf mesophyll compaction, divergent reports are found in the literature. Some studies demonstrate that plants under Cu excess tend to exhibit lower rates of cell elongation and division and smaller intercellular spaces in the leaf blade (Martins et al. 2016; Li et al. 2017), while other studies report that Cu excess can increase the intercellular spaces in the leaf mesophyll (Panou-Filotheo and Bosabalidis 2004; Bini et al. 2012).

Regarding the secretory system of *C. calophylla*, plants from pasture area had higher density of secretory epidermal cells and of glandular emergences than plants of the Atlantic Forest remnant. It is known that both secretory structures produce mucilage and phenolic

compounds (Klider et al. 2020; Seixas in prep. 2021). Mucilage acts in plants as a water supply conferring protection against dehydration, and it can capture some toxic elements and chelate metals, providing a detoxification in plant organism (Kumar et al. 2018; Galloway et al. 2020). Phenolic compounds play an important role as UVB protection and it is a natural antioxidant, capturing excess of ROS (reactive oxygen species) and also some deleterious ions, as metals (Bredenkamp and Van Wyk 1999; Hossain et al. 2018). Therefore, this feature may be important for the resistance of *C. calophylla* in pasture areas.

Despite the hypotheses described above about the possible Zn and Cu excess interference in the leaf anatomy of pasture plants of *C. calophylla*, other environmental factors, besides the variation in the soil nutrients, may have influenced the leaf anatomy features, such as the level of solar radiation, water availability, temperature, among others (Dickison 2000; Rodrigues 2020). Thus, carrying out the experiment in a greenhouse was essential to evaluate the influence by Zn and Cu excess in structural and functional features of *C. calophylla*.

Under experimental conditions it was possible to identify changes in the morphological aspects of the leaf blade of plants exposed to different treatments. Plants under Zn excess had leaves with more evident areas of chlorosis and wrinkling. Leaves with gnarled-looking, wrinkling leaf edges, and areas of chlorosis are common in plants under Zn excess, which may be related to changes in Zn-dependent pathways of chlorophyll biosynthesis and chloroplast degradation under Zn excess (Wang et al. 2009; Ambrosini et al. 2016; Bulgarelli et al. 2016; Kouhi et al. 2016; Hammerschmitt et al. 2020). Our subcellular results corroborate to these changes aforementioned since plants under Zn excess (T2) had chloroplast distortions with poorly internal membranes, which may have influenced the characteristics of the leaf blade of these plants.

Individuals of *C. calophylla* kept under Cu excess presented dark green leaves with chlorosis regions. These features may be related to the interference of Cu in chloroplasts structure and function and in the activation of reactions that lead to a photosynthetic pigment degradation (Yruela 2009; Ambrosini et al. 2016; Martins et al. 2016; Li et al. 2017; Hossain et al. 2018; Hammerschmitt et al. 2020). In addition to the photosynthetic apparatus degradation, in this case chlorosis can also occur due to iron (Fe) deficiency, a necessary element for the plant photochemistry apparatus. It is known that Zn and Cu at high concentrations compete with Fe absorption sites in cell membranes, hindering Fe absorption, which intensify chlorosis and leaf senescence (Yruela 2009; Yang et al. 2011; Hossain et al. 2018; Hammerschmitt et al. 2020). In our results, leaf senescence stood out in plants under both Zn and Cu excess (T4).

Studies describe that many leaf morphological features expressed as a consequence of the toxicity by Zn and/or Cu excess can be similar to the symptoms of deficiency of these elements, such as leaf curling under Zn excess and the development of dark green leaves under Cu excess (Taiz and Zeiger 2017; Hossain et al. 2018). It may happen due to the basal tolerance mechanism or "Bottom-up strategies", since for many plants the absorption of these nutrients is hindered when those are in excess, while for other plants these elements can be accumulated in the roots through a series of chemical reactions to suppress the translocation of Zn and Cu in the plant body (Williams and Milles 2005; Yruela 2009; Kouhi et al. 2016; Li et al. 2017; Taiz and Zeiger 2017; Hossain et al. 2018; Hammerschmitt et al. 2020).

Regarding the leaf area, our results demonstrate that plants under Cu excess (T3) had smaller leaf area than plants submitted to the other experimental treatments. Reduction of the total photosynthetic area has been reported in plants under heavy metals excess (Kouhi et al. 2016; Li et al. 2017; Schwalbert et al. 2019; Hammerschmitt et al. 2020). According to Yruela (2009), Cu excess and toxicity reduce plant growth by interfering in a series of cellular reactions, as respiration and photosynthesis. According to the author, excess Cu can promote the degradation of the photosynthetic apparatus (chlorophyll, chloroplast structure, mitochondrial structure and degradation of photosynthetic cells) and therefore limits resources for cells with high metabolic activity, such as the meristematic cells.

About the anatomical features of the leaf blade, plants under Zn and/or Cu excess (T2, T3 and T4) in greenhouse presented smaller area of the intercellular spaces of the mesophyll and smaller distance between the 4th order vascular bundles, when compared to plants from the control treatment (T1). These results are similar to those found for plants from pasture area, which proves the influence of the excess of Zn (Sridhar et al. 2005; 2007; Kouhi et al. 2016) and Cu (Martins et al. 2016; Li et al. 2017) in the compaction of the leaf mesophyll of *C. calophylla* plants. This mesophyll compaction may benefit the relocation of Zn and Cu to places where they will be accumulated and immobilized, as in epidermal cells, minimizing damage in the photosynthetic tissues (Hossain et al. 2018).

Another outstanding feature was the reduction in the thickness of the outer periclinal wall of the epidermal cells on the adaxial surface of the leaf blade in plants from T3 and T4 compared to the control (T1). It is important to emphasize that most of the epidermal cells are voluminous and secrete mucilage in *C. calophylla*. Considering that there was a reduction in the thickness of the outer periclinal wall and there was no reduction in the total area of these cells, the space filled by mucilage became potentially larger in plants under the treatments with Cu excess (T3 and T4). Studies indicate that mucilage is a sequestering and immobilizing substance of metal ions (Tien et al. 2005; Lefevre et al. 2014; Kumar et al. 2018; Zhou et al.

2020; Hossain et al. 2018), therefore, the presence of mucilaginous cells in leaf epidermis could further contribute to the protection of the photosynthetic cells from the mesophyll. For the plants under Zn excess (T2), the leaves had higher density of secretory mucilaginous cells in epidermis, which can also provide greater protection to the mesophyll cells by sequestering and immobilizing this element in the epidermis (Hossain et al. 2018). In fact, thought the MEV-EDS analysis, it was possible to detect Zn and Cu inside the secretory epidermal cells, proving the uptake of these metals by these cells.

In relation to the glandular emergence, there was no differences in the density of this secretory structure between plants under Zn and/or Cu excess (T2, T3 and T4) and plants from the control treatment (T1). This result suggests that the differential density of glandular emergences found for plants in the field cannot be related to Zn and Cu excesses, but it may be related to other environmental conditions of the pasture area, as hight luminosity, mechanical damage by livestock animals and field animals, and air humidity. However, for plants under Cu excess (T3 and T4), we observed reduction in the length of the glandular emergencies, which may be related to Cu ability to inhibit cell division and elongation (Panou-Filotheou and Bosabalidis 2004; Yruela 2009; Li et al. 2017). Anyway, Zn and Cu were detected in the apex of the glandular emergences of *C. calophylla* by MEV-EDS analysis suggests the role of this structure in detoxification of plant organism by eliminating these metals outside of the plant. Studies showed that metals ions in excess can be exudate by trichomes as a mechanism of metal detoxification in plants organism, excreting the metals in order to protect plants structure against their deleterious effects in cells (Sarret et al. 2006; Harada and Choi 2008; Čiamporová et al. 2021).

Structural differences were also observed in the roots of plants under Zn and/or Cu excess. Plants of *C. calophylla* under Cu (T3) and Cu + Zn (T4) excess presented an increase of intercellular spaces of the cortical parenchyma. Several studies reveal that a higher concentration of Cu promotes the increase of intercellular spaces in the root cortex due to the deleterious effect of the oxidative stress generated (Lequeux et al. 2010; Minkina et al. 2020). Plants under Cu excess (T3) also had vessel members with thicker cell wall than plants from the control treatment (T1) and plants under Zn excess (T2). Studies indicate that Cu can be adsorbed in the cell wall because it has a strong bond with hemicellulose; in addition, this element catalyses the polymerization of lignin. Thus, the increase in Cu concentration often promotes increasement in tissues lignification as a way of retaining this element in the cell walls when it is in excess (Lin et al. 2005; Printz et al. 2016).

Regarding physiological aspects, plants under Zn excess (T2) had higher transpiration rate than the other treatments. Despite the higher transpiration rate, the other indices of gas

exchanges of plants from T2 were similar to the plants from the control treatment, showing the maintenance of photosynthesis. This result suggests that plants of *C. calophylla* under Zn excess may present mechanisms of activation and increase of the expression of Zn-dependent enzymes which are essential for carbohydrate metabolism, as the superoxide dismutase enzyme (SOD) (Hossain et al. 2018; Hammerschmitt et al. 2020). As for the plants under Cu excess (T3 and T4), it was observed that although the plants had an intercellular carbon accumulation in the leaves similar to the plants from the control treatment (T1), the assimilation rate of carbon (*A*) was lower. These results suggest that individuals under Cu and Zn-Cu excess were not efficient in metabolizing the carbon, indicating that Cu excess could reduce the RuBisCO's activity. In fact, studies had demonstrated that copper excess activates enzymatic pathways of acid phosphatase and lipoxygenase, which degrade the RuBisCO (Mira et al. 2002; Khairy et al. 2016).

Our biochemical analyses demonstrate that *C. calophylla* plants under Zn excess had a suppression of the oxidative stress in the aerial vegetative axis when compared to plants from the control treatment, as well as had a reduction of H_2O_2 in the stems and leaves. Considering that the highest density of mucilaginous epidermal cells in plants from T2, this result once more suggests the action of the epidermal mucilaginous cells in uptake Zn, avoiding its deleterious effects in the mesophyll (Kumar et al. 2018; Hossain et al. 2018; Galloway et al. 2020). In addition, these plants had a general DAB staining in the chlorenchyma cells in the leaf mesophyll, suggesting an increase of activity of Zn-dependent enzymes as SOD and ascorbate peroxidase (APX) throughout this tissue. These enzymes act on photosynthetic pathways and plays important antioxidant roles, promoting the capture and degradation of H_2O_2 (Gratão et al. 2005; Bulgarelli et al. 2016).

Regarding the amount of H_2O_2 in the aerial axis of plants under Cu excess (T3 e T4), plants from T3 exhibited results similar to plants from the control group; however, an intense DAB staining was detected mainly in palisade parenchyma cells of the leaves. It is remarkable that palisade parenchyma cells of *C. calophylla* plants under Cu excess exhibited abundant chloroplasts with very large size. Considering that chloroplasts are responsible for H_2O_2 production and accumulation of Cu when it is in excess (Briant e Lebrun 1999; Bulgarelli et al. 2016; Li et al. 2017; Schwalbert et al. 2019), the abundant and larger chloroplasts in palisade parenchyma of *C. calophylla* plants from T3 and T4 could functioning in Cu uptake.

None of the treatments with Zn and/or Cu excess (T2, T3 and T4) were able to change the levels of lipid peroxidation in the aerial vegetative axis of *C. calophylla*. However, subcellular analysis showed that plants under Zn excess (T2) and Zn + Cu excess (T4) had membranous inclusion inside the vacuoles and mitochondria and plastids with alterations in

their internal structure, while plants under Cu excess (T3) had membrane inclusion inside the vacuoles and wide chloroplasts. The occurrence of membranous inclusion in vacuoles and structural changes in the inner membranes of organelles can be signals of degeneration of phospholipid membranes in response to different stimuli, including induction by toxic substances (Nicolai and Rodrigues 2022). However biochemical results indicate that, even with a disorder in cell organelle membranes, the oxidative stress generated by excess of Zn and/or Cu was suppressed in the aerial vegetative axis probably due to the higher activity of antioxidant enzymes under stress conditions by metal toxicity, as SOD, APX, glutathione peroxidase (GPX) and glutathione reductase (GR), mainly in leaves of *C. calophylla*, avoiding higher degradation of cell membranes (Thounaojam et al. 2012; Bulgarelli et al. 2016; Martins et al. 2017; Hossain et al. 2018; Schwalbert et al. 2019).

In plants under both Zn + Cu excess (T4) it was remarkable the juxtaposition of mitochondria and chloroplasts. This organelle association has been described in several studies as a feature related in a greater dynamic in cell metabolism (Machado et al. 2018), mainly as a consequence to harsh environment (Lütz and Engel 2007; Holzinger et al. 2007; Kumar et al. 2014). Thus, this feature may be related to a higher activity of chlorenchyma cells which can promote the photosynthetic metabolism maintenance of *C. calophylla* plants under Zn and Cu excess.

In the roots, our results indicates that plants under Zn excess (T2) had higher levels of lipid peroxidation when compared to plants from the control (T1). This result corroborates the studies that describe that oxidative stress and lipid peroxidation in plants under Zn excess have greater stress expression in roots than in the aerial shoot of plants (Brunetti et al. 2011; Bulgarelli et al. 2016; Kouhi et al. 2016; Hossain et al. 2018). It is known that plants tend to accumulate metals in the root cells, promoting a cascade of reactions that inactivate metal transporting proteins, accumulating these elements mainly in the root cell organelles. This accumulation in the roots prevents the translocation of metals throughout the plant body, thus promote the protection of the photosynthetic apparatus in the aerial axis (Taiz and Zeiger 2017; Hossain et al. 2018; Hammerschmitt et al. 2020).

Furthermore, studies indicate that higher concentrations of Zn in soils favour the absorption and translocation of this element in the root promoting a nutritional disbalance, since Zn competes for absorption sites with other nutrients as Fe, Cu, Mg (Ambrosini et al. 2016; Tiecher et al. 2017). This nutritional disbalance caused by the Zn excess may have influenced the appearance of chlorosis in leaves of T2 plants. In this sense, the higher rate of lipid peroxidation in the root of plants under excess of Zn is consistent with the greater influx of this element into the roots. On the other hand, plants under Cu excess (T3 and T4), especially from

T3, had an intense DAB staining in the tissues involved in the transport of nutrients in the root cortex. This indicates that Cu accumulation in the roots can occur via apoplast, adhering to cell walls, or inside the protoplast with Cu storage inside the vacuole (Hossain et al. 2018).

Subcellular analysis of the root revelled that plants under Zn excess (T2 and T4) had mitochondria devoid of internal membranes, similar of the results found for leaves, proving that Zn acts in the disintegration of inner mitochondrial membranes (Kouhi et al. 2016; Hossain et al. 2018). In general, plants under Zn and/or Cu excess (T2, T3 and T4) had more abundant electron-dense bodies adhered in vessel elements walls of the xylem, suggesting the influx of these metal to the vascular system. Furthermore, electron-dense bodies were also observed in intercellular spaces of the root cortex of plants under Cu excess (T3 and T4), which suggest that Cu was accumulated in the apoplast of *C. calophylla* roots.

Lastly, the chemical analysis revealed that there were no differences in the quantity of ellagic acid and gallic acid produced by *C. calophylla* plants among the different treatments. However, considering the number of peaks of the chromatogram as a number of substances produced (Collins et al. 2006), plants under Cu excess (T3 and T4) had greater number of substances produced when compared to plants from the control (T1). It's known that plants under biotic and abiotic stress have their metabolic partway altered increasing the production of metabolites (Aguirre-Becerra et al. 2020). The excess of toxic metals is one of the factors that can promote changes in substances produced by plants (Lajayer et al. 2017) generating an alert for the consumption of medicinal plants from metal-contaminated soils as they may accumulate these metals in their structure and/or they can also produce harmful substances.

Conclusion

Our results demonstrate that Zn and/or Cu excess induce structural and functional changes in leaves and roots of *C. calophylla* and these organs can respond in different ways to the excess of these elements. However, *C. calophylla* plants subjected to Zn excess, despite to have demonstrated oxidative stress in the roots, had managed the suppression of the oxidative stress in the aerial vegetative axis and maintained their photosynthetic rates similar to the control plants (T1). A different result was found for plants under Cu excess (T3 and T4) that showed a reduction in photosynthetic rates. Thus, considering tolerant plants as those that have mechanisms to maintain high metabolic activity under a specific stress condition (Gaspar et al., 2002), we can suggest the tolerance of *C. calophylla* to Zn and its susceptibility to Cu.

References

AGUIRRE-BECERRA, H.; VAZQUEZ-HERNANDEZ, M.C., SAENZ, D.O.; ALVARADO-MARIANA, A., GUEVARA-GONZALEZ, R.G., GARCIA-TREJO, J.F., FEREGRINO-PEREZ, A.A. Role of stress and defense in plant secondary metabolites production. In: Bioactive natural products for pharmaceutical applications. Springer, Cham, p. 151-195, 2021.

ALEXIEVA. V.; SERGIEV, I.; MAPELLI, S.; KARANOV, E. The effect of drought and ultraviolet radiation on growth and stress markers in pea and wheat. **Plant Cell and Environment**, 24, p.1337-1344, 2001.

AMBROSINI, V.G.; SORIANI, H.H.; ROSA, D.J.; TIECHER, T.L.; GIROTTO, E.; SIMÃO, D.G.; MELO, G.W.B.; ZALAMENA, J.; BRUNETTO, G. **Impacto do excesso de cobre e zinco no solo sobre videiras e plantas de cobertura.** In: Calagem, adubação e contaminação em solos cultivados com videiras. Embrapa Uva e Vinho, p.91-110, 2016.

BELL, R.W.; DELL, B. **Micronutrients in sustainable food, feed, fibre and bioenergy production.** Paris: International Fertiliser Association, 2008.

BINI, C; WAHSHA, M.; FONTANA, S.; MALECI, L. Effects of heavy metals on morphological characteristics of *Taraxacum officinale* web growing on mine soils in NE Italy. **Journal of Geochemical Exploration**, 123, p.101-108, 2012.

BREDENKAMP, C.L; VAN WYK, A.E. Structure of mucilaginous epidermal cell walls in *Passerina* (Thymelaeaceae). **Botanical Journal of the Linnean Society**, 129, p.223-238, 1999.

BRENNAN, R.F.; PENROSE, B.; BELL, R.W. Micronutrients limiting pasture production in Australia. **Crop and Pasture Science**, 70, p.1053-1064, 2019.

BRIAT, J.F.; LEBRUN, M. Plant responses to metal toxicity. Comptes Rendus de l'Académie des Sciences-Series III - **Sciences de la Vie**, 322, p.43-54, 1999.

BRUNETTI, G.; FARRAG, K.; ROVIRA, P.S.; NIGRO, F.; SENESI, N. Greenhouse and field studies on Cr, Cu, Pb and Zn phytoextraction by *Brassica napus* from contaminated soils in the Apulia region, Southern Italy. **Geoderma**, 160, p.517-523, 2011.

BRUNETTO, G.; MIOTTO, A.; CERETTA, C.A.; SCHMITT, D.E.; HEINZEN, J.; DE MORAES, M.P.; CANTON, L.; TIECHER, T.L.; COMIN, J.J.; GIROTTO, E. Mobility of

copper and zinc fractions in fungicide-amended vineyard sandy soils. **Archives of Agronomy Soil Science**. 60, p.609–624, 2014.

BULGARELLI, R.G.; ARAUJO, P.; TEZOTTO, T.; MAZZAFERA, P.; ANDRADE, S. A. L. Expression of metallothionein genes in coffee leaves in response to the absence or excess of Cu and Zn. **Theoretical and Experimental Plant Physiology**, 28, p.371-383, 2016.

CAVALCANTI, T.B.; GRAHAM, S. **Lythraceae**. In: Wanderley, M.G.L., Shepherd, G.J., Giulietti, A.M., Melhem, T.S., Bittrich, V., Kameyama, C. (eds.) - Flora Fanerogâmica do Estado de São Paulo. Instituto de Botânica, São Paulo, 2, p.163-180, 2002.

ČIAMPOROVÁ, M.; NADUBINSKÁ, M.; BANÁSOVÁ, V.; ĎURIŠOVÁ, E.; ZELINOVÁ, V.; HORAK, O.; GRUBER, D.; LICHTSCHEIDL, I.K. Structural traits of leaf epidermis correspond to metal tolerance in *Rumex acetosella* populations growing on metal-contaminated soils. **Protoplasma**, p.1-14, 2021.

COLLINS, C.H.; BRAGA, G.L.; BONATO, P.S. Fundamentos de cromatografia. In **Fundamentos de cromatografia**, Universidade Estadual de Campinas, editora da Unicamp, 2006.

CUNHA, A.R.; MARTINS, D. Classificação climática para os municípios de Botucatu e São Manuel, SP. **Irriga**, 14, p.1-11, 2009.

DE CONTI, L.; CERRETA, C.A.; FERREIRA P.A.A.; LOURENZI, C.R.; GIROTTO, E.; LOURENSINI, F.; TIECHER, T.L.; MARCHEZEN, C.; ANCHIETA, M.G.; BRUNETTO, G. Soil solution concentrations and chemical species of copper and zinc in a soil with a history of pig slurry application and plant cultivation. **Agriculture, Ecosystems and Environment**, 216, p.374-386, 2016.

DEMBOGURSKI, D.S.O.; TRENTIN, D.S.; BOARETTO, A.G.; RIGO, G.V.; SILVA, R.C.; TASCA, T.; MACEDO, A.J.; CAROLLO, C.A.; SILVA, D. B. Brown propolis-metabolomic innovative approach to determine compounds capable of killing *Staphylococcus aureus* biofilm and *Trichomonas vaginalis*. **Food Research International**, 111, p.661-673, 2018.

DICKISON, W. **Integrative Plant Anatomy**. New York, 2000.

FACCO, M. G. **Estudo taxonômico do gênero *Cuphea* P. Browne (Lythraceae) no Rio Grande do Sul.** Federal University of Rio Grande do Sul, Brasil. 2015.

GALLOWAY, A.F.; KNOX, P.; KRAUSE, K. Sticky mucilages and exudates of plants: putative microenvironmental design elements with biotechnological value. **New Phytologist**, 225, p.1461-1469, 2020.

GASPAR, T., FRANCK, T., BISBIS, B., KEVERS, C., JOUVE, L., HAUSMAN, J. F., DOMMES, J. Concepts in plant stress physiology. Application to plant tissue cultures. **Plant Growth Regulation**, 37, p.263-285, 2002.

GIAMPAOLI, P.; TRESMONDI, F.; LIMA, G.P.P.; KANASHIRO, S.; ALVES, E.S.; DOMINGOS, M.; TAVARES, A.R. Analysis of tolerance to copper and zinc in *Aechmea blanchetiana* grown in vitro. **Biologia Plantarum**, 56, p.83-88, 2012.

GIROTTO, E. **Cobre e zinco no solo sob uso intensive de dejeto líquido de suínos**. Universidade Federal de Santa Maria, Centro de Ciências Rurais, p.01-121, 2007.

GIROTTO, E.; CERETTA, C.A.; ROSSATO, L.V.; FARIAS, J.G.; TIECHER, T.L.; DE CONTI, L.; SCHMATZ, R.; BRUNETTO, G.; SCHETINGER, M.R.C.; NICOLOSO, F.T. Triggered antioxidant defense mechanism in maize grown in soil with accumulation of Cu and Zn due to intensive application of pig slurry. **Ecotoxicology and Environmental Safety**. 93, p.145–155, 2013.

GRATÃO, P.L.; POLLE, A.; LEA, P.J.; AZEVEDO, R.A. Making the life of heavy metal-stressed plants a little easier. **Functional Plant Biology**, 32, p.481-494, 2005.

GUIMARÃES, P.R., AMBROSINI, V.G., MIOTTO, A., CERETTA, C.A., SIMÃO, D.G., BRUNETTO, G. Black oat (*Avena strigosa* Schreb.) growth and root anatomical changes in sandy soil with different copper and phosphorus concentrations. **Water Air Soil Pollution**. 227, 192, 2016.

HAMMERSCHMITT, R.K.; TIECHER, T.L.; FACCO, D.B.; SILVA, L.O.; SCHWALBERT, R.; DRESCHER, G. L.; TRENTIN, E.; SOMAVILLA, L.M.; KULMANN, M.S.S.; SILVA, I.C.B.; TAROUCO, C.P.; NICOLOSO, F.T.; TIECHER, T.; MAYER, N.A; KRUG, A.V.; BRUNETTO, G. Copper and zinc distribution and toxicity in 'Jade'/'Genovesa' young peach tree. **Scientia Horticulturae**, 259, n.108763, 2020.

HARADA, E.; CHOI, Y.E. Investigation of metal exudates from tobacco glandular trichomes under heavy metal stresses using a variable pressure scanning electron microscopy system. **Plant Biotechnology**, 25, p. 407-411, 2008.

HEATH, R.L.; PACKER, L. Photoperoxidation in isolated chloroplasts. I. Kinetics and stoichiometry of fatty acid peroxidation. **Archives in Biochemistry and Biophysics**, 125, p.189-198, 1968.

HOAGLAND, D.R.; ARNON, D.I. **The water culture method for growing plants without soils.** California Agriculture Experimental Station, Berkeley, CA, 1950.

HOLZINGER, A.; BUCHNER, O.; LÜTZ, C.; HANSON, M.R. Temperature sensitive formation of chloroplast protrusions and stromules in mesophyll cells of *Arabidopsis thaliana*. **Protoplasma**, 230, p. 23-30, 2007.

HOSSAIN, M.A.; KAMIYA, T.; BURRITT, D.; TRAN, L.S.P.; FUJIWARA, T. (EDS.). **Plant macronutrient use efficiency: molecular and genomic perspectives in crop plants**. Academic Press, Elsevier Inc, 2018.

JOHANSEN, D.A. **Plant microtechnique**. New York: Mc. Graw-Hill Book, p 530, 1940.

KHAIRY, A.I.H.; OH, M.J.; LEE, S.M.; ROH, K.S. Nitric oxide overcomes Cd and Cu toxicity in in vitro-grown tobacco plants through increasing contents and activities of rubisco and rubisco activase. **Biochimie open**, 2, p.41-51, 2016.

KLIDER, L. M. MACHADO, C.D.; ALMEIDA, V.P.; TIRLONI, C.A.S.; MARQUES, A.A.M.; PALOZI, R.A.C.; LORENÇONE, B.R.; ROMÃO, P.V.M.; GUARNIER, L.P.; CASSERIMO, N.S.; SILVA, D.B.; CAVALCANTI, T.B.; RAMAN, V.; KHAN, I.A.; JUNIOR, A.G.; BUDEL, J.M. Cuphea calophylla var. mesostemon (Koehne) SA Graham: A Whole-Ethnopharmacological Investigation. **Journal of Medicinal Food**, 24, p.394-410, 2020.

KOUHI, S.M.M.; LAHOUTI, M.; GANJEALI, A.; ENTEZARI, M.H. Anatomical and ultrastructural responses of *Brassica napus* after long-term exposure to excess zinc. **Turkish Journal of Biology**, 40, p.652-660, 2016.

KUMAR, A.; DINESH-KUMAR, S.P.; CAPLAN, J. STROMULES. In: **Theg S, Wollman F (eds) Adv plant biol: plastid biology**, 5. Springer, New York, p. 189–207, 2014.

KUMAR, S.S.; GIRISH-PATIL, B.G.; GIRIDHAR, P. Mucilaginous polysaccharides from vegetative parts of *Bixa orellana* L.: Their characterization and antioxidant potential. **Journal of food biochemistry**, 43, e12747, 2018.

LAJAYER, B.A.; GHORBANPOUR, M.; NIKABADI, S. Heavy metals in contaminated environment: destiny of secondary metabolite biosynthesis, oxidative status and

phytoextraction in medicinal plants. **Ecotoxicology and Environmental Safety**, 145, p.377-390, 2017.

LEFÈVRE, I.; VOGEL-MIKUS, K.; JEROMEL, J.; VAVPETIČ, P.; PLANCHON, S.; ARČON, I.; VAN ELTEREN, J.T.; LEPOINT, G.; GOBERT, S.; RENAUT, J.; PELICON, P.; LUTTS, S. Cadmium and zinc distribution in relation to their physiological impact in the leaves of the accumulating *Zygophyllum fabago* L. **Plant, Cell & Environment**, 37, p.1299-1320, 2014.

LEQUEUX, H.; HERMANS, C.; LUTTS, S.; VERBRUGGEN, N. Response to copper excess in *Arabidopsis thaliana*: impact on the root system architecture, hormone distribution, lignin accumulation and mineral profile. **Plant Physiology and Biochemistry**, 48, p.673-682, 2010.

LI, S.; WANG, Y.; MAHMOOD, Q.; CHEN, J.; WU, J.; YE, Z.; LIU, D. Cu induced changes of ultrastructure and bioaccumulation in the leaf of *Moso bamboo* (Phyllostachys pubescens). **Journal of Plant Nutrition**, 41, p.288-296, 2017.

LIN, C.C.; CHEN, L.M.; LIU, Z.H. Rapid effect of copper on lignin biosynthesis in soybean roots. **Plant Science**, 168, p.855-861, 2005.

LORENZI, H.; MATOS, F.J.A. **Plantas medicinais no Brasil: nativas e exóticas cultivadas**. Nova Odessa: Instituto Plantarum, p.512, 2002.

LUSA, M.G.; BIASI, L.A. Estaquia de *Cuphea calophylla* subsp. *mesostemon* (Koehne) Lourteig (Lythraceae). **Revista Brasileira de Plantas Medicinais,** 13, p.52-57, 2011.

LÜTZ, C.; ENGEL, L. Changes in chloroplast ultrastructure in some high-alpine plants: adaptation to metabolic demands and climate? **Protoplasma**, 231, p.183–192, 2007.

MACHADO, S.R.; GREGÓRIO, E.A.; RODRIGUES, T.M. Structural associations between organelle membranes in nectary parenchyma cells. **Planta,** v. 247, p.1067-1076, 2018.

MANTOVI, P.; BONAZZI, G.; MAESTRI, E.; MARMIROLI, N. Accumulation of copper and zinc from liquid manure in agricultural soils and crop plants. **Plant and soil**, 250, p.249–257, 2003.

MARSOLA, T.; MIYAZAWA, M.; PAVAN, M.A. Acumulação de cobre e zinco em tecidos do feijoeiro em relação com o extraído do solo. **Revista Brasileira de Engenharia Agrícola e Ambiental**, 9, p.92-98, 2005.

MARTINS, J.P.R.; MARTINS, A.D.; PIRES, M.F.; JUNIOR, R.A.B.; REIS, R.O.; DIAS, G.D.M.G.; PASQUAL, M. Anatomical and physiological responses of *Billbergia zebrina* (Bromeliaceae) to copper excess in a controlled microenvironment. **Plant Cell, Tissue and Organ Culture** (PCTOC), 126, p.43-57, 2016.

MATIAS, J.L.; CERETTA, C.A.; NESI, C.N.; GIROTTO, E.; TRENTIN, E.E.; LOURENZI, C.R.; VIEIRA, R.C. Cupper, zinc and manganese in soils of two watersheds in Santa Catarina with intensive use of pig slurry. **Revista Brasileira de Ciências do Solo**, 34, p.1445-1454, 2010.

MINKINA, T.; RAJPUT, V.; FEDORENKO, G.; FEDORENKO, A.; MANDZHIEVA, S.; SUSHKOVA, S.; MORIN, T.; YAO, J. Anatomical and ultrastructural responses of Hordeum sativum to the soil spiked by copper. **Environmental Geochemistry and Health**, 42, p.45-58, 2020.

MIRA, H.; MARTÍNEZ, N.; PEÑARRUBIA, L. Expression of a vegetative-storage-protein gene from *Arabidopsis* is regulated by copper, senescence and ozone. **Planta**, 214, p.939-946, 2002.

NAGAJYOTI, P.C.; LEE, K.D.; SREEKANTH, T.V.M. Heavy metals, occurrence and toxicity for plants: a review. **Environmental Chemistry Letters**, 8, p.199-261, 2010.

NICOLAI, J.; RODRIGUES, T.M. Cell wall thickenings and tylosoid: developmental morphology reveals novelties for secretory canals in *Protium ovatum* (Burseraceae). **Journal of Plant Research**, 1-11, 2022.

O'BRIEN, T.P.; FEDER N.; MCCULLY M.E. Polychromatic staining of plant cell walls by toluidine blue. **Protoplasma**, 59, p. 368-373, 1964.

PANOU-FILOTHEOU, H.; BOSABALIDIS, A.M. Root structural aspects associated with copper toxicity in oregano (*Origanum vulgare* subsp. *hirtum*). **Plant Science**, 166, p.1497-1504, 2004.

PRINTZ, B.; LUTTS, S.; HAUSMAN, J. F.; SERGEANT, K. Copper trafficking in plants and its implication on cell wall dynamics. **Frontiers in Plant Science**, 7, p.601, 2016.

RAMÍREZ-ATEHORTÚA, A.M.; MORALES-AGUDELO, L.; OSORIO, E.; LARA-GUZMÁN, O.J. The traditional medicinal plants *Cuphea calophylla*, *Tibouchina kingii*, and

Pseudelephantopus spiralis attenuate inflammatory and oxidative mediators. **Evidence-Based Complementary and Alternative Medicine**, p.01-11, 2018.

REYNOLDS, E.S. The use of lead citrate at high pH as an electron-opaque stain in electron microscopy**. Journal of Cell Biology**, 17, PMID:13986422, 1963.

RODRIGUES, M.; ROCHA, D.I.; MENDONÇA, A.M.D.C.; SILVA, L.C.D.; FESTUCCI-BUSELLI, R.A.; OTONI, W.C. Leaf anatomy micromorphometry plasticity and histochemistry of *Azadirachta indica* during acclimatization. **Rodriguésia**, 71, 2020.

ROSSETTI, S.; BONATTI, P.M. In situ histochemical monitoring of ozone-and TMV-induced reactive oxygen species in tobacco leaves. **Plant Physiology and Biochemistry**, 39, p.433-442, 2001.

SANTOS, M. C., TOSON, N. S., PIMENTEL, M. C., BORDIGNON, S. A., MENDEZ, A. S., & HENRIQUES, A. T. Polyphenols composition from leaves of *Cuphea* spp. and inhibitor potential, in vitro, of angiotensin I-converting enzyme (ACE). **Journal of ethnopharmacology**, 255, p.112781, 2020.

SARRET, G.; HARADA, E.; CHOI, Y.E.; ISAURE, M.P.; GEOFFROY, N.; FAKRA, S.; MARCUS, M.A.; BIRSCHWILKS, M.; CLEMENS, S.; MANCEAU, A. Tobacco detoxify toxic levels of zinc by exuding Zn-substituted calcite and Zn phosphate through the trichomes. Plant Physiology, 41, p.1021–1034, 2006.

SCHEID, D.L.; SILVA, R.F.D.; SILVA, V.R.D.; ROS, C.O.D.; PINTO, M.A.B.; GABRIEL, M.; CHERUBIN, M.R. Changes in soil chemical and physical properties in pasture fertilised with liquid swine manure. **Scientia Agricola**, 77, e20190017, 2019.

SCHWALBERT, R.; SILVA, L.O.; SCHWALBERT, R.A.; TAROUCO, C.P.; FERNANDES, G.S.; MARQUES, A.C.; COSTA, C.C.; HAMMERSCHMITT, R.K.; BRUNETTO, G.; NICOLOSO, F.T. Physiological responses of soybean (*Glycine max* (L.) Merrill) cultivars to copper excess. **Anais da Academia Brasileira de Ciências**, 91, e20190121, 2019.

SILVA, A.L.O.; BARROCAS, P.R.; JACOB, S.C.; MOREIRA, J.C. Dietary intake and health effects of selected toxic elements. **Brazian Journal of Plant Physiology**, 17, p.79–93, 2005.

SRIDHAR, B.B.M.; DIEHL, S.V.; HAN, F.X.; MONTS, D.L.; SU, Y. Anatomical changes due to uptake and accumulation of Zn and Cu in Indian mustard (*Brassica juncea*). **Environmental and Experimental Botany**, 54, p.131-141, 2005.

SRIDHAR, B.B.M.; HAN, F.X.; DIEHL, S.V.; MONTS, D.L.; SU, Y. Effects of Zn e Cu accumulation on structural and physiological characteristics of barley plants. **Brazilian Plant Physiology**, 19, p.15-22, 2007.

TAIZ, L.; ZEIGER, E.; MØLLER, I.M.; MURPHY, A. **Fisiologia e desenvolvimento vegetal**. Artmed Editora, 2017.

TIECHER, T.L.; TIECHER, T.; CERETTA, C.A.; FERREIRA, P.A.A.; NICOLOSO, F.T.; SORIANI, H.H.; DE CONTI, L.; KULMANN, M.S.S.; SCHNEIDER, R.O.; BRUNETTO, G. Tolerance and translocation of heavy metals in young grapevine (*Vitis vinifera*) grown in sandy acidic soil with interaction of high doses of copper and zinc. **Science Horticulturae**, 222, p.203-212, 2017.

TIECHER, T.L.; SORIANI, H.H.; TIECHER, T.; CERETTA, C.A.; NICOLOSO, F.T.; TAROUCO, C.P.; CLASEN, B.E.; DE CONTI, L.; TASSINARI, A.; MELO, G.W.B.; BRUNETTO, G. The interaction of high copper and zinc doses in acid soil changes the physiological state and development of the root system in young grapevines (*Vitis vinifera*). **Ecotoxicology and Environmental Safety**, 148, p.985-994, 2018.

TIEN, C.J.; SIGEE, D.C.; WHITE, K.N. Copper adsorption kinetics of cultured algal cells and freshwater phytoplankton with emphasis on cell surface characteristics. **Journal of Applied Phycology**, 17, p.379-389, 2005.

THOMPSON, A.E. *Cuphea* - a potential new crop. **HortScience**, p.352-354, 1984.

THOUNAOJAM, T.C.; PANDA, P.; MAZUMDAR, P.; KUMAR, D.; SHARMA, G.D.; SAHOO, L.; SANJIB, P. Excess copper induced oxidative stress and response of antioxidants in rice. **Plant Physiology and Biochemistry**, 53, p.33-39, 2012.

VERKLEJI, J.A.S. **The effects of heavy metals stress on higher plants and their use as bio monitors.** In: Markert, B. (ed) Plant as bioindicators: indicators of heavy metals in the terrestrial environment. New York: VCH, p.415-424, 1993.

WANG, C.; ZHANG, S.H.; WANG, P.F.; HOU J.; ZHANG W.J.; LI, W.; LIN, Z.P. The effect of excess Zn on mineral nutrition and antioxidative response in rapeseed seedlings. **Chemosphere**, 75, p.1468-1476, 2009.

WATSON, M.L. Staining of tissue sections for electron microscopy with heavy metals. **The Journal of Biophysical and Biochemical Cytology**, 4, p.475–478, 1958.

WILLIAMS, L.E.; MILLS, R.F. P1B-ATPases – an ancient family of transition metal pumps with diverse functions in plants. **Trends Plant Science,** 10, p.491-502, 2005.

YANG, Y.; SUN, C.; YAO, Y.; ZHANG, Y.; ACHAL, V. Growth and physiological responses of grape (*Vitis vinifera* "Combier") to excess zinc. **Acta Physiologiae Plantarum,** 33, p.1483-1491, 2011.

YRUELA, I. Copper in plants. **Brazilian Journal of Plant Physiology**, 17, p.145-156, 2005.

YRUELA, I. Copper in plants: acquisition, transport and interactions. **Functional Plant Biology**, 36, p.409-430, 2009.

ZHANG, S.; LI, Q.; MA, K.; CHEN, L. Temperature-dependent gas exchange and stomatal/non-Stomatal limitation to CO2 assimilation of *Quercus liaotungensis* under midday high irradiance. **Photosynthetica**, 39, p.383-388, 2001.

ZHOU, M.X.; CLASSEN, B.; AGNEESSENS, R.; GODIN, B.; LUTTS, S. Salinity improves Zinc resistance in *Kosteletzkya pentacarpos* in relation to a modification in mucilage and polysaccharides composition. **International Journal of Environmental Research**, 14, p.323-333, 2020.

Tables

Table 1. Chemical analysis of soil from the Atlantic Forest remnant and pasture area.

Area		Chemical features														
		pH	M.O.	P.resin	H+Al	K	Ca	Mg	SB	CTC	V%	B	Cu	Fe	Mn	Zn
		$CaCl_2$	g/dm^3	mg/dm^3	----------$mmol_c/dm^3$----------							---------mg/dm^3-------				
Atlantic Forest remnant	Sample 1	4,4	28	9	33	1,0	11	10	22	54	40	0,27	0,3	103	10,4	1,4
	Sample 2	4,3	16	6	30	0,4	3	3	6	36	18	0,24	0,2	55	11,6	0,7
Pasture area	Sample 1	5,1	42	34	26	2,6	41	24	67	93	72	0,41	1,5	101	8,3	22,0
	Sample 2	5,0	49	39	29	3,2	35	28	67	96	69	0,40	1,2	76	6,8	6,8

Table 2. Morphological features of *Cuphea calophylla* plants under different concentrations of Zn and/or Cu.

Treatments	Morphological features						
	Diameter of the apical buds (mm)	Length of the leaf blade (mm)	Width of the leaf blade (mm)	Area of the leaf blade (cm^2)	Length of the stem (cm)	Diameter of the stem (mm)	Length of the root system (cm)
T1	1,02 ± 0,06	15,52 ± 0,78	10,57 ± 0,77	1,45 ± 0,14 a	26,75 ± 1,05	0,90 ± 0,07	21,8 ± 2,93
T2	1,05 ± 0,10	19,07 ± 1,55	13,20 ± 1,34	1,44 ± 0,14 a	28,70 ± 0,81	0,82 ± 0,06	31,2 ± 1,60
T3	1,16 ± 0,05	15,26 ± 0,53	09,94 ± 0,54	0,95 ± 0,07 b	30,10 ± 0,95	1,08 ± 0,06	25,7 ± 2,13
T4	1,01 ± 0,06	16,82 ± 1,26	11,34 ± 0,76	1,11 ± 0,09 ab	30,60 ± 1,42	0,97 ± 0,04	24,4 ± 1,46

T1 = control (0.11g/ L of Zn and 0.04g/L of Cu); T2 = excess of Zn (0.22g/L); T3 = excess of Cu (0.10g/L); T4 = excess of Zn and Cu (0.22g/L of Zn and 0.10g/L of Cu).
Mean values ± standard error (n=10). Means were compared using the Tukey test.
Values followed by different letters indicate significant differences ($p < 0.05$).

Table 3. Leaf blade anatomical measurements of *Cuphea calophylla* plants from a remnant of Atlantic Forest and a pasture area.

Anatomical features	**Areas**		**Significance***
	Atlantic Forest remnant	**Pasture area**	**(p < 0,05)**
Length of glandular emergencies (µm)	461,16 ± 131,97	534,32 ± 104,86	n.s.
Density of glandular emergencies (glandular emergencies /µm^2)	0,67 ± 0,24	1,51 ± 0,53	*
Thickness of the outer periclinal wall of epidermal cells (adaxial face) (µm)	4,64 ± 0,14	5,73 ± 0,46	n.s.
Area of the secretory epidermal cells (adaxial face) (µm^2)	666,08 ± 35,94	575,12 ± 58,31	n.s.
Density of secretory epidermal cells (adaxial face) (µm^2)	28,12 ± 4,34	39,79 ± 6,37	*
Thickness of the leaf blade (µm)	130,79 ± 5,57	138,20 ± 2,92	n.s.
Thickness of the mesophyll (µm)	96,65 ± 5,61	105,24 ± 2,64	n.s.
Thickness of the palisade parenchyma (µm)	41,78 ± 2,52	49,03 ± 3,06	n.s.
Thickness of the spongy parenchyma (µm)	55,33 ± 3,79	60,15 ± 3,55	n.s.
Width of palisade parenchyma cells (µm)	11,14 ± 0,45	9,54 ± 0,40	*
Area occupied by intercellular spaces in the spongy parenchyma (µm^2)	380,56 ± 17,96	242,14 ± 17,94	*

Area of 4th order vascular bundles (μm^2)	1744,93 ± 148,51	1217,58 ± 102,59	*
Distance between the 4th order vascular bundles (µm)	330,53 ± 27,55	142,52 ± 12,76	*
Area occupied by vascular tissues in the midrib (μm^2)	27572,56 ± 1950,56	30104,17 ± 1846,94	n.s.

Mean ± standard error (n=10). Means were compared using the Student t test. Significant differences ($p < 0.05$) were indicated with (*) and non-significant differences indicated with (n.s.).

Table 4. Leaf blade anatomical measurements of *Cuphea calophylla* plants under different concentrations of Zn and/or Cu.

Anatomical features	**Treatments**			
	T1	T2	T3	T4
Length of glandular emergencies (µm)	532,41 ± 36,48 a	466,61 ± 78,82 ab	372,38 ± 74,16 b	405,04 ± 58,26 b
Density of glandular emergencies (glandular emergencies /µm^2)	0,34 ± 0,10	0,41 ± 0,13	0,36 ± 0,21	0,32 ± 0,09
Thickness of the outer periclinal wall of epidermal cells (adaxial face) (µm)	5,55 ± 0,57 a	4,14 ± 0,20 ab	3,77 ± 0,26 b	3,98 ± 0,31 b
Area of the secretory epidermal cells (adaxial face) (µm^2)	693,18 ± 52,89	563,17 ± 59,05	597,50 ± 34,08	637,89 ± 57,33
Density of secretory epidermal cells (adaxial face) (µm^2)	10,17 ± 2,36 ab	15,98 ± 5,57 a	12,72 ± 5,72 ab	06,73 ± 03,06 b
Thickness of the leaf blade (µm)	109,96 ± 1,85	109,99 ± 3,96	112,52 ± 3,01	109,48 ± 1,32
Thickness of the mesophyll (µm)	80,72 ± 1,54	80,75 ± 3,14	84,28 ± 2,50	79,65 ± 1,58
Thickness of the palisade parenchyma (µm)	55,84 ± 1,55	54,59 ± 1,47	53,69 ± 1,36	52,29 ± 1,75
Thickness of the spongy parenchyma (µm)	31,55 ± 1,02	31,29 ± 1,40	30,52 ± 1,34	29,73 ± 0,94
Width of palisade parenchyma cells (µm)	8,87 ± 0,31	8,37 ± 0,28	8,62 ± 0,26	8,58 ± 0,44
Area occupied by intercellular spaces in the spongy parenchyma (µm^2)	155,58 ± 7,25 a	141,72 ± 9,50 ab	113,37 ± 8,09 bc	93,50 ± 9,08 c

Area of 4th order vascular bundles (μm^2)	930,17 ± 35,42 b	1176,46 ± 111,88 ab	976,21 ± 32,08 ab	1280,69 ± 107,20 a
Distance between the 4th order vascular bundles (µm)	198,19 ± 14,64 a	178,83 ± 20,72 a	109,43 ± 10,57 b	153,97 ± 11,78 ab
Area occupied by vascular tissues in the main vein (μm^2)	17107,00 ± 1545,52	18764,10 ± 1649,78	20148,82 ± 2180,99	25249,59 ± 2678,64

T1 = control (0.11g/ L of Zn and 0.04g/L of Cu); T2 = excess of Zn (0.22g/L); T3 = excess of Cu (0.10g/L); T4 = excess of Zn and Cu (0.22g/L of Zn and 0.10g/L of Cu).
Mean ± standard error (n=10). Means were compared using the Tukey test. Values followed by different letters indicate significant differences ($p < 0.05$).

Table 5. Root anatomical measurements of *Cuphea calophylla* plants under different concentrations of Zn and/or Cu.

Anatomical features	**Treatments**			
	T1	T2	T3	T4
Thickness of the epidermis (µm)	16,64 ± 0,60	16,26 ± 0,61	17,09 ± 0,60	17,22 ± 0,53
Thickness of the cortex (µm)	109,11 ± 7,63	130,32 ± 6,69	130,82 ± 5,01	128,12 ± 5,55
Area occupied by intercellular spaces in the cortex (μm^2)	572,38 ± 66,96 b	769,80 ± 84,89 ab	951,35 ± 104,86 a	1097,43 ± 71,00 a
Area of the vascular system (μm^2)	13924,09 ± 2040,42	14464,26 ± 799,31	16147,26 ± 1123,66	15932,07 ± 1844,37
Thickness of vessel member walls (µm)	1,87 ± 0,10 b	1,83 ± 0,13 b	2,52 ± 0,11 a	2,33 ± 0,17 ab

T1 = control (0.11g/ L of Zn and 0.04g/L of Cu); T2 = excess of Zn (0.22g/L); T3 = excess of Cu (0.10g/L); T4 = excess of Zn and Cu (0.22g/L of Zn and 0.10g/L of Cu).
Mean ± standard error (n=10). Means were compared using the Tukey test. Values followed by different letters indicate significant differences ($p < 0.05$).

Table 6. Chemical characteristics and quantity of ellagic acid and gallic acid by high-performance liquid chromatography (HPLC) in the methanolic extract of *Cuphea calophylla* aerial vegetative axis under different concentrations of Zn and/or Cu.

Treatments	Number of peaks in the chromatogram	[ellagic acid] (mg ellagic acid g^{-1} dry aerial vegetative axis)	[gallic acid] (mg gallic acid g^{-1} dry aerial vegetative axis)
T1	43,33 ± 1,53 b	08,94 ± 01,48	173,75 ± 57,25
T2	48,33 ± 3,06 ab	08,89 ± 04,06	180,75 ± 78,24
T3	49,67 ± 1,53 a	07,68 ± 02,03	189,23 ± 04,67
T4	50,33 ± 3,06 a	10,16 ± 03,09	220,27 ± 06,82

T1 = control (0.11g/ L of Zn and 0.04g/L of Cu); T2 = excess of Zn (0.22g/L); T3 = excess of Cu (0.10g/L); T4 = excess of Zn and Cu (0.22g/L of Zn and 0.10g/L of Cu).
Mean values ± standard error (n=10). Means were compared using the Tukey test. Values followed by different letters indicate significant differences ($p < 0.05$).

Figures

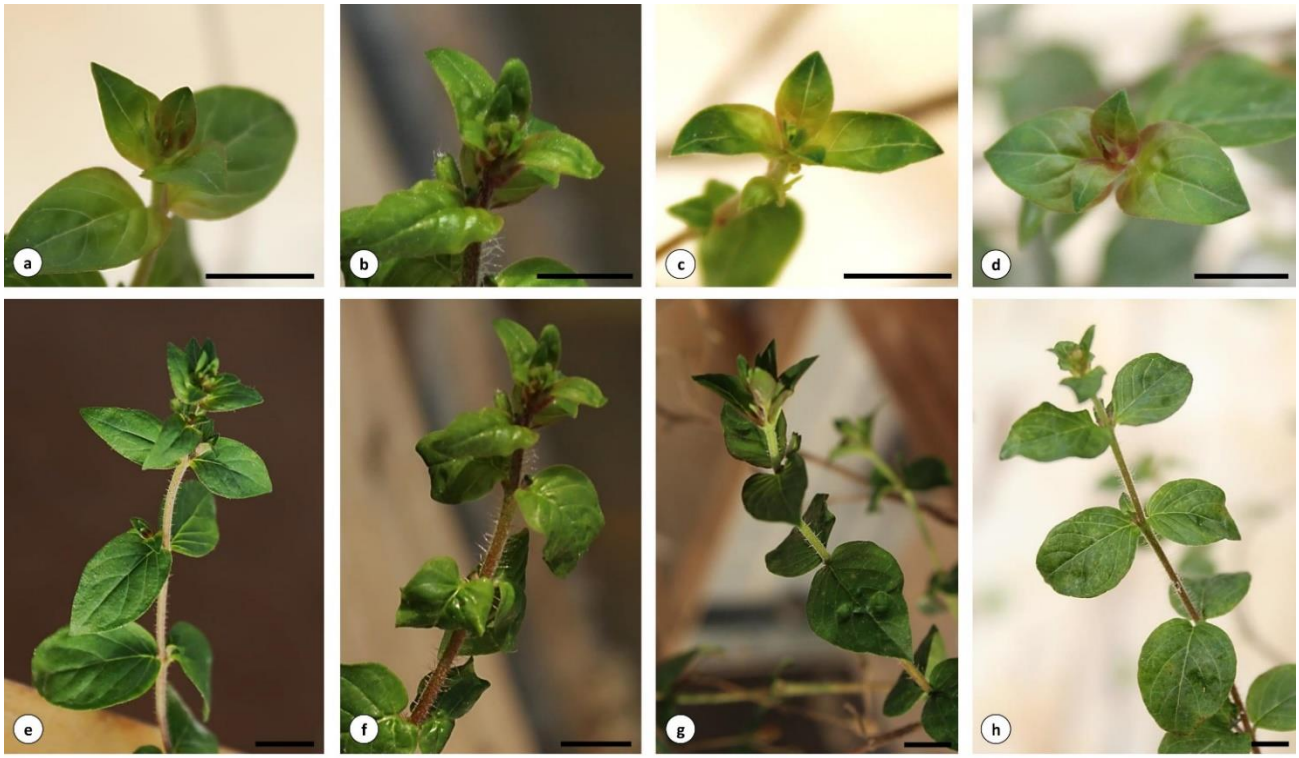

Figure 1. Photographs of *C. calophylla* plants under the experimental treatments with Zn and/or Cu excess. **a**, **e**. T1 = control (0.11g/ L of Zn and 0.04g/L of Cu). **b**, **f**. T2 = excess of Zn (0.22g/L). **c**, **g**. T3 = excess of Cu (0.10g/L). **d**, **h**. T4 = excess of Zn and Cu (0.22g/L of Zn and 0.10g/L of Cu). **a.** Leaf primordia showed a greenish colour. **b-d**. Leaf primordia and young leaves from plants under T2, T3 and T4 treatments showed scattered chlorosis regions, wrinkled appearance and reddish basal portion. **e**. Expanded leaves of plants under T1 treatment with greenish leaf blade, without chlorosis. **f**. Expanded leaves of plants under T2 treatment showed greenish leaf blade with scattered chlorosis, and leaf blade with wrinkled and twisted edge facing downwards. **g**. Expanded leaves of plants under T3 treatment with leaf blade in dark green colour and portions close to the midrib showed with a wrinkled appearance. **h**. Expanded leaves of plants under T4 treatment with green leaf blade, wrinkled appearance and slightly twisted edge, presenting a senescent appearance, with scattered chlorosis. Scale bars: 5 mm (a-h).

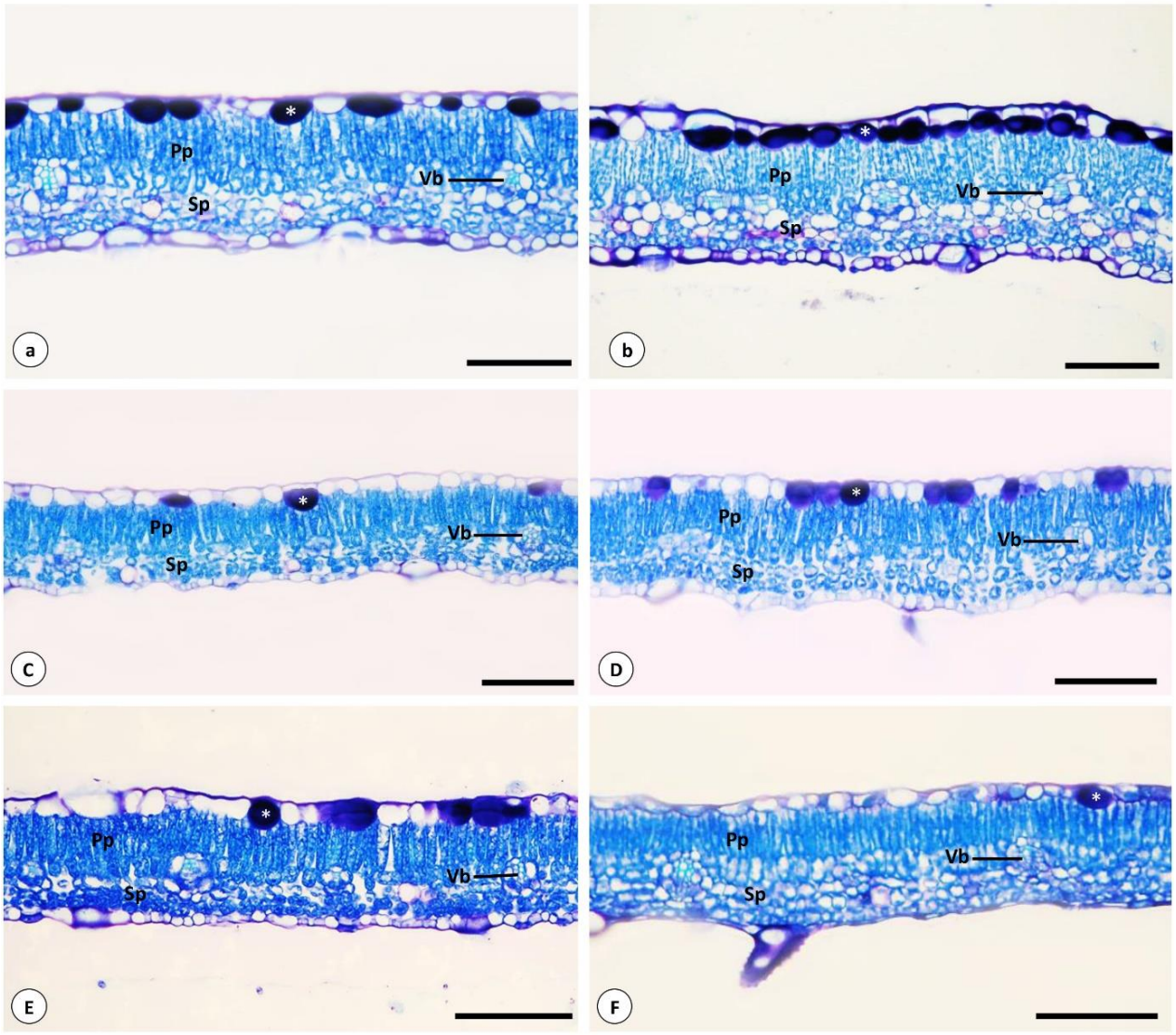

Figure 2. Photomicrographs of cross-sections of the leaf blade of *C. calophylla* plants from field conditions (**a**, **b**) and plants from the greenhouse experiment (**c-f**) showing uniseriate epidermis with secretory cells in the adaxial surface of the leaf blade, dorsiventral mesophyll and collateral vascular bundles. **a**. Plant from Atlantic Forest remnant. **b**. Plant from pasture area. **c**. Plant from T1 = control (0.11g/ L of Zn and 0.04g/L of Cu). **d**. Plant from T2 = excess of Zn (0.22g/L). **e**. Plant from T3 = excess of Cu (0.10g/L). **f**. Plant from T4 = excess of Zn and Cu (0.22g/L of Zn and 0.10g/L of Cu). **Pp** - palisade parenchyma; **Sp** - spongy parenchyma; **Vb** - vascular bundle; (*) secretory epidermal cell. Scale bars: 100 µm (a-f).

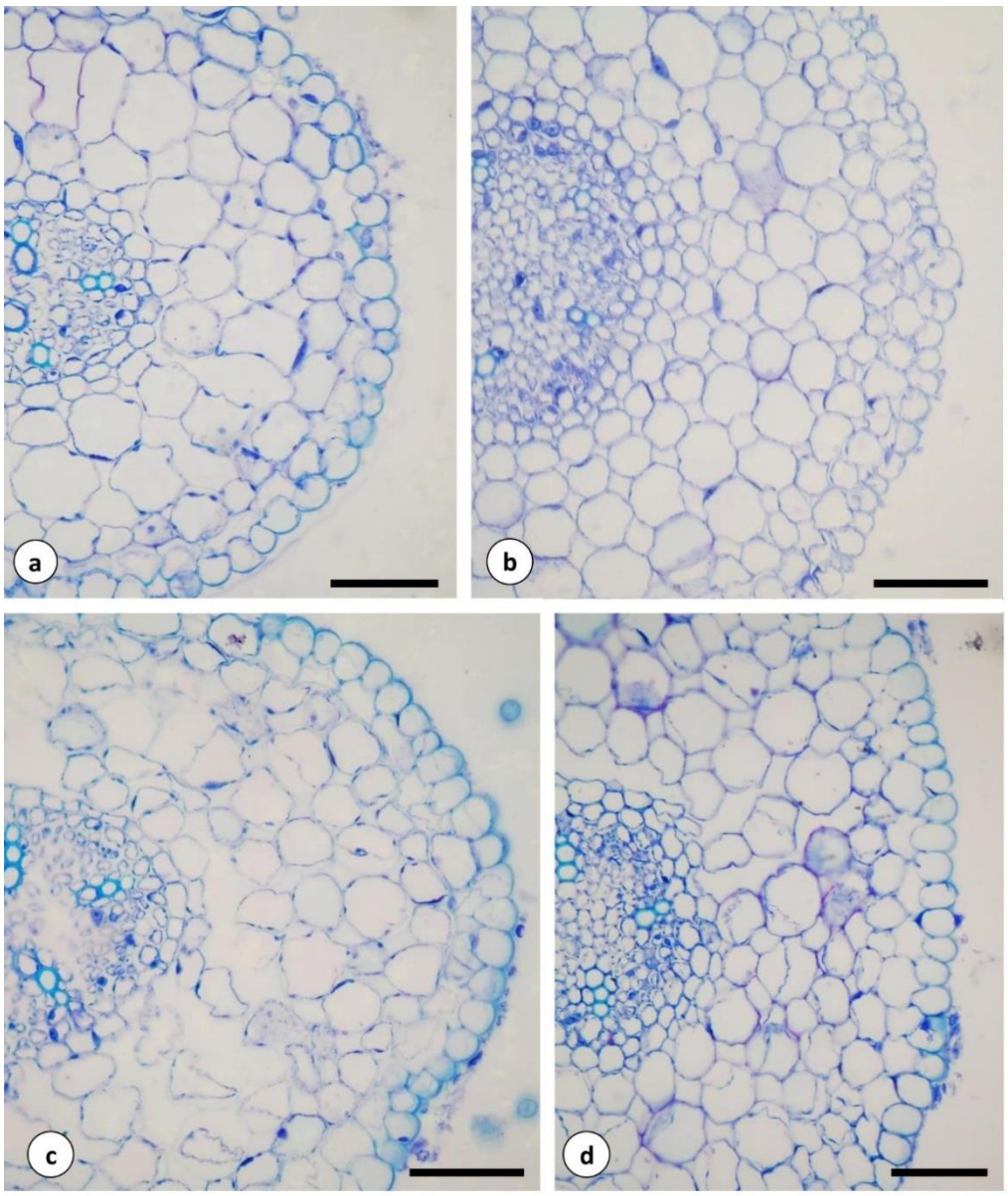

Figure 3. Photomicrographs of the cross sections of roots from *C. calophylla* plants under the experimental treatments with Zn and/or Cu excess. **a**. T1 = control (0.11g/ L of Zn and 0.04g/L of Cu). **b**. T2 = excess of Zn (0.22g/L). **c**. T3 = excess of Cu (0.10g/L). **d**. T4 = excess of Zn and Cu (0.22g/L of Zn and 0.10g/L of Cu). Scale bars: 50 μm (a-d).

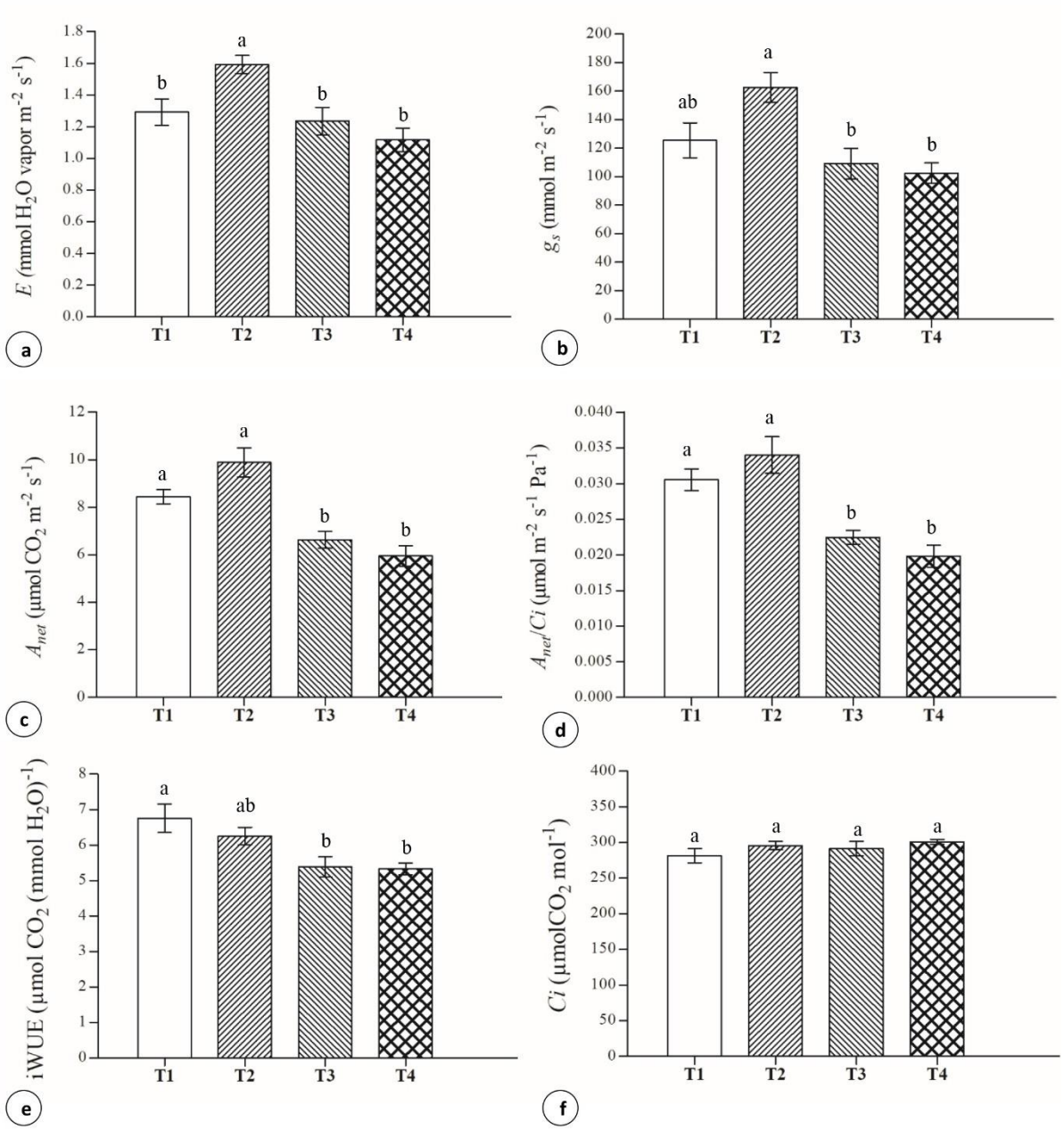

Figure 4. Gas exchange measurements from *C. calophylla* plants under the experimental treatments with Zn and/or Cu excess. **a**. Transpiration rate (*E*). **b**. Stomatal conductance (g_s). **c**. carbon assimilation (*A*). **d**. RuBisCO efficiency (A_{net}/Ci). **e**. Instantaneous water use efficiency (iWUE). **f**. Internal CO_2 concentration in the leaf (*Ci*). T1 = control (0.11g/ L of Zn and 0.04g/L of Cu); T2 = excess of Zn (0.22g/L); T3 = excess of Cu (0.10g/L); T4 = excess of Zn and Cu (0.22g/L of Zn and 0.10g/L of Cu).

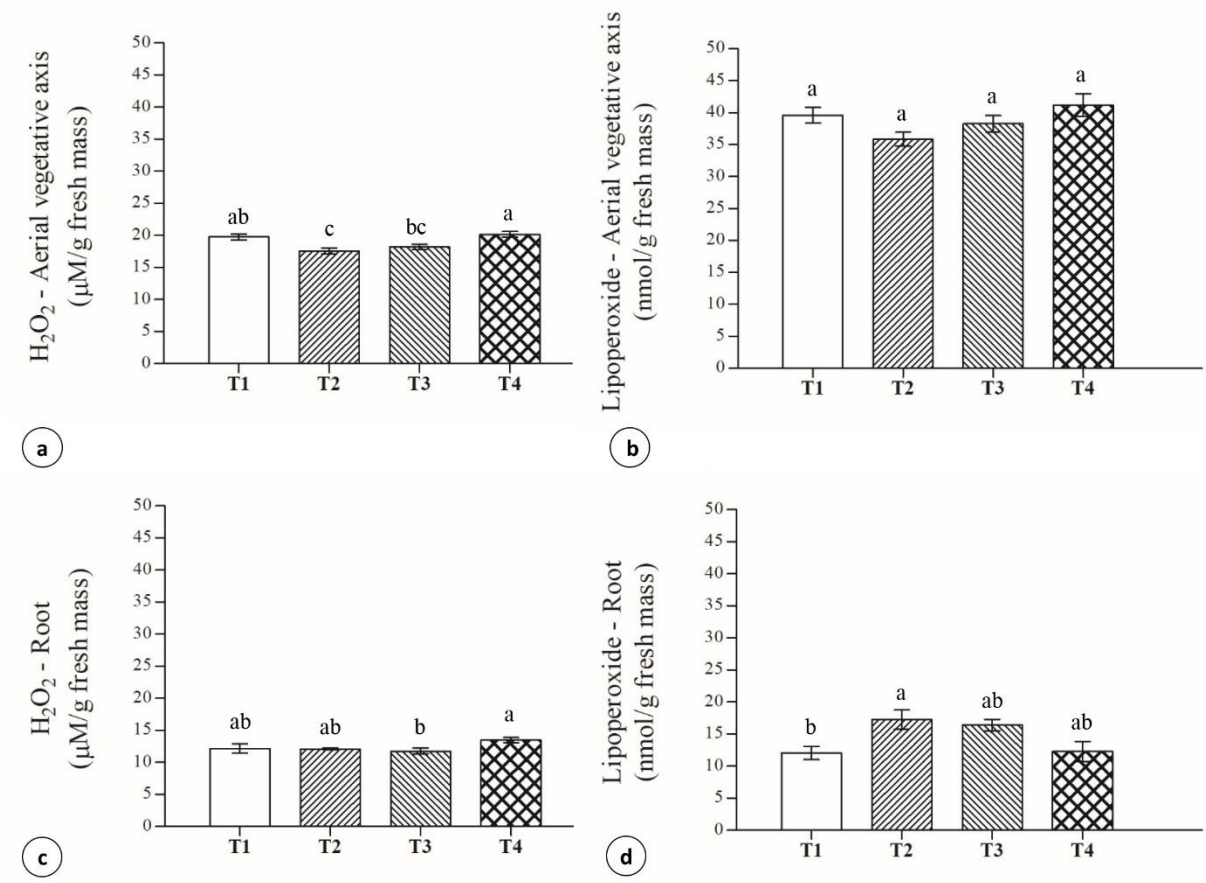

Figure 5. Peroxidation level in *C. calophylla* plants under the experimental treatments with Zn and/or Cu excess. **a**. Quantification of hydrogen peroxide (H_2O_2) in the aerial shoots. **b**. Lipid peroxidation in the aerial shoots. **c**. Quantification of hydrogen peroxide (H_2O_2) in roots. **d**. Lipid peroxidation in roots. T1 = control (0.11g/ L of Zn and 0.04g/L of Cu); T2 = excess of Zn (0.22g/L); T3 = excess of Cu (0.10g/L); T4 = excess of Zn and Cu (0.22g/L of Zn and 0.10g/L of Cu).

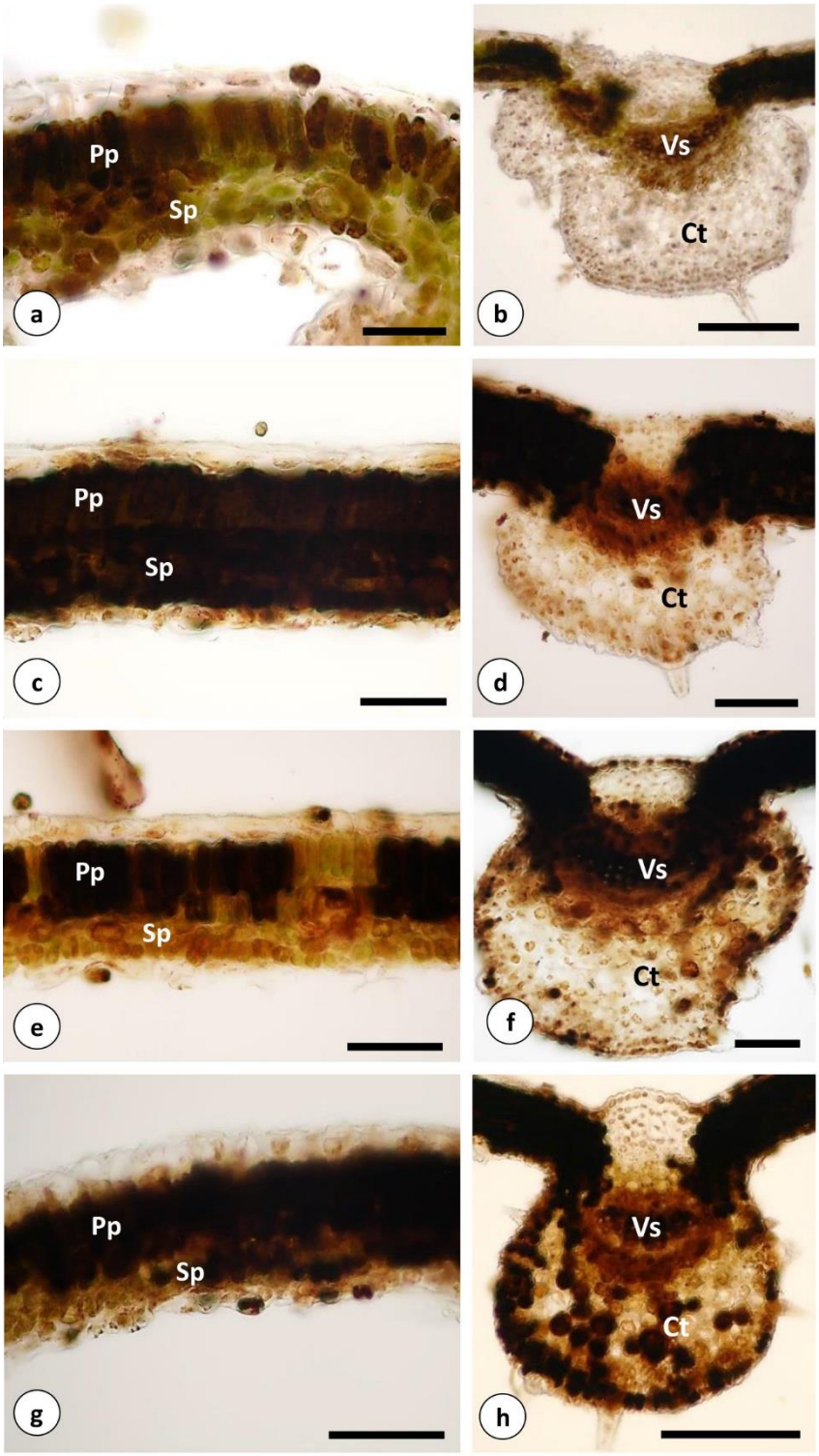

Figure 6. Histolocalization of hydrogen peroxide (H_2O_2) using DAB reagent in cross sections of the leaf blade of *C. calophylla* plants under the experimental treatments with Zn and/or Cu excess. **a**, **c**, **e**, **g**. Histolocalization of H_2O_2 in the mesophyll. **b**, **d**, **f**, **h**. Histolocalization of H_2O_2 in the midrib. **a-b**. T1 = control (0.11g/ L of Zn and 0.04g/L of Cu). **c-d.** T2 = excess of Zn (0.22g/L). **e-f**. T3 = excess of Cu (0.10g/L). **g-h**. T4 = excess of Zn and Cu (0.22g/L of Zn and 0.10g/L of Cu). **Ct** - cortex; **Pp** - palisade parenchyma; **Sp** - spongy parenchyma; **Vs** - vascular system. Scale bars: 100 μm (b, d, f, h); 50 μm (a, c, e, g).

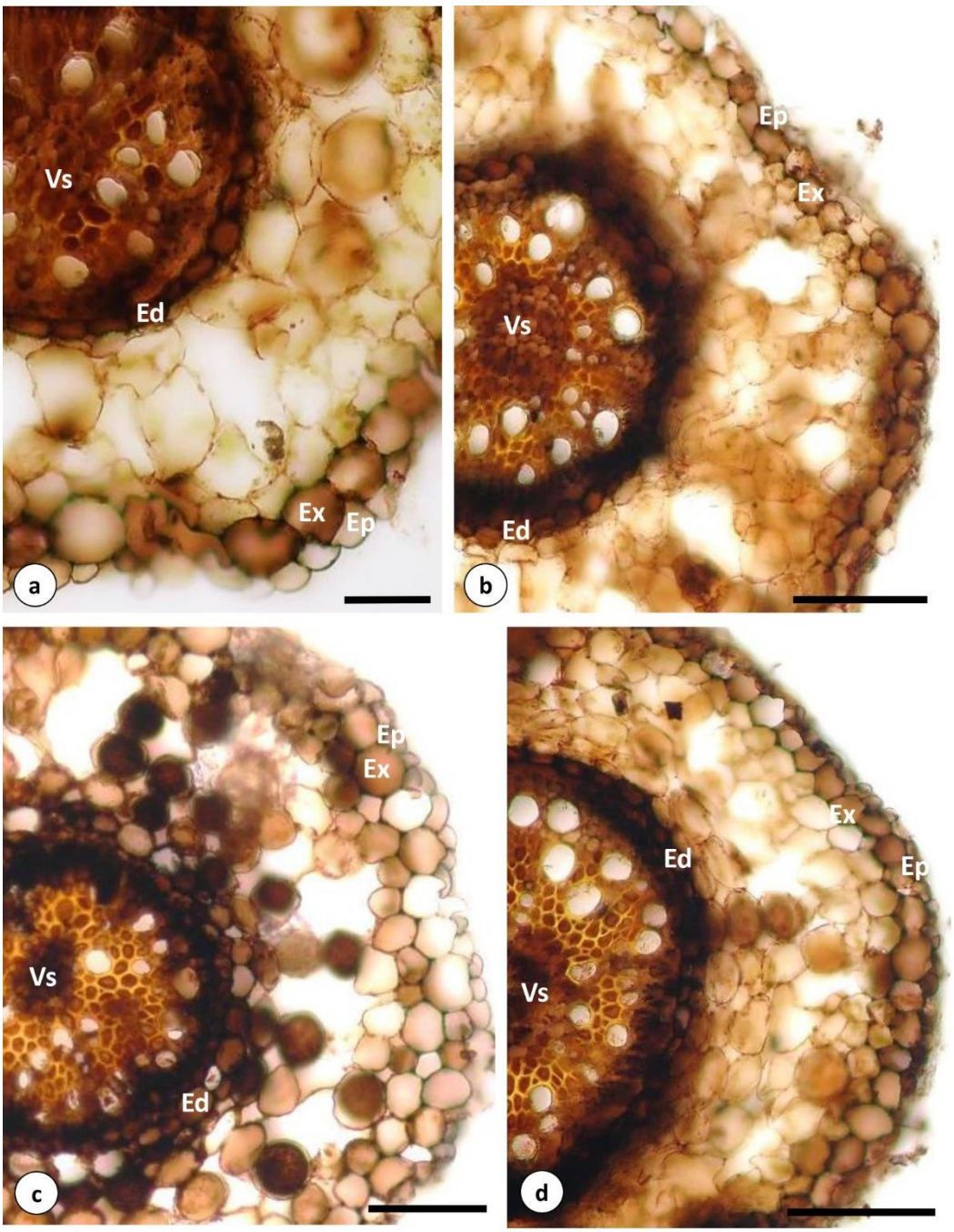

Figure 7. Histolocalization of hydrogen peroxide (H_2O_2) using DAB reagent in cross sections of the root of *C. calophylla* plants under the experimental treatments with Zn and/or Cu excess. **a**. T1 = control (0.11g/ L of Zn and 0.04g/L of Cu). **b**. T2 = excess of Zn (0.22g/L). **c**. T3 = excess of Cu (0.10g/L). **d**. T4 = excess of Zn and Cu (0.22g/L of Zn and 0.10g/L of Cu). **Ed** - endoderm; **Ep** - epidermis; **Ex** - exodermis; **Vs** - vascular system. Scale bars: 100 µm (a-d).

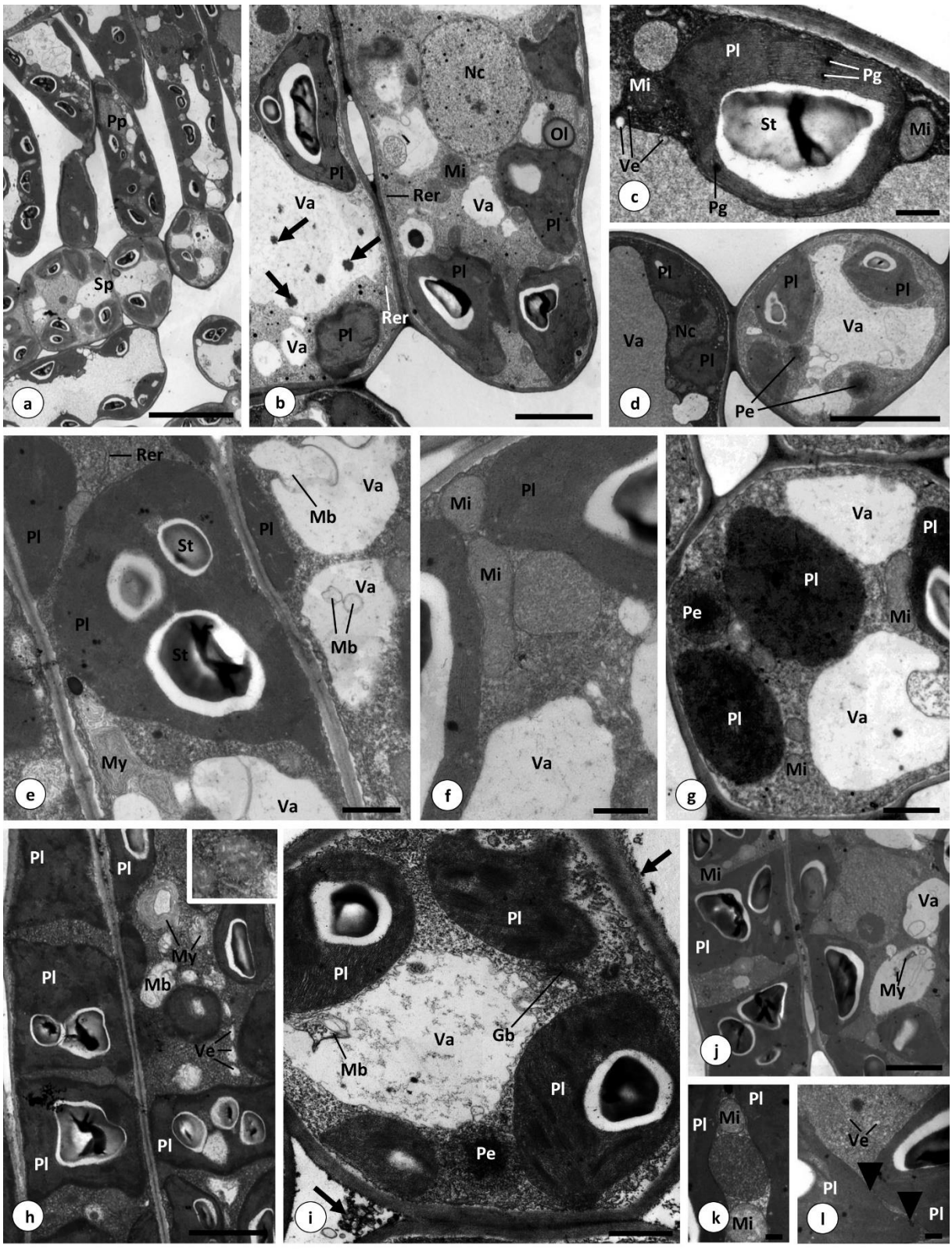

Figure 8. Transmission electron micrographs of the mesophyll in the leaf blade of *C. calophylla* plants under the experimental treatments with Zn and/or Cu excess. **a-d**. Plant from T1 = control (0.11g/ L of Zn and 0.04g/L of Cu). **a**. General view the chlorenchyma cells from the mesophyll showing their thin walls, dense cytoplasm with abundant well-developed organelles and large vacuoles. **b**. Palisade parenchyma cells with chloroplast containing starch grains and plastoglobuli, oil droplets, vacuoles with electron-dense inclusions and, round nucleus with evident nucleolus. **c**. Detail of the periphery cytoplasm with vesicles and a chloroplast with developed thylakoids

and starch grain. **d**. Spongy parenchyma cells with chloroplasts in an irregular contour and peroxisomes. **e**-**g**. Plant from T2 = excess of Zn (0.22g/L). **e**. Palisade parenchyma cells with very large plastids, voluminous mitochondria and myelin figures. **f**. Detail of the plastids and mitochondria with dilated cristae. **g**. Spongy parenchyma cells with some chloroplast devoid of starch grains and membrane inclusion in the vacuoles. **h**-**i**. Plant from T3 = excess of Cu (0.10g/L). **h**. Palisade parenchyma cells with dense cytoplasm containing large square chloroplasts occupying almost the entire cells, myelin figures and mitochondria (insert). **i**. Detail of plastids with well-developed thylakoids, membranous and fibrillar material occurred in the vacuoles and, electron-dense bodies in the spaces of the spongy parenchyma cells. **j**-**l**. Plant from T4 = excess of Zn and Cu (0.22g/L of Zn and 0.10g/L of Cu). **j**. General view of palisade parenchyma cells with dense granular cytoplasm, abundant organelles, large square chloroplasts and vesicles; vacuoles with membranous inclusions and myelin figures. **k**. Detail of mitochondria with poorly developed cristae and juxtaposition points of chloroplasts and mitochondria. **l**. Juxtaposition points between chloroplasts. **Gb** - Golgi body; **Mb** - membrane inclusion; **Mi** - mitochondria; **My** - myelin figures; **Nc** - nucleus; **Ol** - oil droplet; **Pe** - peroxisome; **Pg** - plastoglobuli; **Pl** - Plastids; **Pp** - Palisade parenchyma; **Rer** - rough endoplasmic reticulum; **Sp** - Spongy parenchyma; **St** - starch grains; **Va** - vacuole; **Ve** - vesicles. (Arrow head) connection point between chloroplasts. (Arrow) Electron-dense body. Scale bars: 10 μm (b, d); 5 μm (a, h, j); 2 μm (e, g, i); 1 μm (f, c); 0,5 μm (k, l).

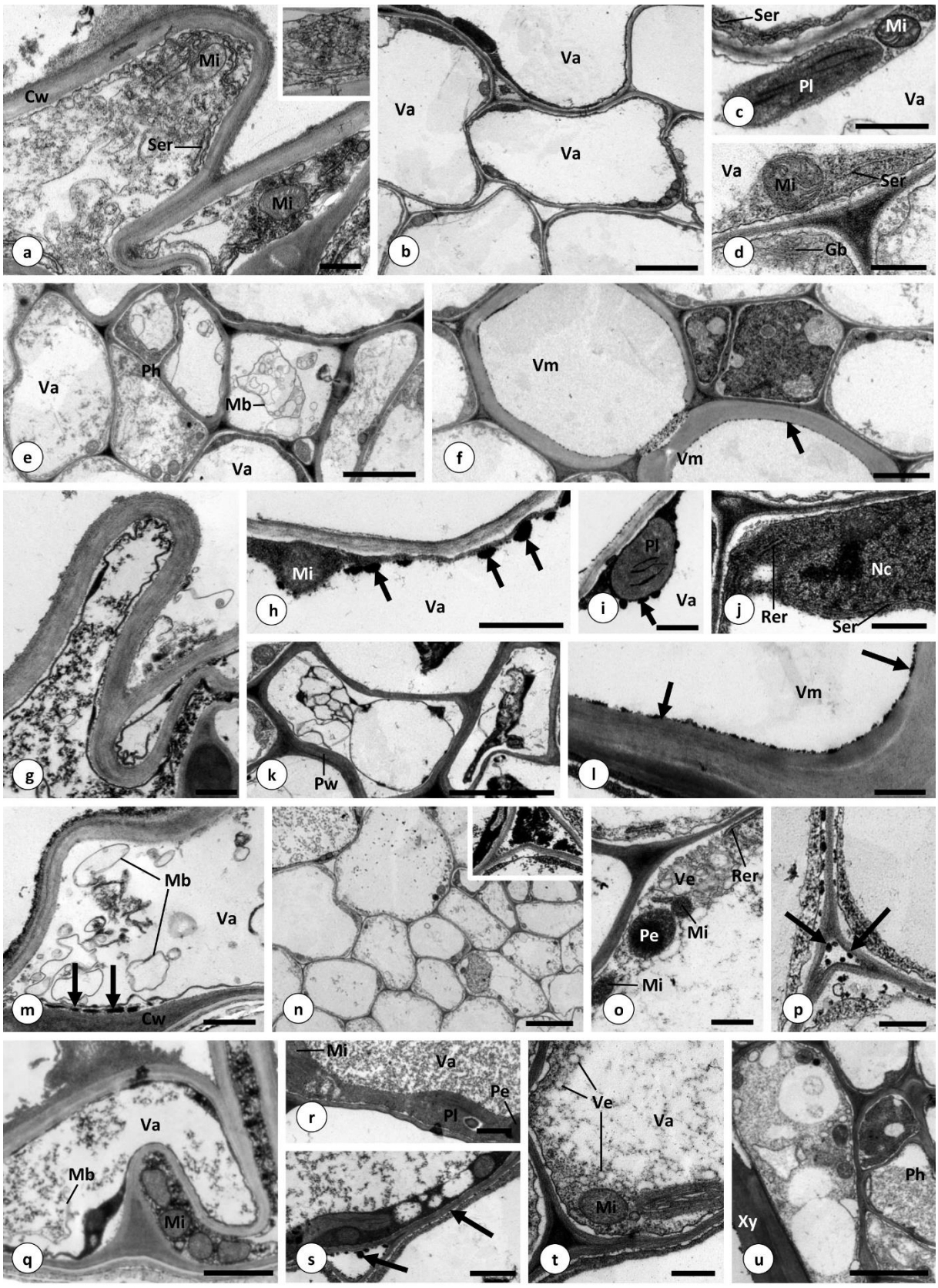

Figure 9. Transmission electron micrographs of the root of *C. calophylla* plants under the experimental treatments with Zn and/or Cu excess. **a-d**. Plant from T1 = control (0.11g/ L of Zn and 0.04g/L of Cu). **a**. Sinuous epidermal cells containing abundant organelles, mitochondria with developed cristae (insert) and small electro-lucent vacuoles. **b**. Cortical parenchyma cells with large vacuole and cytoplasm comprised in cell periphery. **c-d**. Detail

of the cytoplasm of the cortical parenchyma cells with abundant organelles. **e**. Phloem cells showing cytoplasm comprised in cell periphery and membrane inclusions in the vacuole. **f**. Vessel members from xylem with thick walls and electron-dense bodies adhered on it. **g-l**. Plant from T2 = excess of Zn (0.22g/L). **g**. Sinuous epidermal cell showing a flocculent and electron-dense cytoplasm with few organelles. **h**. Cortical parenchyma cell with reduced and electron-dense cytoplasm, mitochondria with unclear cristae and electron-dense bodies are observed in the attached in the internal face of the tonoplast. **i**. Detail of a plastid with poorly developed internal membrane. **J**. Detail of the nucleus with rough and smooth endoplasmic reticulum. **k**. Phloem cells with thick wall. **l**. Vessel members of xylem with electron-dense bodies adhered in the internal cell wall. **m-p**. Plant from T3 = excess of Cu (0.10g/L). **m**. Epidermal cell with electron-dense bodies in the periplasmic space and wide vacuole containing membrane inclusions. **n**. Cortical parenchyma cells with grainy and reduced cytoplasm; electron-dense material accumulated in the intercellular space (insert). **o**. Endodermal cell with abundant organelles and vesicles. **p**. Vascular parenchyma cells with electron-dense bodies in the periplasmic and intercellular spaces. **q-u**. Plant from T4 = excess of Zn and Cu (0.22g/L of Zn and 0.10g/L of Cu). **q**. Epidermal cell with wide vacuole and electron-dense granular cytoplasm with abundant mitochondria. **r**. Cytoplasm of a cortical parenchyma cells with abundant organelles and vacuole containing fibrillar material. **s**. Electron-dense bodies in the intercellular spaces of cortical parenchyma cells. **t**. Grainy cytoplasm of a vascular parenchyma cell with mitochondria, plastids and vesicles. **u**. Vacuole of cortical parenchyma cells with fibrillar material and membrane inclusions. **Cw** - cell wall; **Gb** - Golgi bodies; **En** – endodermis; **Mb** - membrane inclusion; **Mi** - mitochondria; **Nc** - nucleus; **Pe** - peroxisome; **Ph** - phloem; **Pl** - plastid; **Pw** - pearly wall; **Rer** - rough endoplasmic reticulum; **Ser** - smooth endoplasmic reticulum; **Va** - vacuole; **Ve** – vesicle; **Vm** - vessel member; **Xy** - xylem. (Arrow) Electron-dense body. Scale bars: 10 μm (n); 5 μm (b, e, f, k, u); 2 μm (c, h, i, q, r, s); 1 μm (a, d, g, j, l, m, o, p, t).

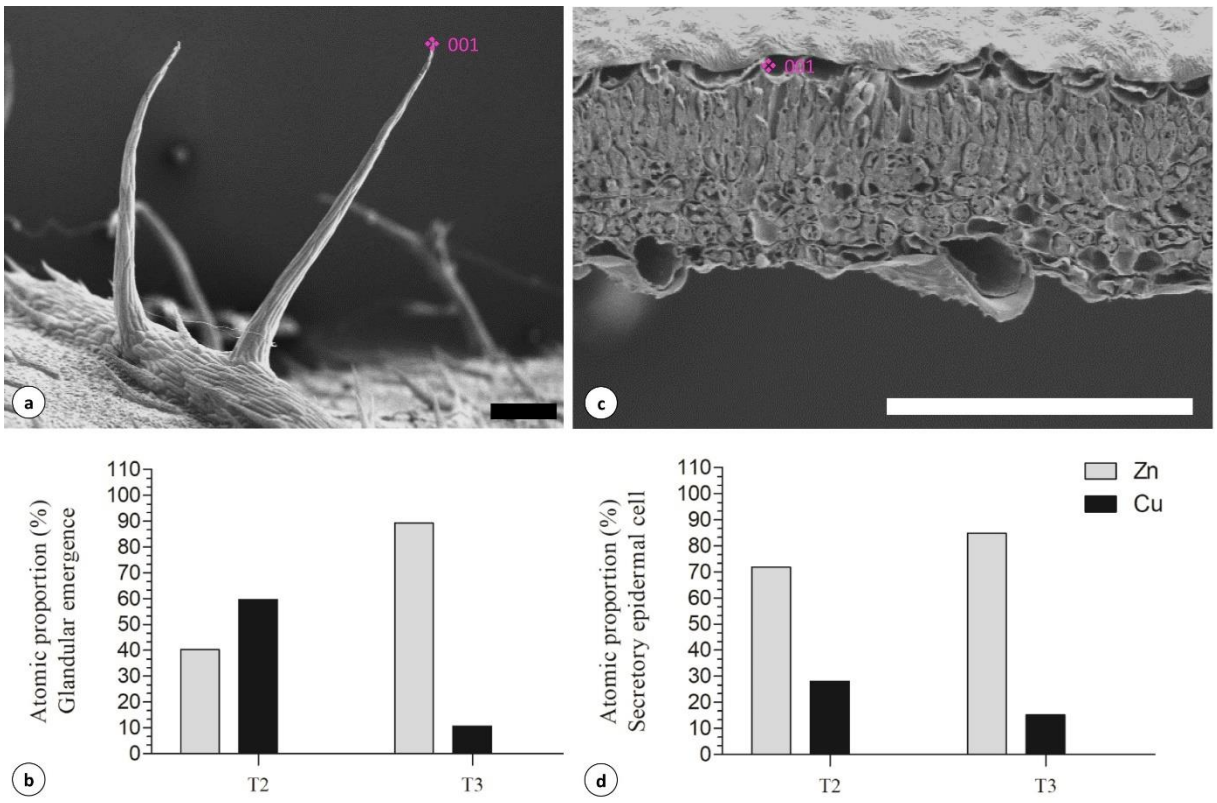

Figure 10. Detection of Zn and Cu in the secretory system *C. calophylla* plants under excess of Zn (T2 = 0.22g/L) and Cu (T3 = Cu 0.10g/L) using MEV-EDS. **a**. Scanning electron micrographs of the glandular emergence showing the exact point of Zn and Cu measurements. **b**. Atomic proportion (%) of Zn and Cu in the apex of the glandular emergence. **c**. Scanning electron micrographs of the epidermal secretory cell showing the exact point of Zn and Cu measurements. **d**. Atomic proportion (%) of Zn and Cu in the inner wall of the secretory epidermal cell. Scale bars: 100 µm (a, c).

Apêndices

Equações para calcular as concentrações das substâncias químicas estudadas no capítulo 2 e cromatogramas.

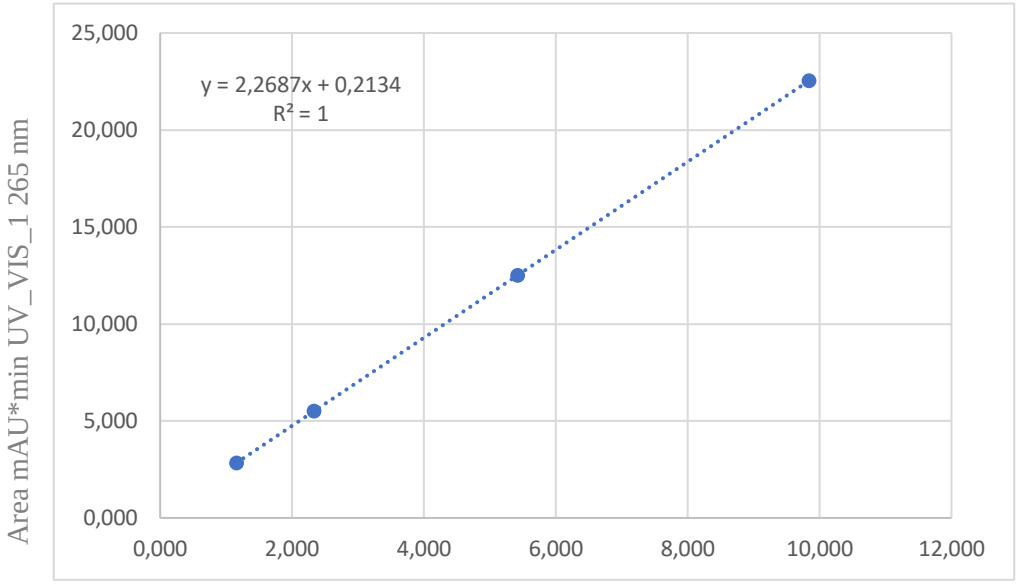

a

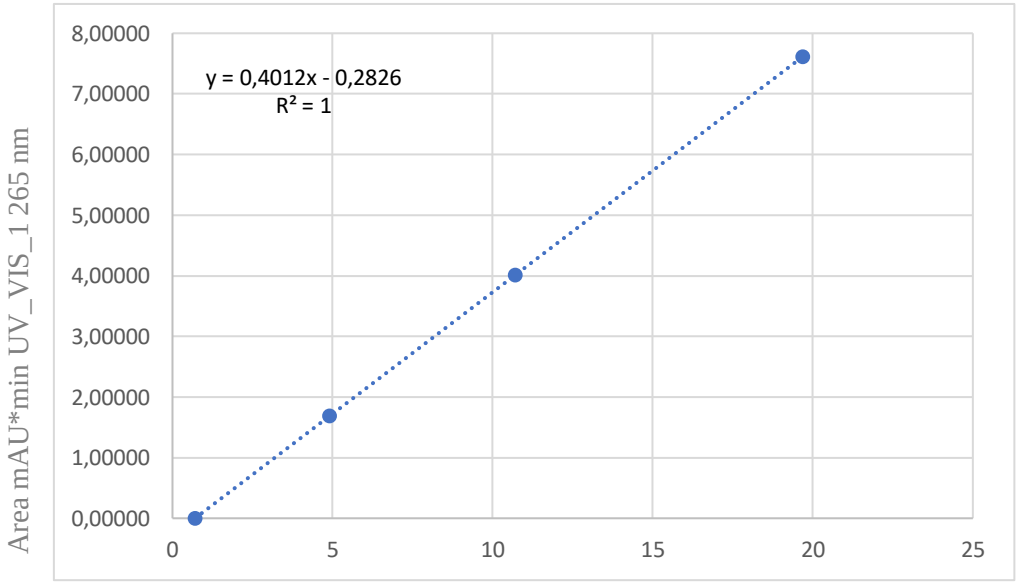

b

Appendix 1. Curves and equations for ellagic acid (a) and gallic acid (b) concentrations. The equations were calculated through the injection of authentic standards solutions in different concentrations in high-resolution liquid chromatography (uv HPLC - Thermo Fisher-Scientific). These equations were used to calculate the concentration of these substances in methanol extracts of *Cuphea calophylla* plants under the four different experimental treatments. The detection wavelength was 365 nm.

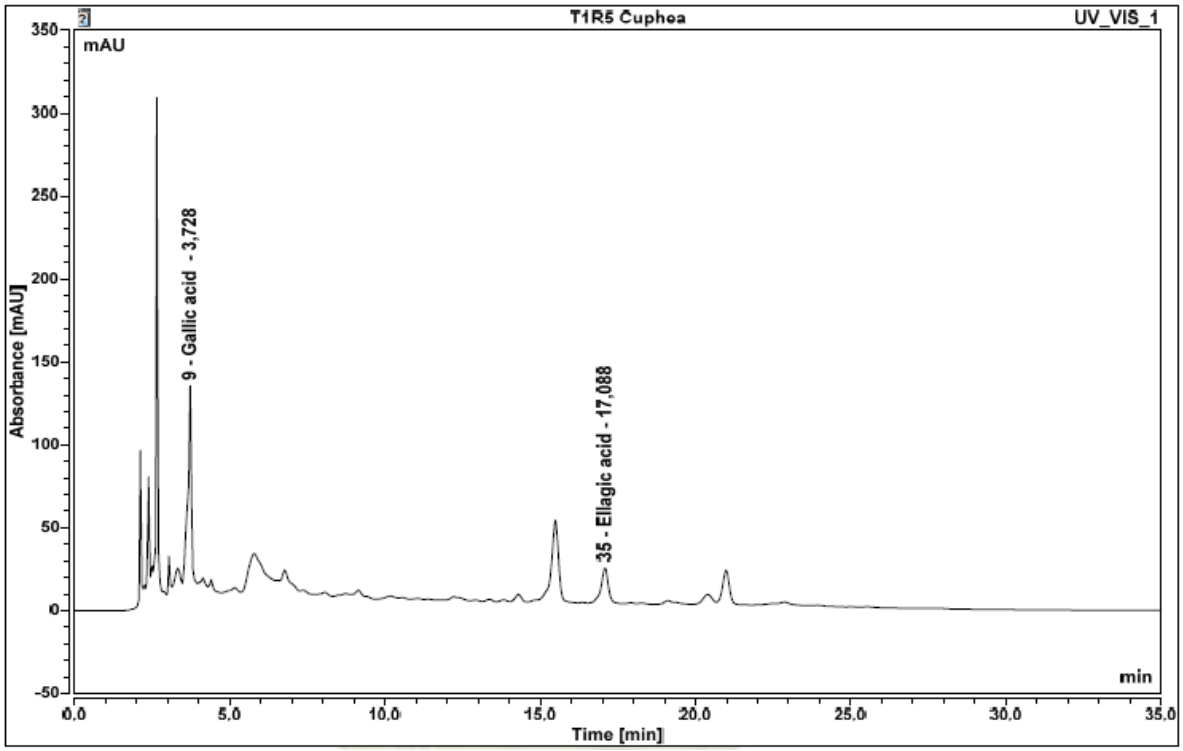

Appendix 2. Chromatogram showing the chemical profile of methanolic extract of a *Cuphea calophylla* plant under control treatment (T1).

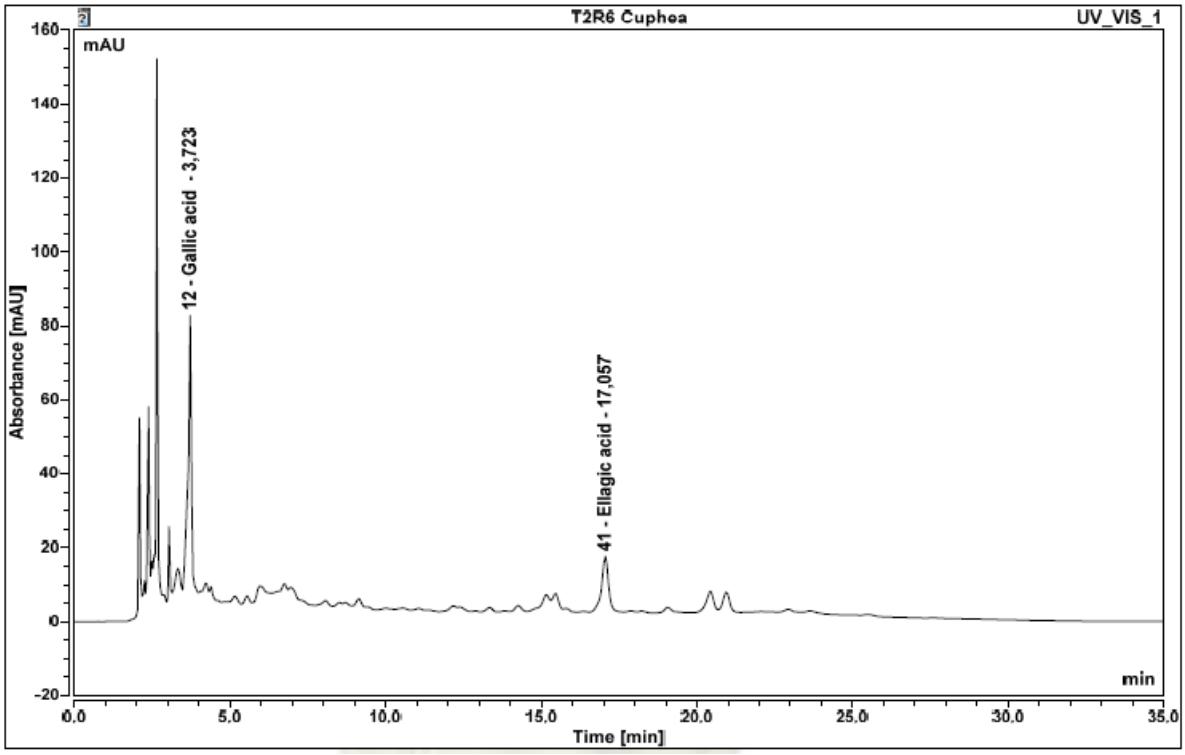

Appendix 3. Chromatogram showing the chemical profile of methanolic extract of a *Cuphea calophylla* plant under Zn excess (T2).

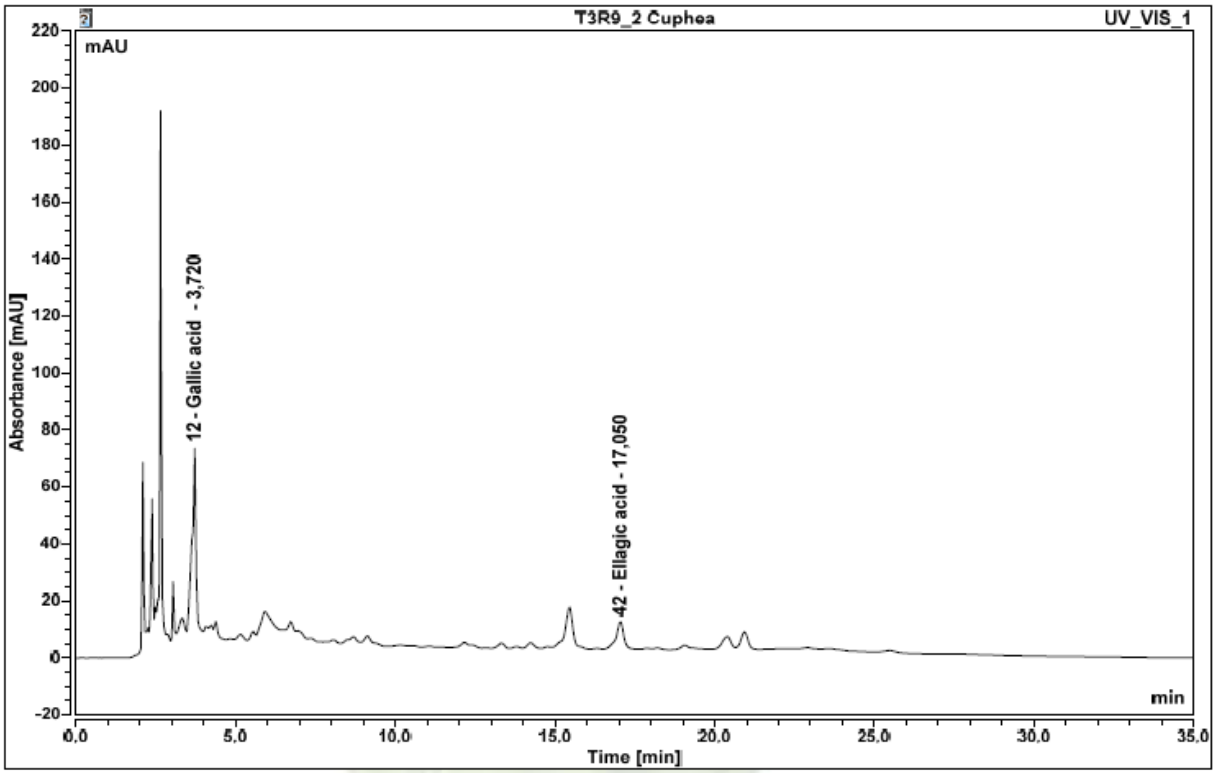

Appendix 4. Chromatogram showing the chemical profile of methanolic extract of a *Cuphea calophylla* plant under Cu excess (T3).

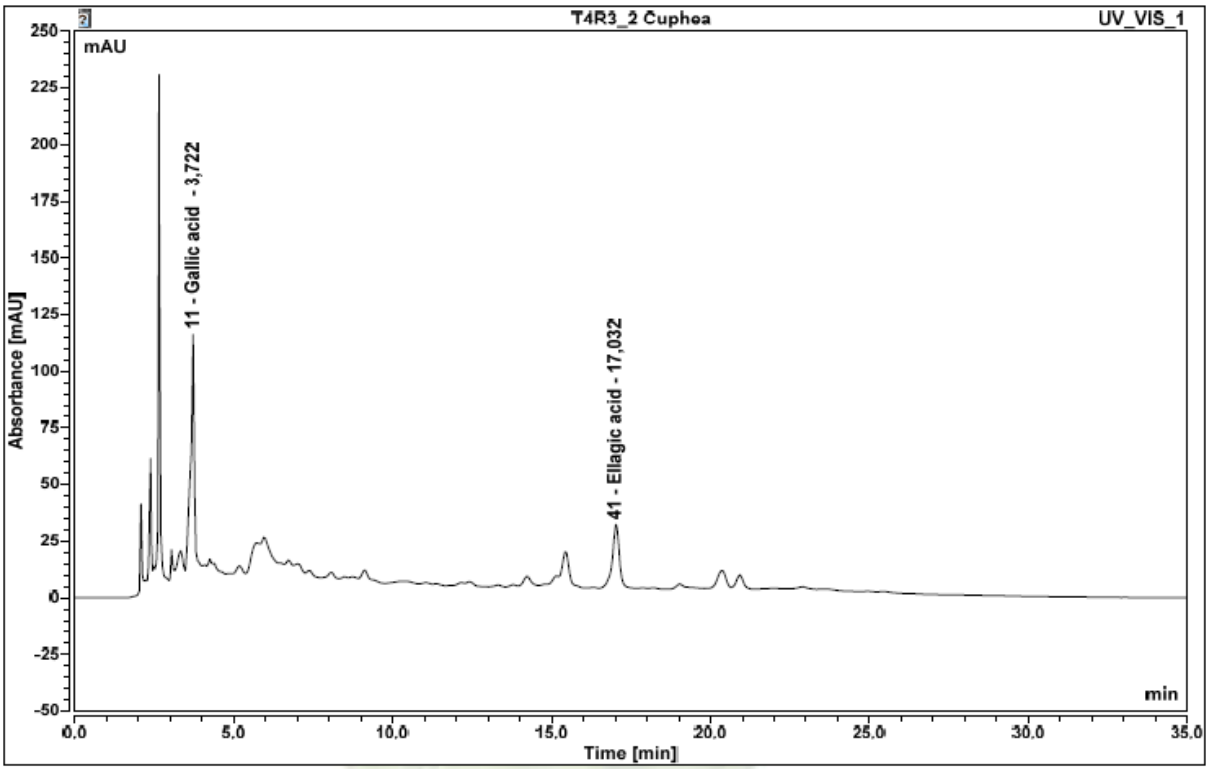

Appendix 5. Chromatogram showing the chemical profile of methanolic extract of a *Cuphea calophylla* plant under Zn and Cu excess (T4).

Considerações finais

Considerando o potencial medicinal e econômico de *C. calophylla* e sua ampla distribuição no Brasil, a ampliação do conhecimento sobre aspectos estruturais e funcionais dessa espécie é de grande relevância. Em especial, quando se considera sua ocorrência natural em ambientes ruderais e de pastagem contaminados por excesso de metais potencialmente tóxicos e o aumento de áreas destinadas à agropecuária no Brasil, entender o efeito do excesso de cobre e zinco na morfologia e fisiologia dessa espécie é de fundamental importância na predição dos efeitos das ações antrópicas na flora nativa.

Os resultados obtidos quanto à morfologia e desenvolvimento das células e tecidos secretores no eixo vegetativo aéreo de *C. calophylla* têm especial relevância quando se reconhece tais estruturas como os sítios produtores das substâncias bioativas com potencial farmacológico e econômico. Nossos dados preenchem lacunas e elucidam aspectos negligenciados na literatura sobre a morfologia do gênero *Cuphea*. Relatamos pela primeira vez a presença de hidatódios no bordo do limbo foliar de uma espécie do gênero. A origem mista dos apêndices glandulares, descrita aqui, esclarece que tais estruturas são emergências glandulares ao invés de tricomas secretores como tradicionalmente considerado para espécies do gênero, inclusive *C. calophylla*. Ainda, a bicompartimentalização por meio de um septo de material celulósico e o acúmulo de compostos fenólicos, além de mucilagem, nas células da epiderme foliar também são aspectos inovadores, uma vez que essas células têm sido descritas em literatura apenas como células secretoras de mucilagem.

Os dados obtidos por meio da investigação das respostas de *C. calophylla* ao excesso de cobre e zinco corroboram com a ideia de que o excesso de metais tóxicos em áreas utilizadas para agropecuária pode levar a alterações estruturais e fisiológicas nas plantas; além disso, a investigação da influência do excesso de Zn e/ou Cu no sistema secretor *C. calophylla* também merece destaque quando se considera o papel dessas estruturas nas interações ecológicas dessa espécie e como fonte de matéria-prima com valor econômico e medicinal.

Os resultados anatômicos, ultraestruturais, bioquímicos e fisiológicos obtidos a partir do experimento realizado em casa de vegetação nos permitiram sugerir que *C. calophylla* é uma espécie tolerante ao excesso de Zn e susceptível ao excesso de Cu. Ainda, a detecção de Zn e Cu no ápice da emergência glandular e no interior das células epidérmicas secretoras, sugerem o papel das células e tecidos secretores na liberação e imobilização desses metais. Por fim, estima-se que o potencial medicinal de *C. calophylla* não seja afetado em condições de excesso de Zn e Cu, uma vez que os compostos químicos que conferem as propriedades terapêuticas conhecidas dessa espécie - ácido elágico e ácido gálico - não sofreram alterações nas diferentes

condições experimentais. Entretanto, este resultado deve ser tratado com cautela visto que as plantas sob o excesso de Cu e Zn+Cu apresentaram um maior número de substâncias produzidas, as quais devem ter as suas características estudadas, principalmente quanto a nocividade.

Em suma, nossos resultados, além de ampliar o conhecimento sobre aspectos estruturais e funcionais de *C. calophylla*, trazem novas interpretações a estruturas já conhecidas e geram subsídios para estudos com abordagem ecológica, taxonômica e medicinal. As diferentes abordagens empregadas nesse estudo favorecem o entendimento das respostas das plantas nativas ao excesso de metais tóxicos e produzem informações úteis para o manejo de espécies vegetais e para o estabelecimento de estratégias de conservação.